Inelastic X-Ray Scattering as a Probe of Materials under Extreme Conditions

E. Ercan Alp

Argonne National Laboratory

Collaborators:
W. Sturhahn, H. Sinn, T. Toellner, J. Zhao, A. Alatas, A. Said, M. Lerche, H. Yavas, Y. Xiao

ERL X-ray Science Workshop 3

"Almost Impossible Materials Science:
Pushing the Frontier with ERL X-Ray Beams"

Inelastic Scattering as a Probe of Materials under Extreme Conditions

- Inelastic x-ray scattering
  - Nuclear Resonant Scattering
  - High resolution, momentum-resolved IXS
  - X-Ray Raman Scattering
  - Resonant IXS
  - X-Ray emission spectroscopy
  - Compton Scattering
- Extreme conditions for solids & liquids
  - High pressure: up to several megabar
  - High temperature: up to 3000 K
  - High magnetic field: up to 30 T
  - Low temperature: 0.1 K
  - Monolayers or islands on surfaces or buried interfaces
- ERL vs 3rd Generation Storage Rings
  - Brightness, flux, polarization, space
- Some new ideas

Why an ERL for IXS ?

- Brightness:
  - E > 12 keV, brightness translates into flux and resolution for high resolution crystal optics (especially above 20 keV)
  - B > 10^{23} ph/sec/mm^2/mrad^2/0.1%BW
- Flux:
  - F > 10^{15} ph/sec/eV (thus 50 m + undulator with a short period)
- Polarization in the vertical plane
  - Easier to build large horizontal instruments than vertical instruments:
- Focusing:
  - Efficient focussing for ~ 1 μm spot for high pressure measurements
- Space
  - Large instruments extending both ways difficult at circular rings:

What can we study with IXS ?

- Thermoelasticity:
  - Speed of sound, elastic constants and tensor, kinematic and dynamic viscosity, thermal conductivity, relaxation times at and beyond the hydrodynamic limit
  - At P > 2 Mb, and 1 < T < 4000 K
- Phonon dispersion and density of states in nano-size systems, buried interfaces, and multilayers:
  - Boson peak, non-Debye behaviour, magnon-phonon coupling
- Dynamics of proteins, enzymes, and their model compounds such as porphyrins, and cubanes

  Anisotropy, effect of ligands, effect of charge transport

  Membrane fluidity, DNA dynamics in confined fluids
- Element and isotope specific magnetometry of monolayers:
- Valence electron excitations
  - Hubbard U, t
  - Plasmons
- Low-Z element (H, B, C, N, O) K-edge measurements with hard x-rays: in-situ, extreme conditions, bond formations

Inelastic x-ray scattering geometry and physics

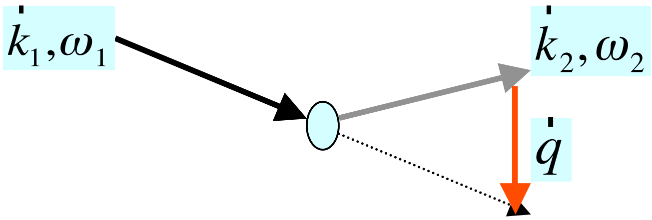

$\omega = \omega_1 - \omega_2$ energy transferred

$\mathbf{q} = \mathbf{k}_1 - \mathbf{k}_2$ momentum transferred

The goal of the experiments is to measure the scattering cross-section

$$\frac{\mathrm{d}^2\sigma}{d\Omega d\omega}(\mathbf{q},\mathrm{h}\omega)$$

$$\frac{\mathrm{d}^2\sigma}{d\Omega d\omega}(q,\mathrm{h}\omega) \approx \left(\frac{\mathrm{d}\sigma}{d\Omega}\right)_{T\,\mathrm{hom}\,pson} S(\mathbf{q},\omega) + \text{ resonant terms}$$

$$S(\mathbf{q},\omega) = \frac{1}{2\pi}\int dt e^{-i\omega t}\left\langle i \left| \sum_{jj'} e^{-i\mathbf{q}r_{j'}(t)} e^{i\mathbf{q}r_j(0)} \right| f \right\rangle$$

is the Fourier transform of the correlation of the phase of the scattering amplitude at different times

Scattering geometry and physics

The physical origin of the correlations depends on how $1/\mathbf{q}$ compares with l_c, the characteristic length, of the system related to the spatial inhomogeneity.

$$\text{when} \quad \mathbf{q}\cdot l_c << 1 \qquad \Rightarrow \quad \text{COLLECTIVE BEHAVIOUR}$$

$$\text{when} \quad \mathbf{q}\cdot l_c >> 1 \qquad \Rightarrow \quad \text{SINGLE PARTICLE BEHAVIOUR}$$

$$\text{when} \quad \frac{1}{\mathbf{q}} \approx d \text{ and } \omega \approx \text{ phonon frequency } \Rightarrow \text{ Collective ion excitation}$$

$$\text{when} \quad \frac{1}{\mathbf{q}} \approx r_c \text{ and } \omega \approx \text{ plasma frequency } \Rightarrow \text{ Valence electron excitation}$$

What is being measured ?

$$\frac{d^2\sigma}{d\Omega\, \mathrm{d}\omega} = \underbrace{r_0^2\, \frac{\omega_f}{\omega_i} \left|\mathbf{e}_i \cdot \mathbf{e}_f\right|^2 N \sum_{i,f}}_{\textbf{Thomson cross section}} \underbrace{\left| \langle i | \sum e^{i\mathbf{Q}\mathbf{r}_{\mathrm{j}}} | f \rangle \right|^2 \delta(E_f - E_i - \mathbf{h}\omega)}_{\textbf{Dynamical structure factor S(Q,w)}}$$

$$S(\mathbf{Q},\omega) = \frac{1}{2\pi} \int dt\, e^{-i\omega t} \underbrace{\langle \phi_i | \sum_{ll'} f_l(\mathbf{Q}) e^{-i\mathbf{Q}\cdot \mathbf{r}_l(t)} f_{l'}(\mathbf{Q}) e^{i\mathbf{Q}\cdot \mathbf{r}_{l'}(0)} | \phi_i \rangle}_{\textbf{Density-density correlations}}$$

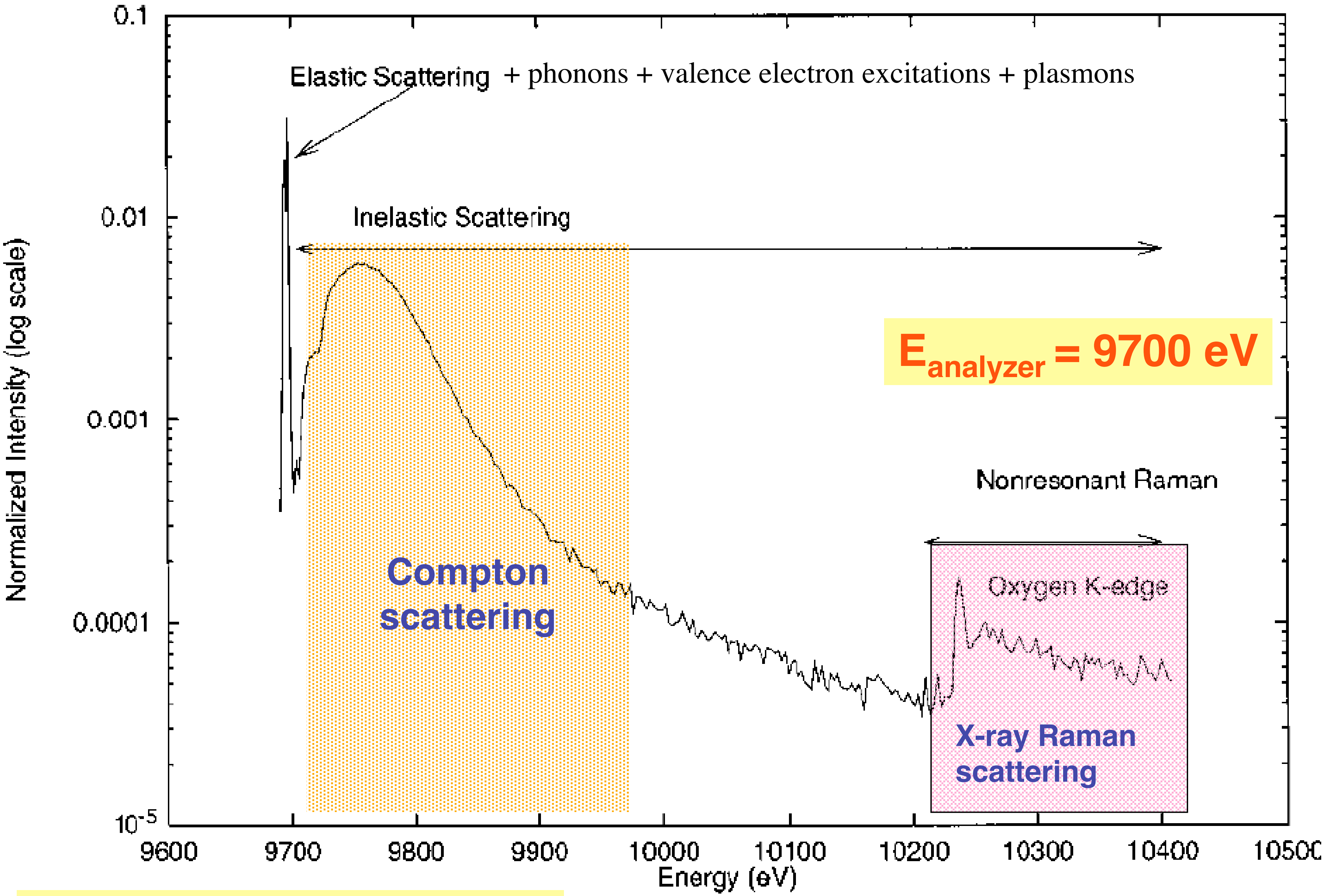

(D.T. Bowron et al, Phys. Rev. B 62 R9223)

A SHORT SUMMARY OF CURRENT INELASTIC X-RAY SCATTERING TECHNIQUES

Technique	Source of interaction	Typical resolution	Deetection method	Location at the APS
Momentum-resolved, high energy resolution IXS: HERIX	Collective excitations of atoms, ions, molecules, PHONONS	1-3 meV	Back-scattering, curved and diced crystal analyzer	3-ID, 30-ID
Momentum-resolved, medium energy resolution resonant IXS: MERIX	Valence electrons near Fermi level	100-500 meV	Near-back-scattering, curved and diced crystal analyzer	9-ID, 12-ID, 30-ID, 33-ID
Momentum-integrated, nuclear resonant IXS: NRIXS	Collective excitations monitored through a nuclear resonance	0.5-2 meV	Nano-second time resolved detectors monitoring nuclear level decay	3-ID, 16-ID
High resolution Compton scattering: CS	Core and valence electrons	1 eV	Triple Laue crystal analyzer, PSD detector	
Magnetic Compton scattering: MCS	Spin polarized electrons	100 eV	Solid state detector	11-ID
X-ray Raman spectroscopy: XRS	Core electron excitations of low-Z elements	1 eV	Back-scattering curved flat analyzers	13-ID, 16-ID, 20-ID
X-ray emission spectroscopy: XES	X-ray fluorescence by incident photons: photon-in/photon-out	0.5 eV	Back-scattering curved flat analyzers	13-ID, 16-ID, 10-ID
Soft-X-ray IXS : PEEM	x-ray induced photoemission: photon-in/electron-out	5 meV	Electron spectrometer	4-ID

Inelastic X-Ray Scattering in the Synchrotron Era

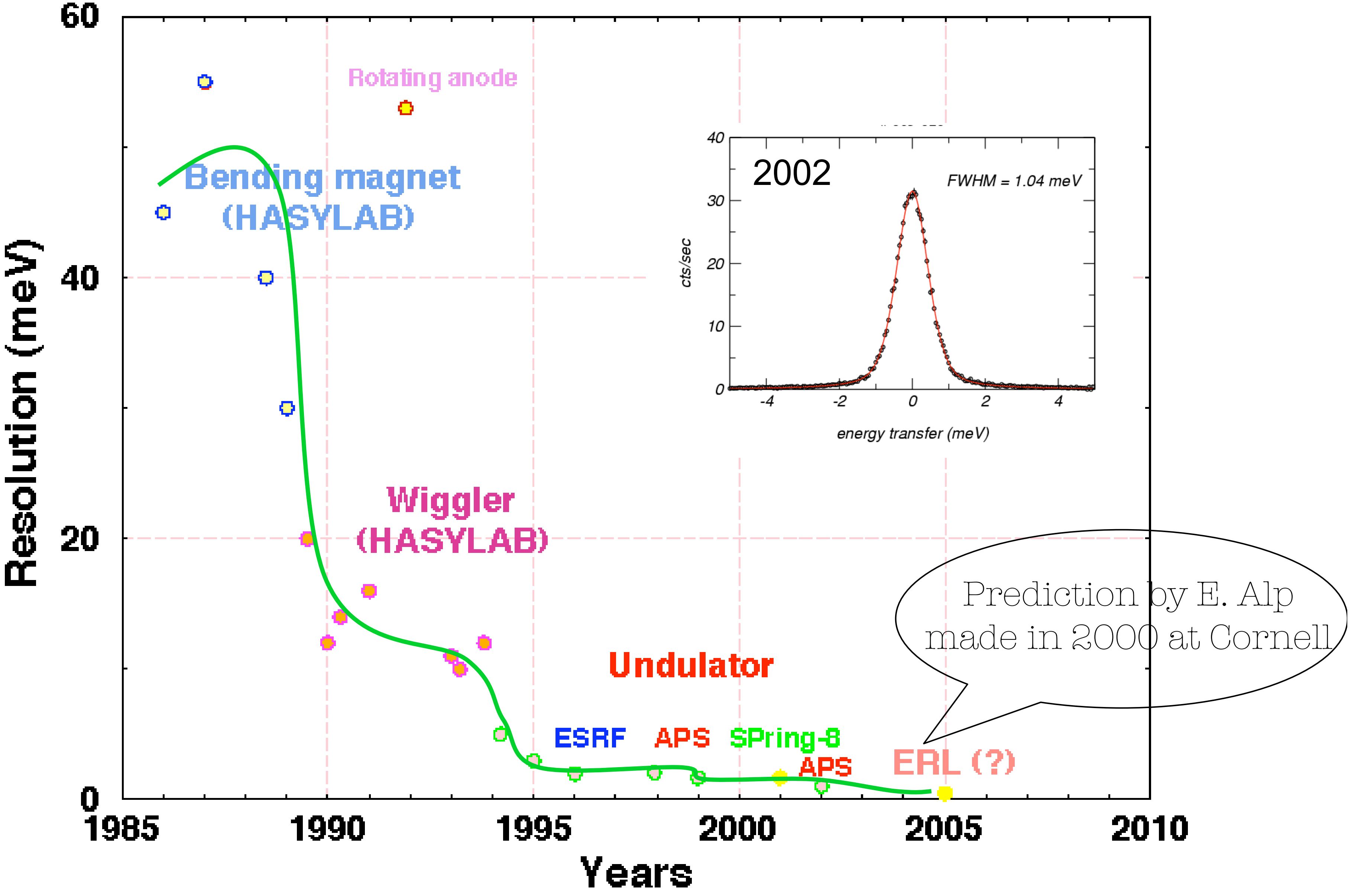

source: E. Burkel, Rep. Prog. Phys. 63 (2000) 171, (modified)

Prediction by E. Alp made in 2000 at Cornell

Why X-Rays ?

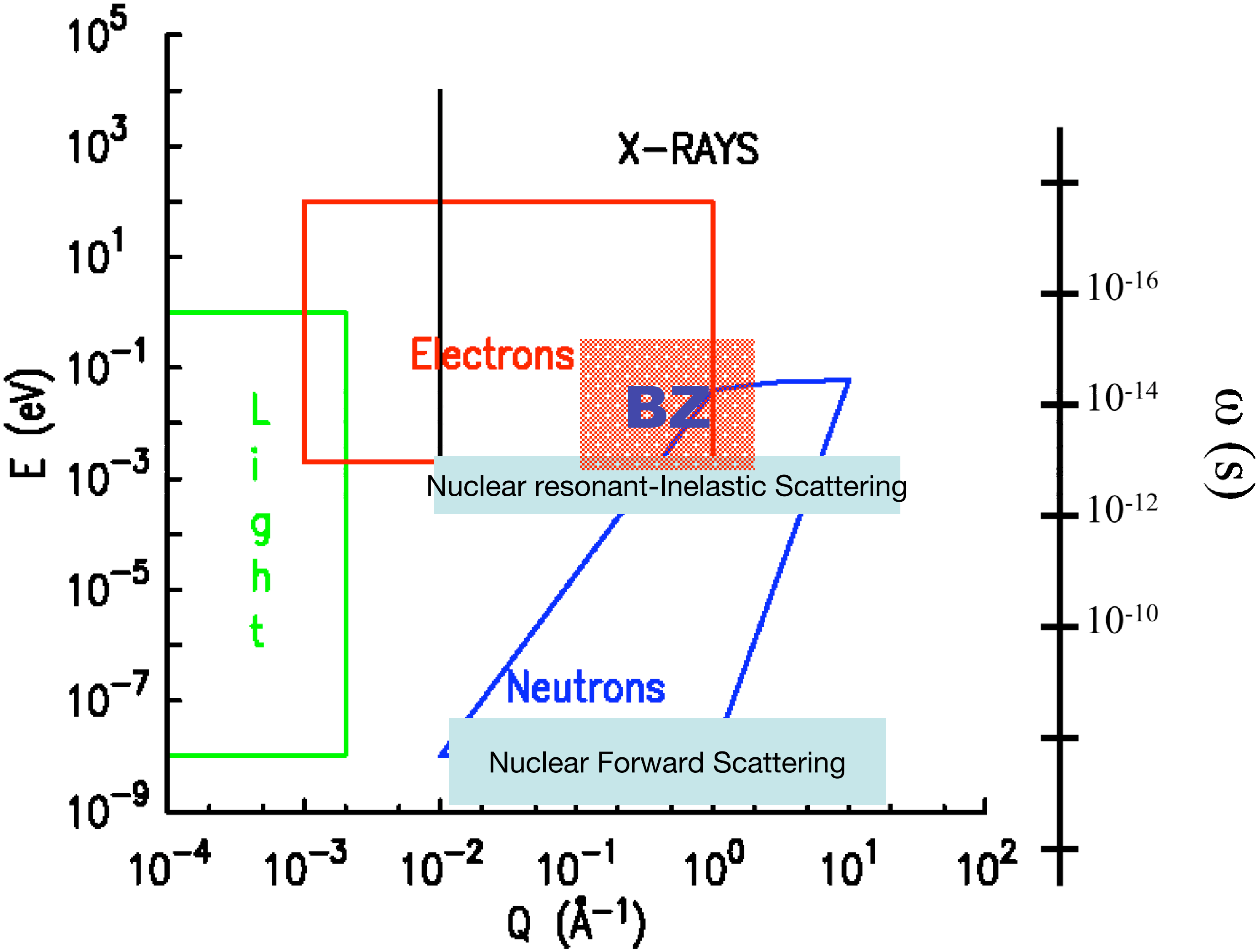

10^{5}
10^{3}
10^{1}
10^{-1}
10^{-3}
10^{-5}
10^{-7}
10^{-9}
E (eV)
X-RAYS
Electrons
BZ
Light
Nuclear resonant-Inelastic Scattering
Neutrons
Nuclear Forward Scattering
10^{-4}
10^{-3}
10^{-2}
10^{-1}
10^{0}
10^{1}
10^{2}
Q (Å^{-1})
10^{-16}
10^{-14}
10^{-12}
10^{-10}
ω (s)

Generations of high resolution monochromators

@ CHESS, 1991

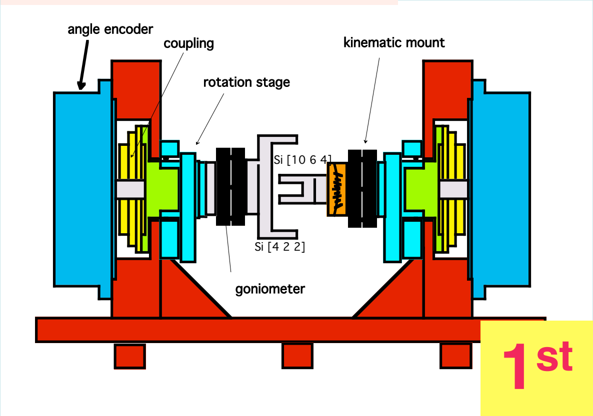

@ APS, 1998

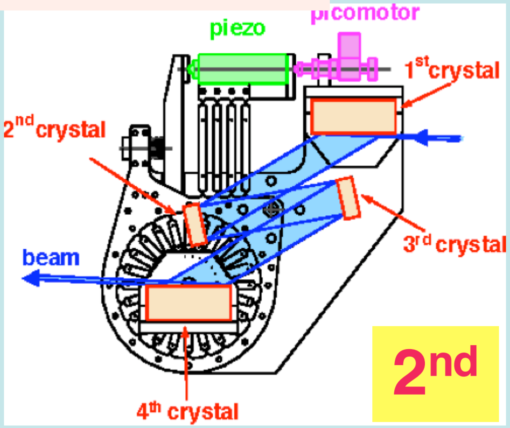

@ APS, 2001

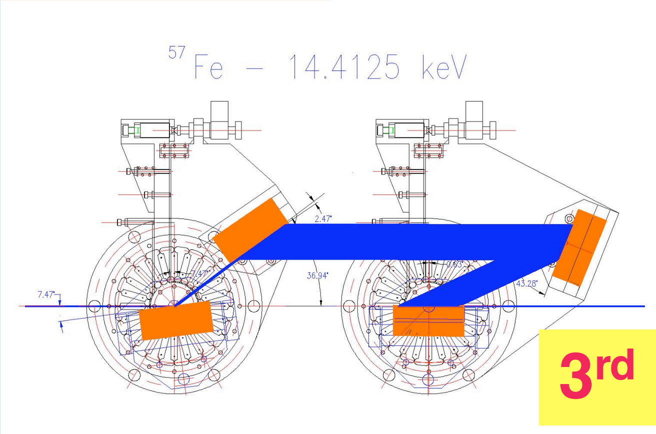

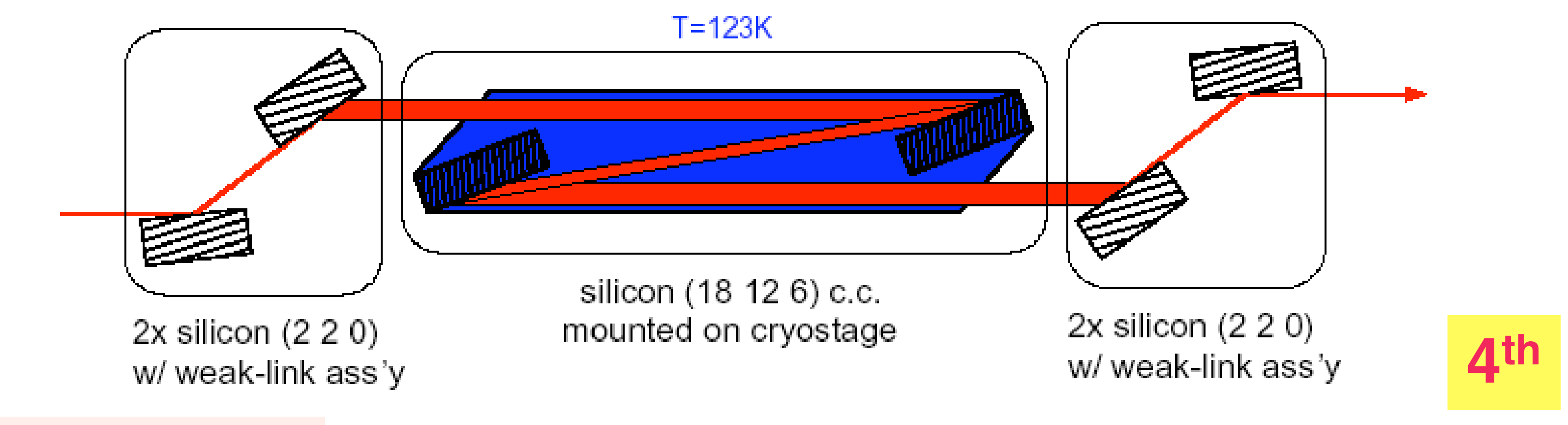

@ APS, 2003

Record resolution at 23.870 keV
^{119}Sn nuclear resonance
T. Toellner, 2003

$$E / \Delta E = 1.7 \cdot 10^8$$

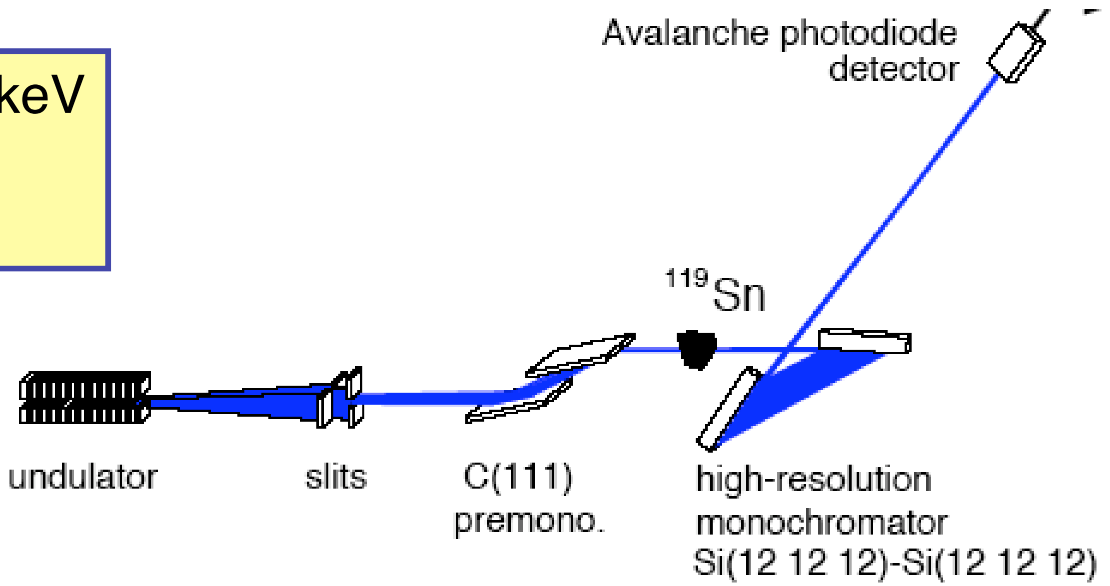

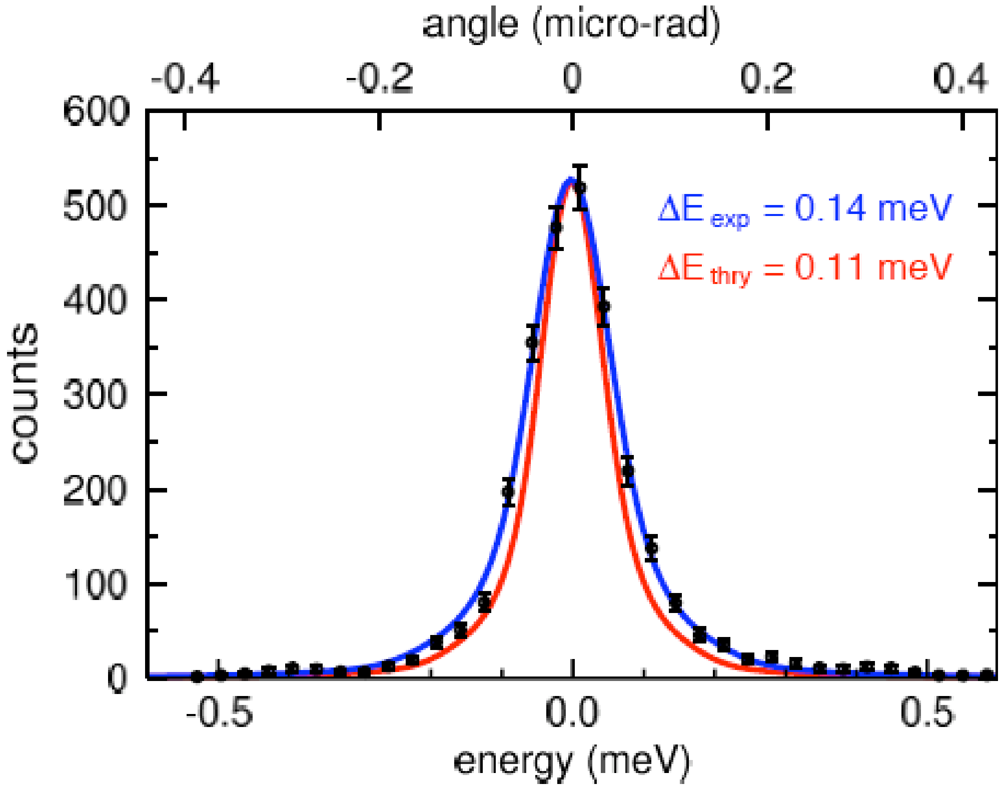

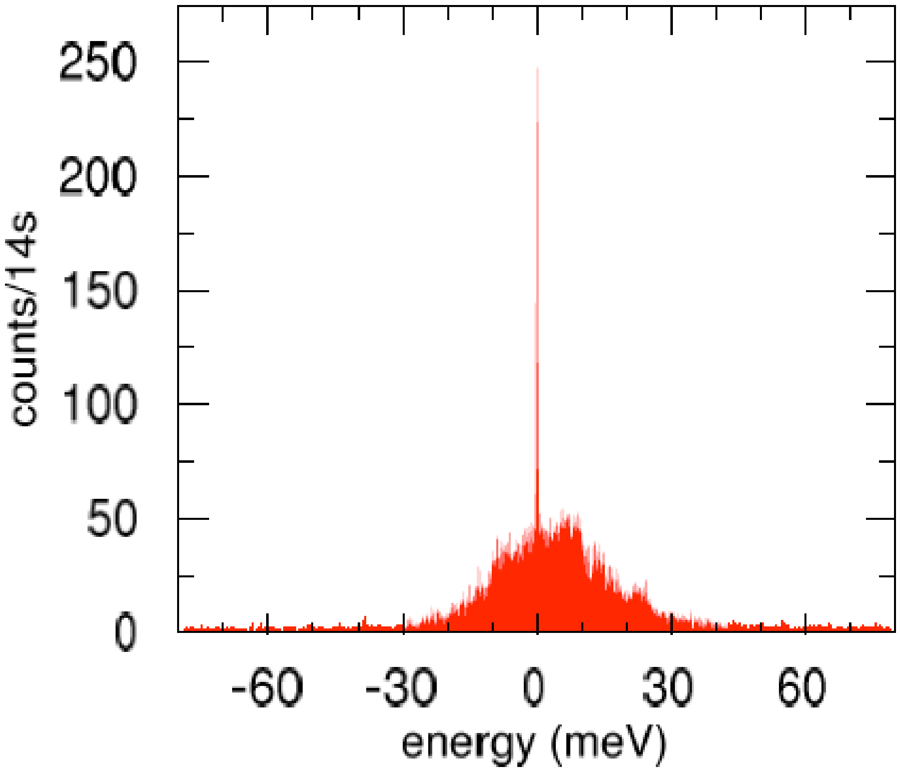

IXS Spectrometer at 3 ID-C

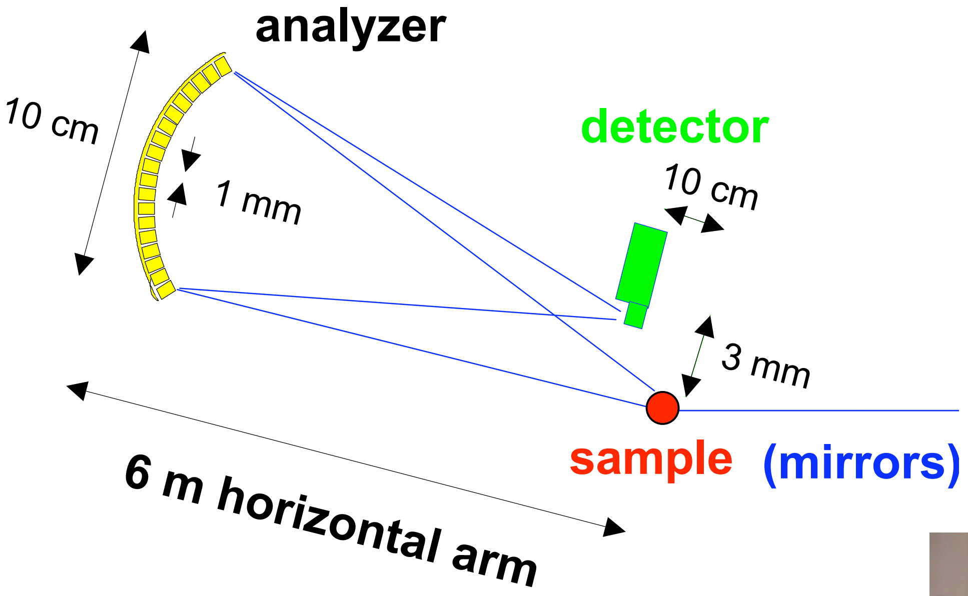

analyzer

10 cm

1 mm

detector

10 cm

3 mm

sample

(mirrors)

6 m horizontal arm

in-line, cryogenic monochromator

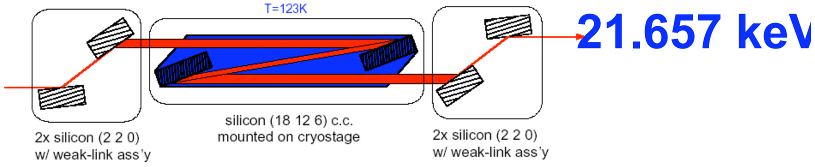

Energy resolution: 1.8 -2.0 meV
1-4 analyzers

H. Sinn
T. Toellner

Energy Scans in [0 0 ζ] direction

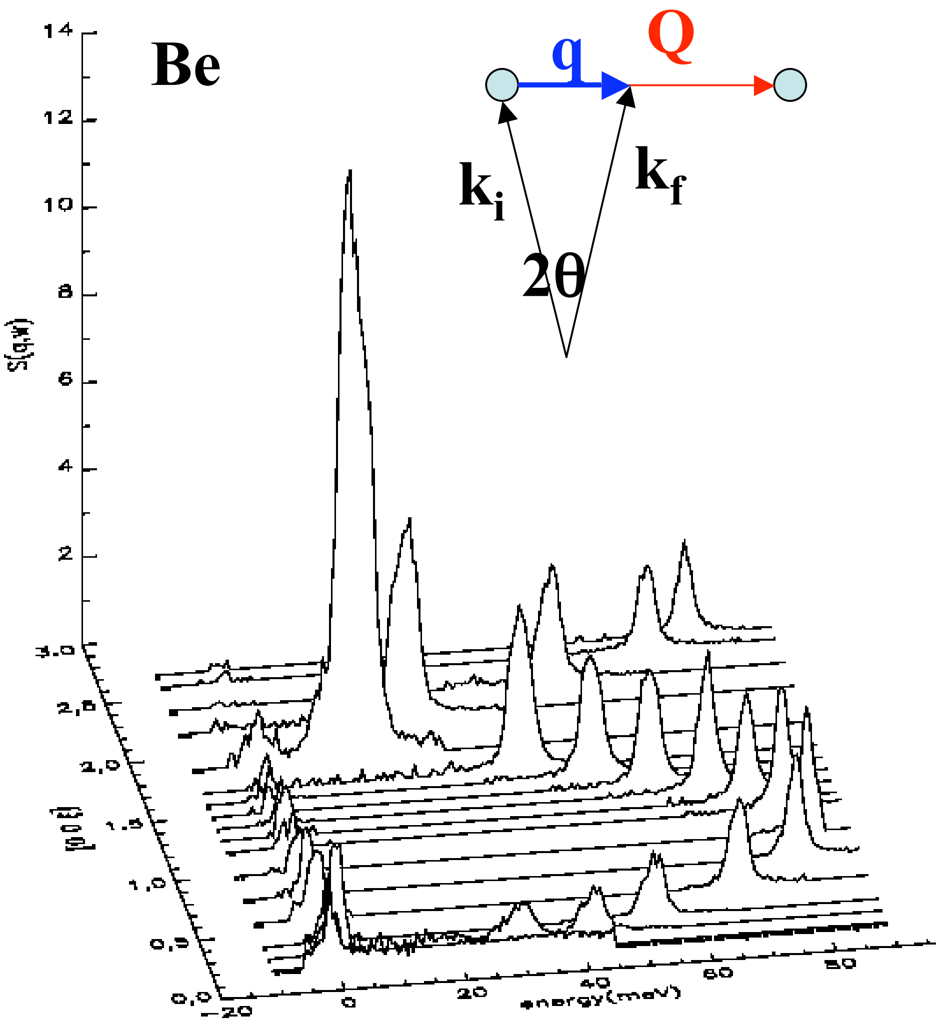

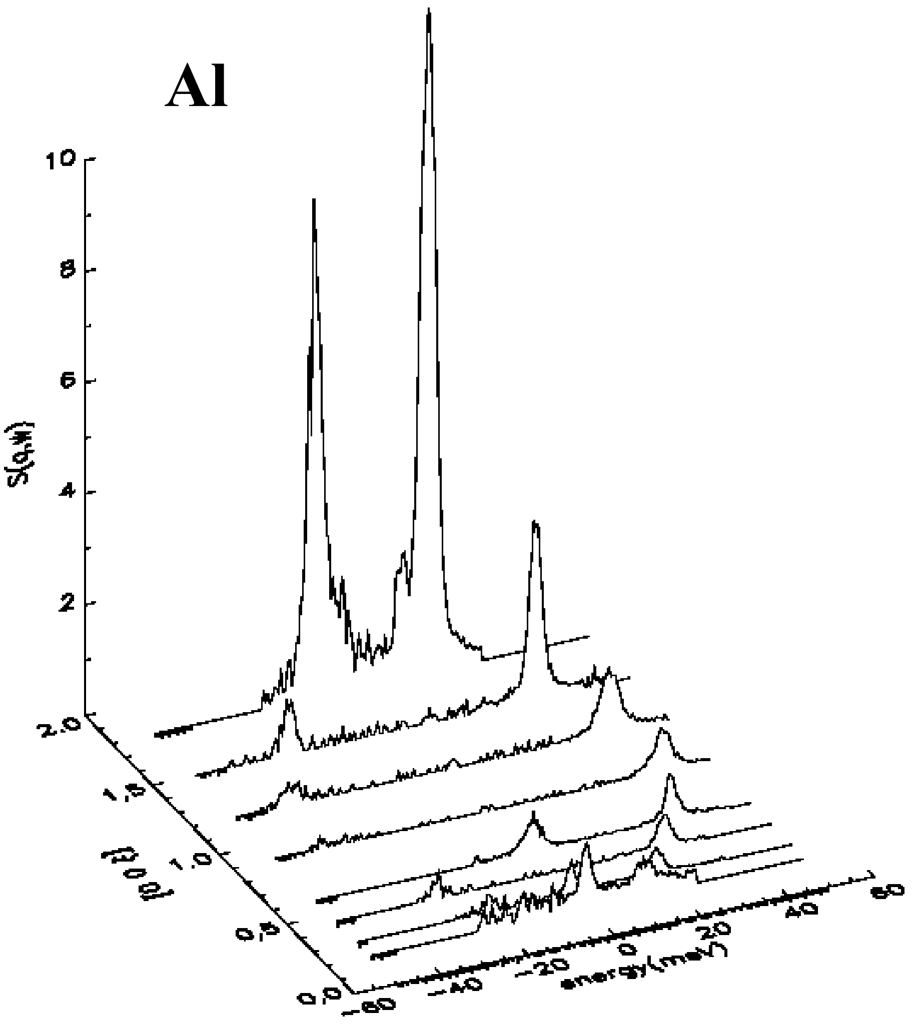

Dispersion relations for Li, Be and Al

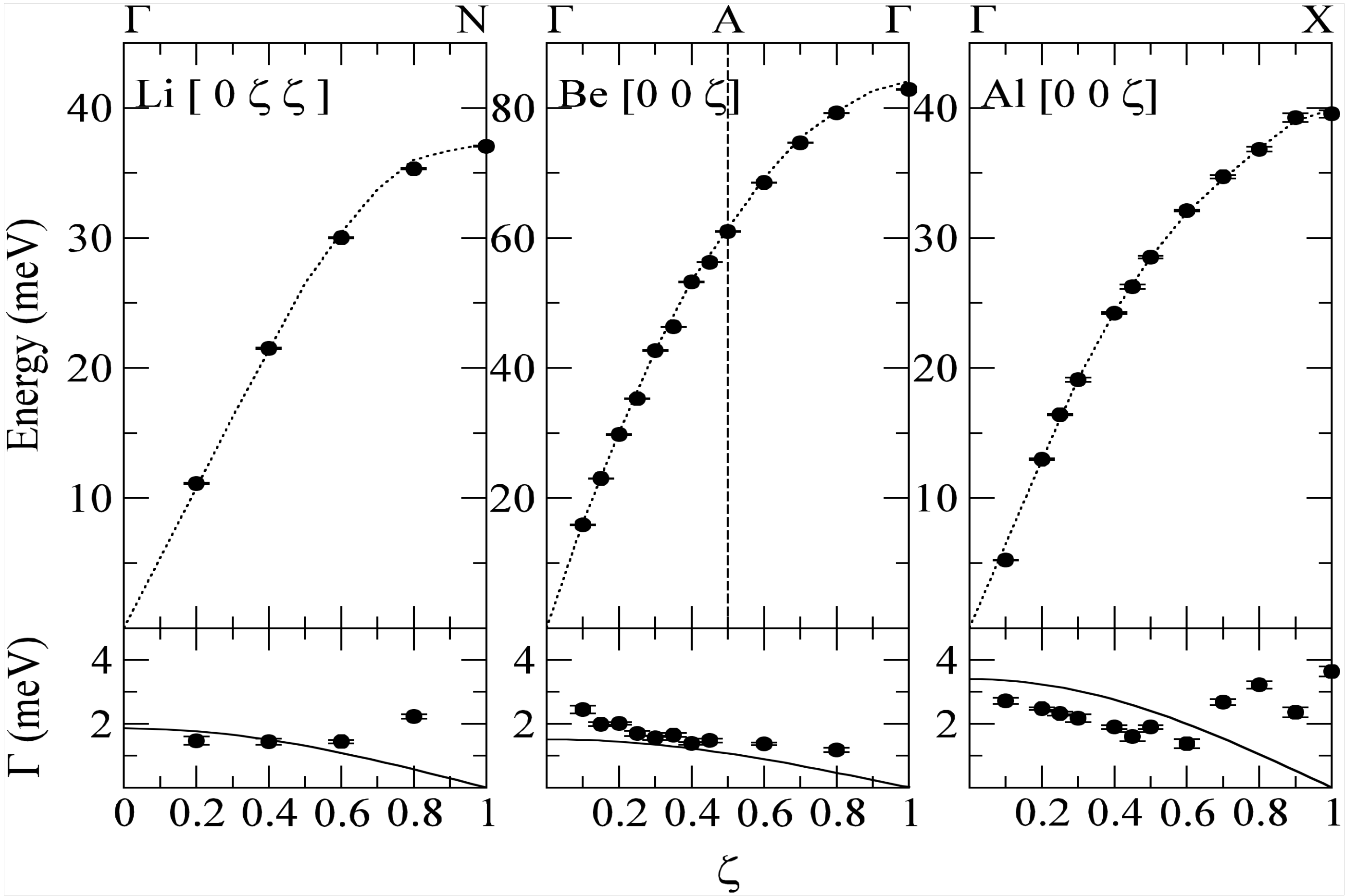

Why x-rays instead of neutrons or visible light ?

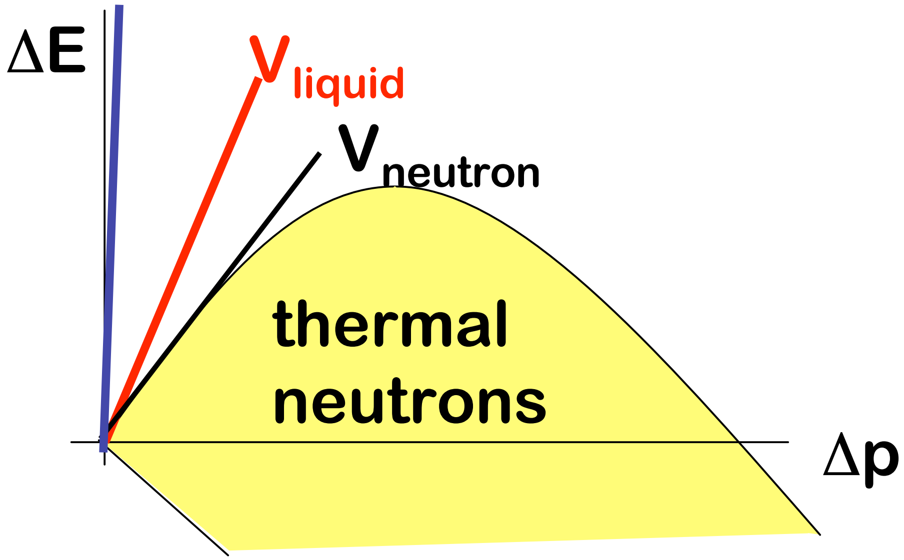

Limited momentum transfer capability of neutrons at low energies favor x-rays to study collective excitations with large dispersion, like sound modes.

When the sound velocity exceeds that of neutrons in the liquid, x-rays become unique. The low-momentum/high-energy transfer region is only accessible by x-rays.

High Melting Point Substances

Lindemann criterion: $mv_{sound}^{2} \propto T_{melt}$

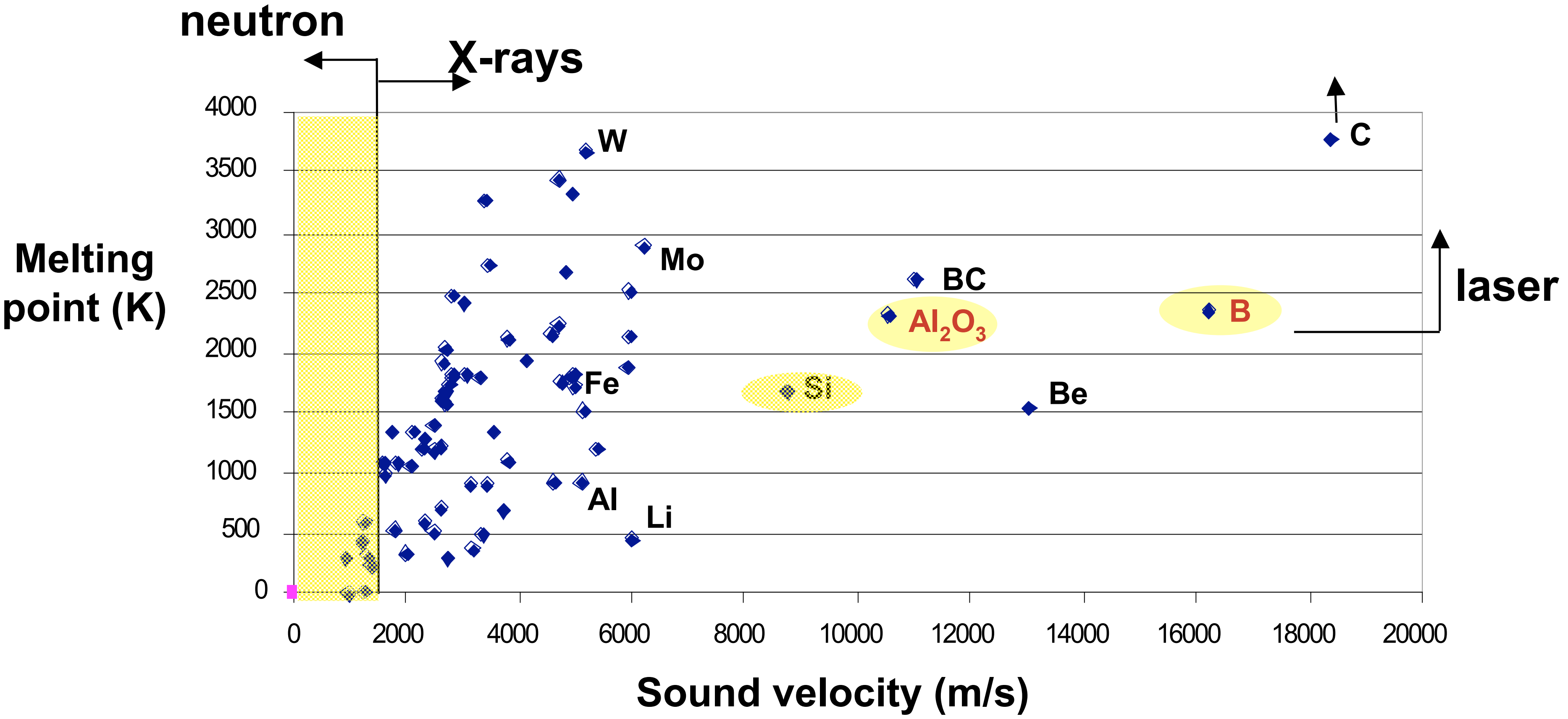

Hydrodynamics: 3 Peaks

Rayleigh-peak **FWHM ~ κ Q^2**

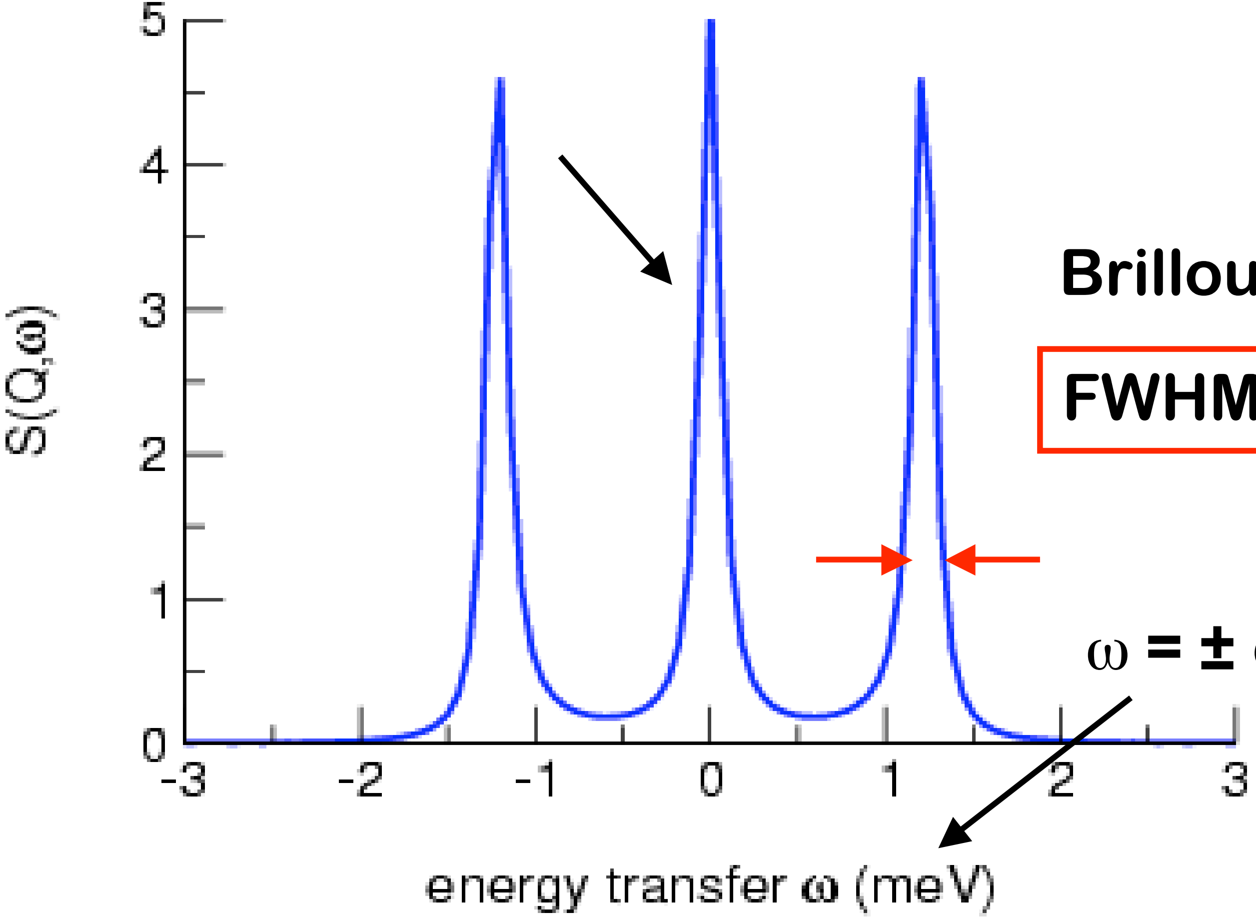

Brillouin doublet:

FWHM ~ η Q^2

$\omega = \pm c Q$

κ : thermal conductivity

η; kinematic viscosity

c : sound velocity

Containerless Research

Liquid Alumina Al_2O_3

Sapphire
Melting point: 2050°C

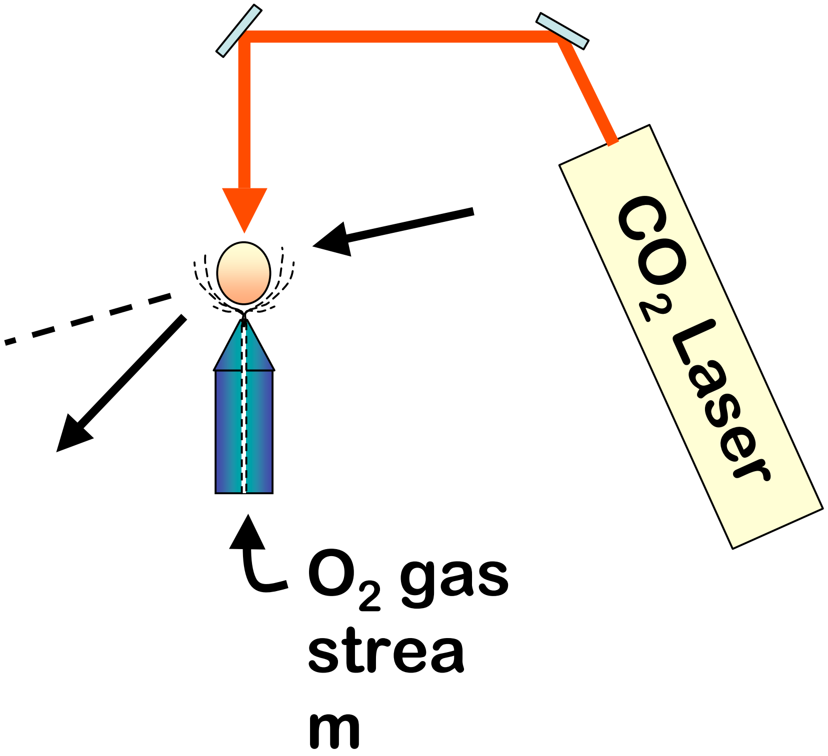

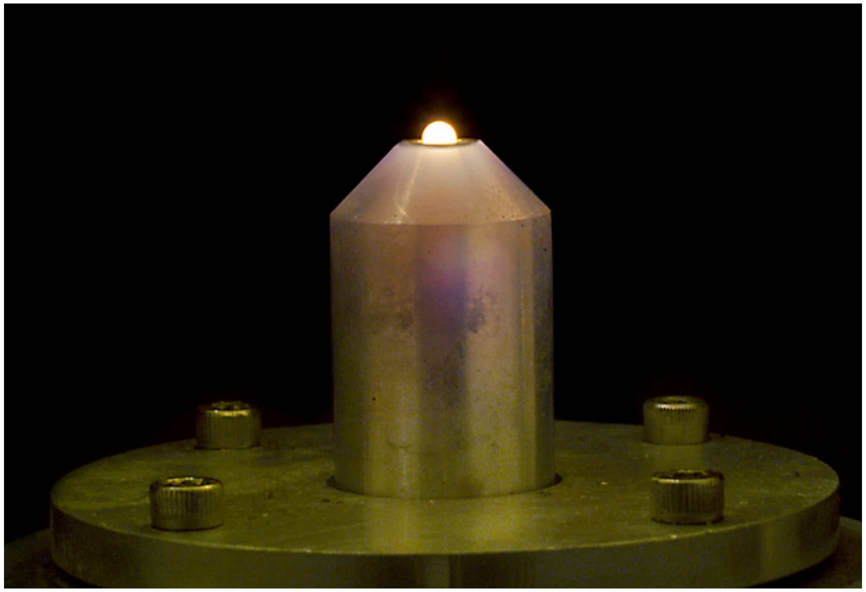

H. Sinn *et al.* Science, **299**: 2047, (2003)

Liquid Al_2O_3 @ 2050°C

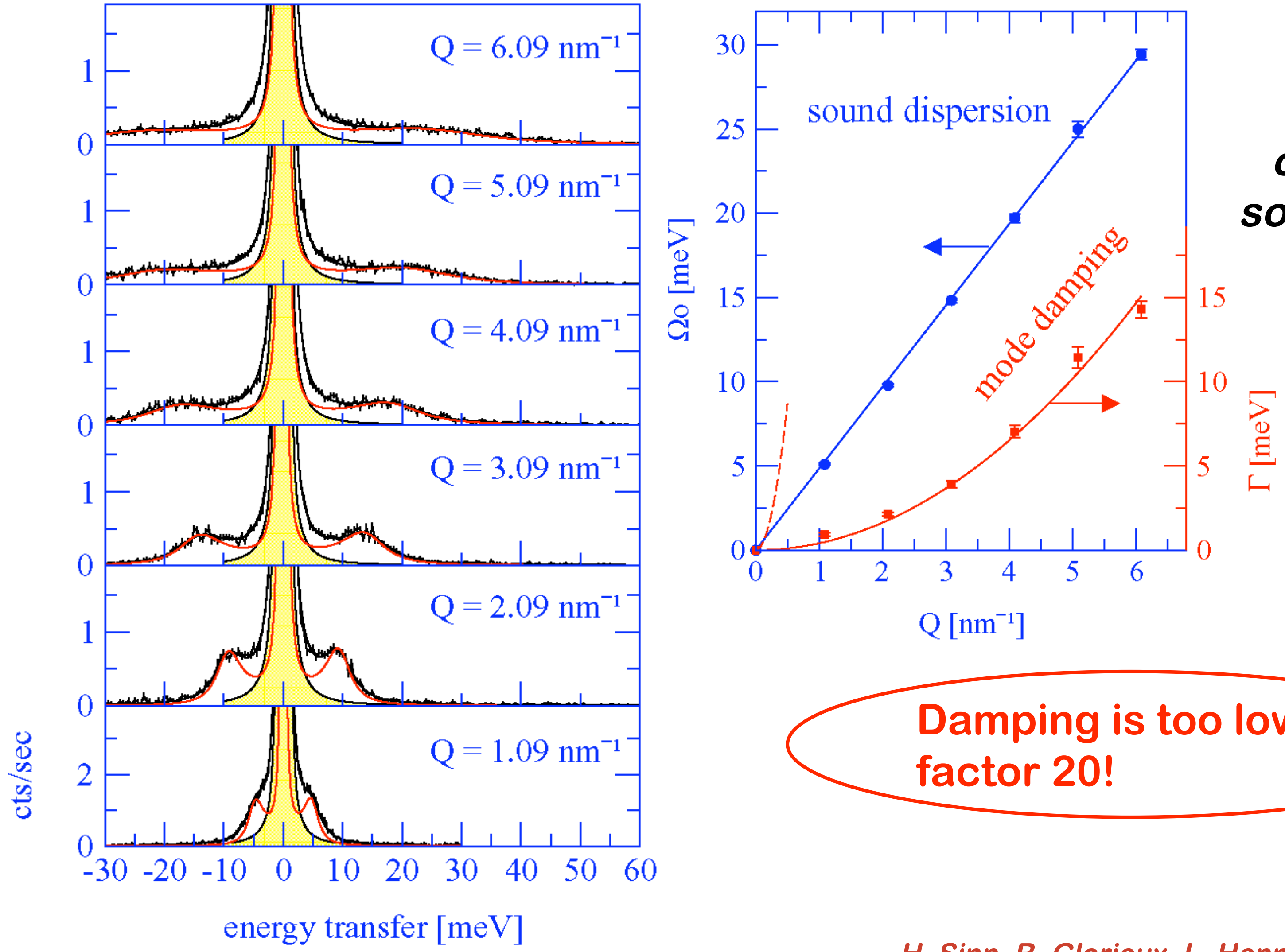

c = 7350 m/s
solid:10500 m/s

Damping is too low by factor 20!

H. Sinn, B. Glorieux, L. Hennet, A. Alatas, M. Hu, E. Alp, F. Bermejo, D. Price, M. Saboungi: Science, 299: 2047, 2003

Viscoelasticity, η(ω)

$$\eta(\omega) = \frac{\eta_0}{1 + i\omega\tau} + \eta_\infty$$

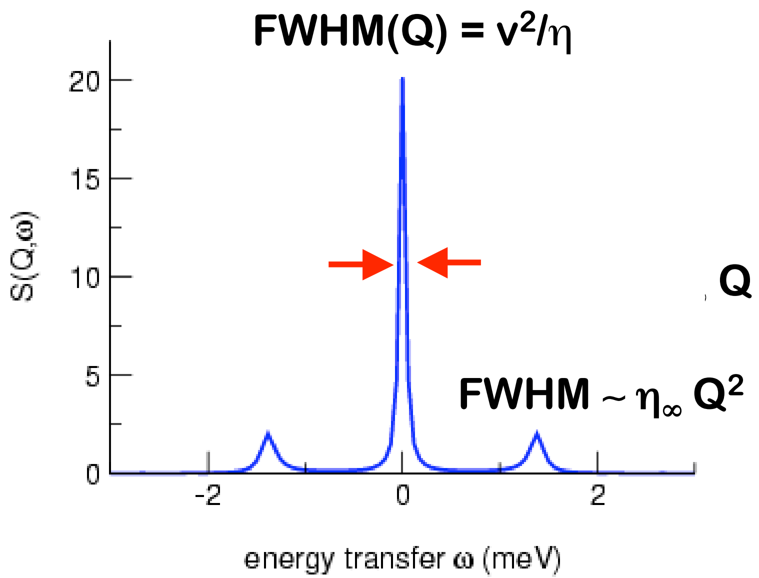

FWHM(Q) = v^2/η

Q

FWHM ~ $\eta_\infty Q^2$

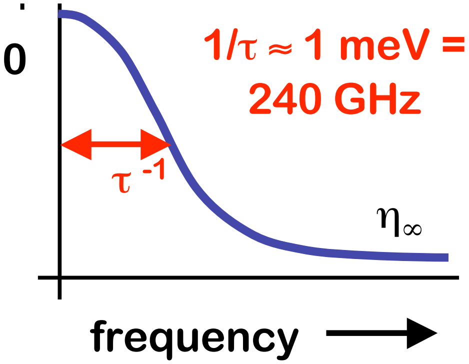

$1/\tau \approx 1$ meV = 240 GHz

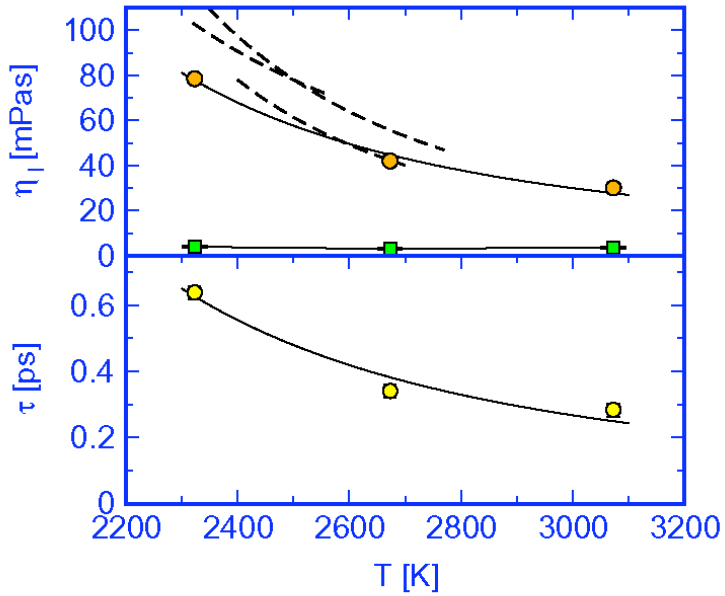

H. Sinn, B. Glorieux, L. Hennet, A. Alatas, M. Hu, E. Alp, F. Bermejo, D. Price, M. Saboungi: Science, 299: 2047, 2003

IXS Experiment: Melting of Al_2O_3

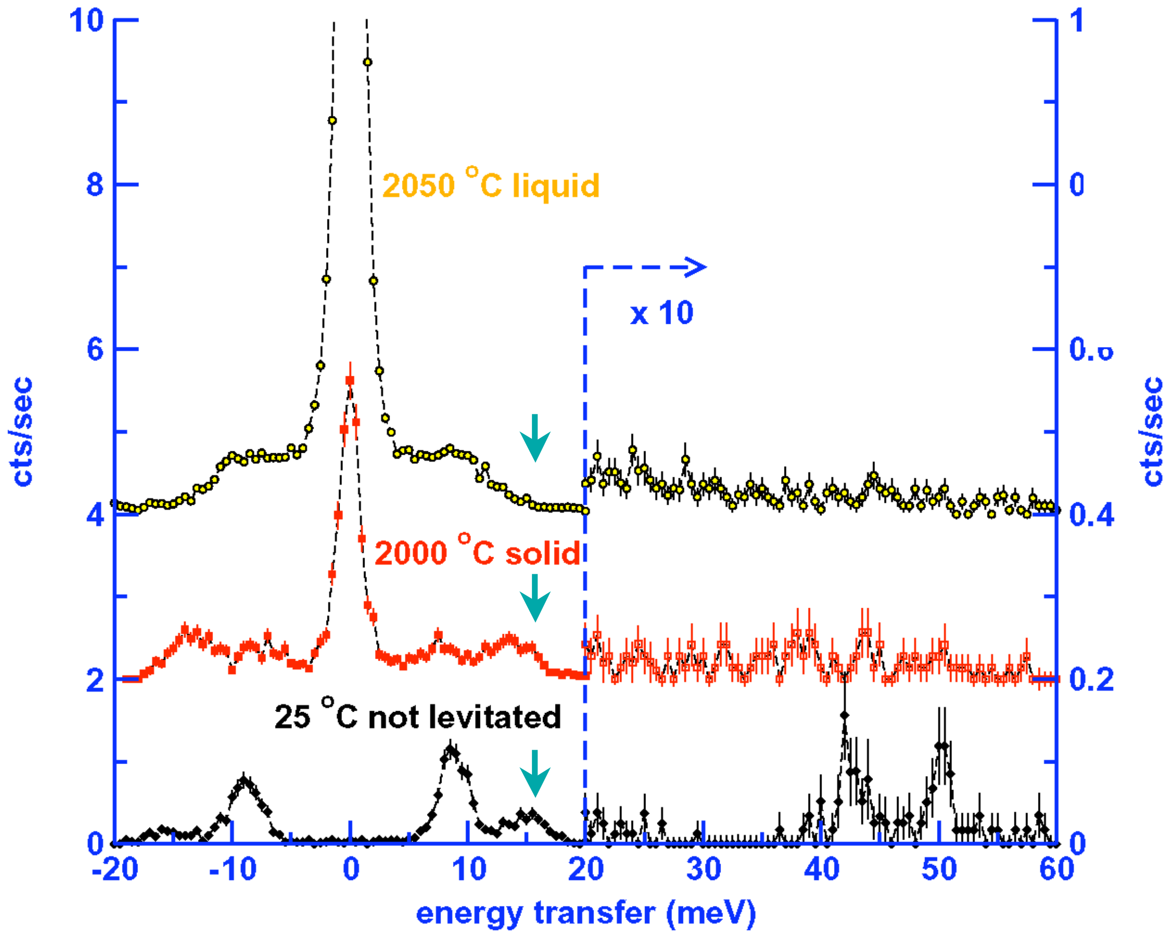

Sapphire
Melting point: 2050°C

6 hours/spectrum

Disappearance of transverse phonons and appearance of strong elastic peak signal melting. So it might be possible o determine solid/liquid phase boundary under high pressure where diffraction may not work such as amorphization may precede melting.

Silicon - IXS spectra

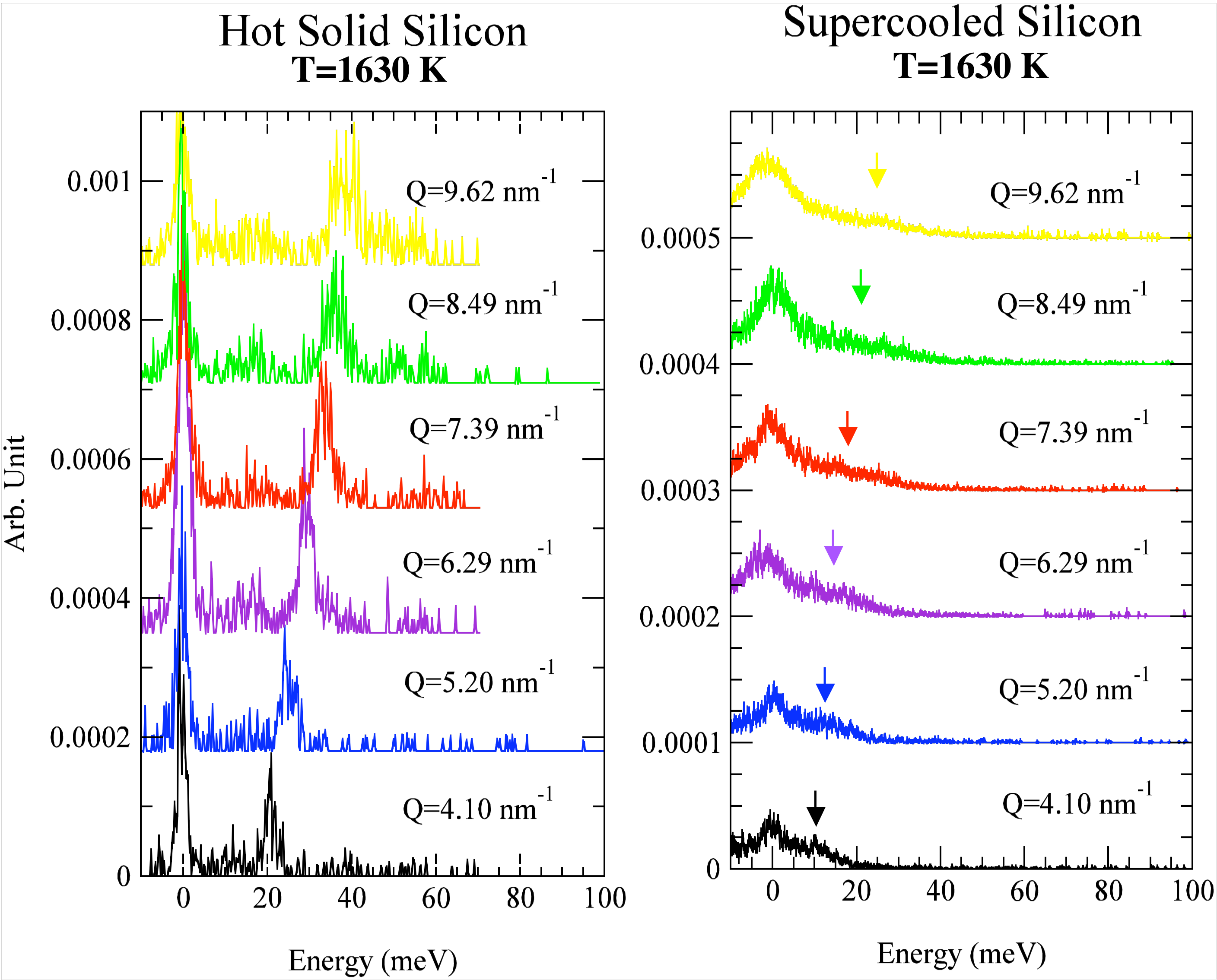

Silicon - Dispersion relation

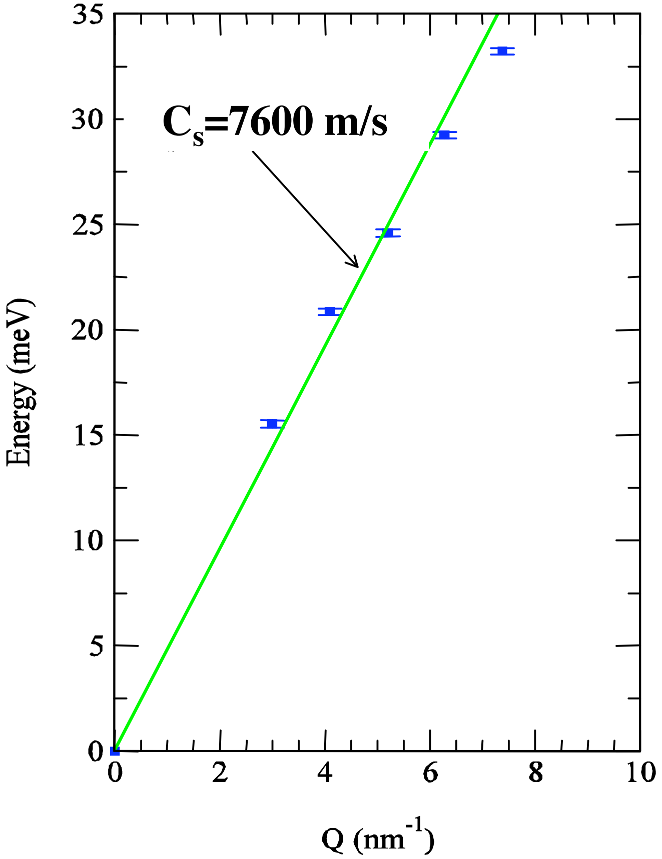
Hot Solid Si

T=1630 K

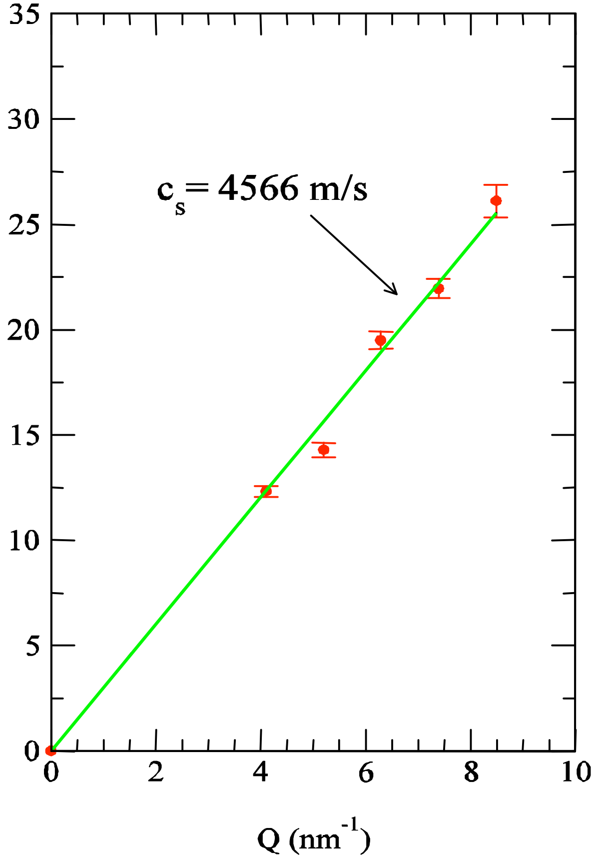
Supercooled Si

T=1630 K

Sound dispersion in boron

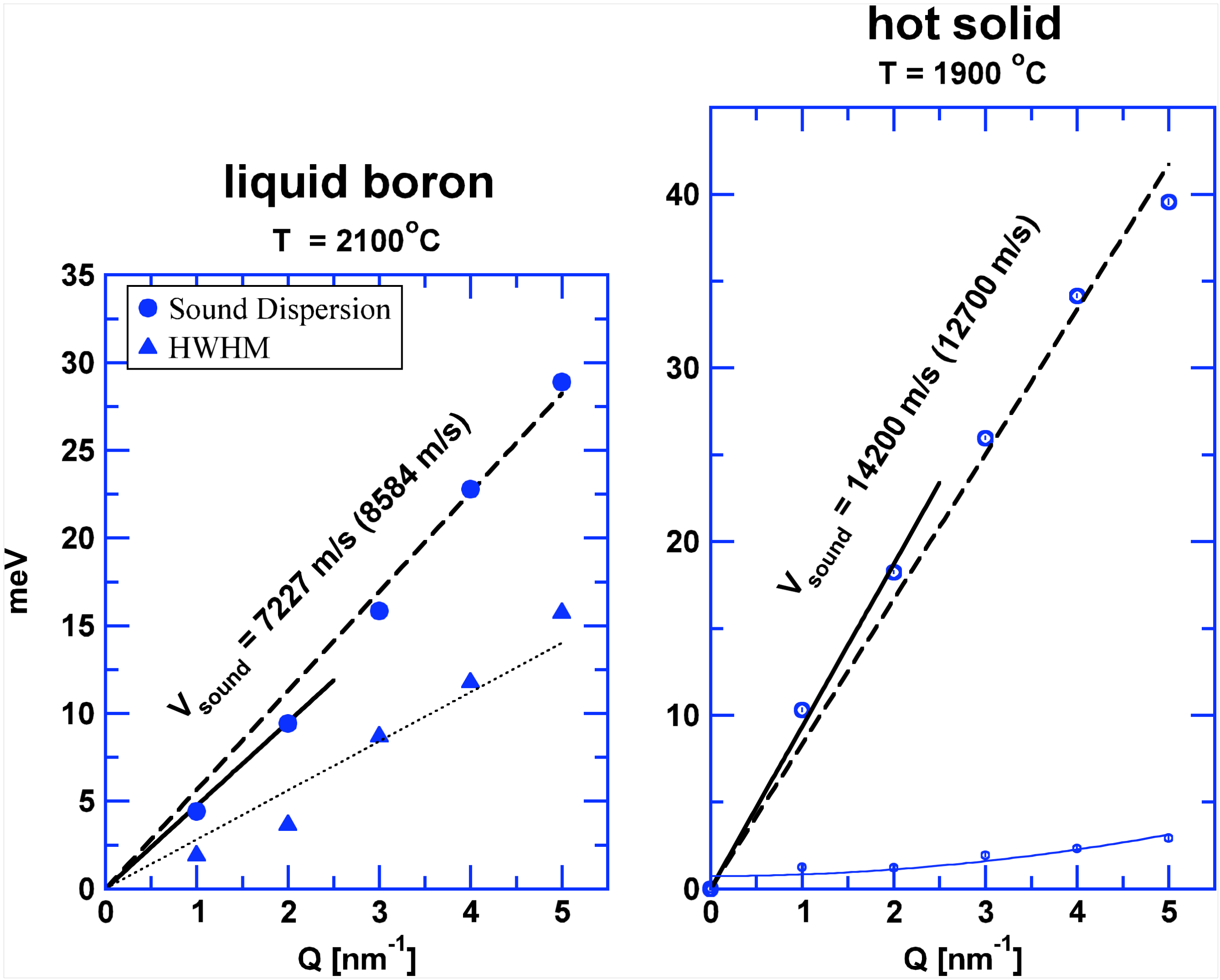

Literature:
14300 -
16000 m/s

49 % reduction in sound velocity upon melting

Si: 47%

Ge: 50 %

η_l (ω=0) = 14 mPas

$\eta_s \approx$ 1.5 mPas (est.)

τ(Q=0) = 0.2 ps

IXS Spectrometer at 3 ID-C

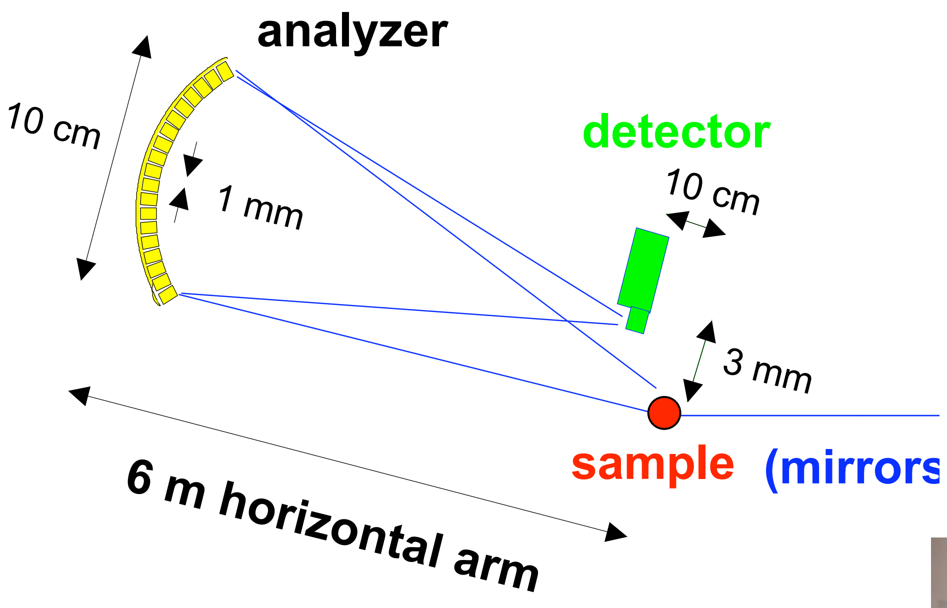

in-line, cryogenic monochromator

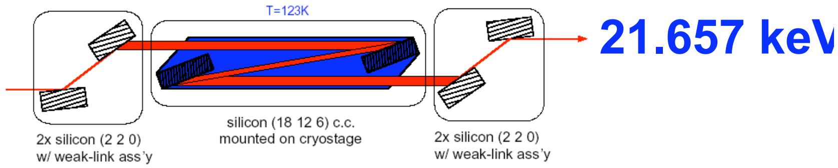

Energy resolution: 1.8 -2.0 meV
1-4 analyzers

H. Sinn
T. Toellner

cholesterol.jpg 509×359 pixels 06/11/2006 06:12 PM

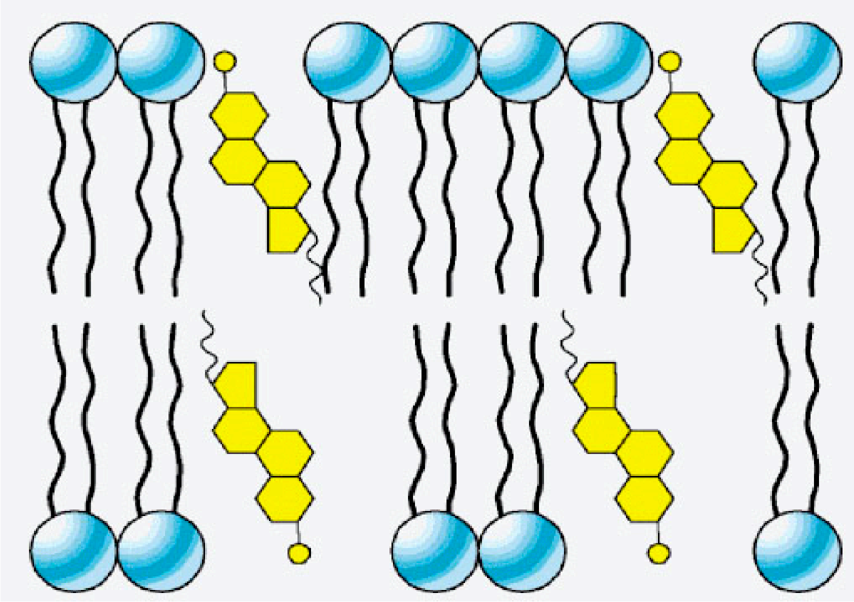

http://www.uic.edu/classes/bios/bios100/lectf03am/cholesterol.jpg

Dynamics of lipid bilayers:

Effect of cholestrol intercalation

intper.jpg 517×366 pixels 06/11/2006

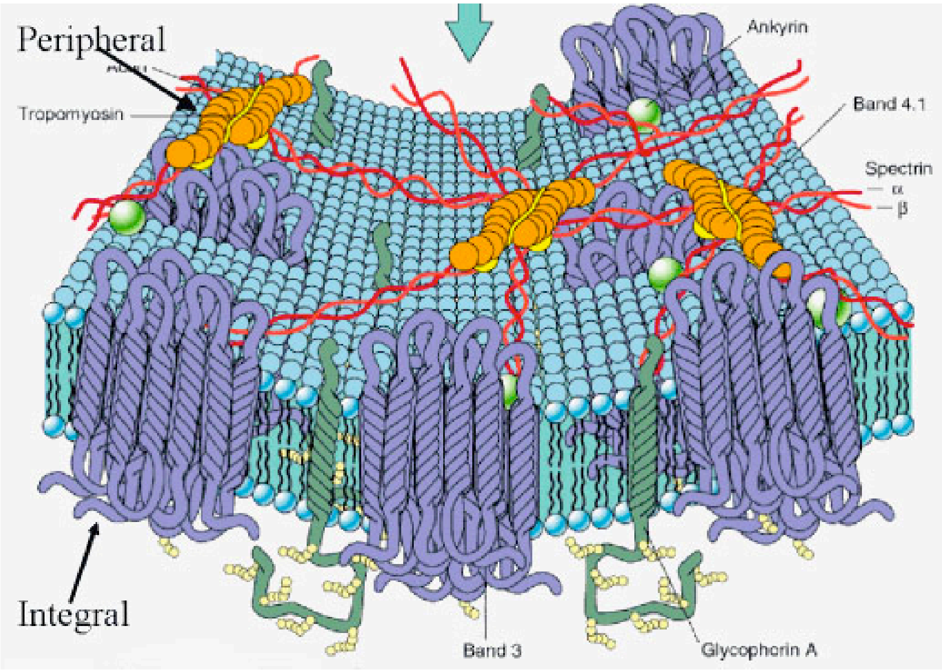

A typical data set: the need for higher resolution

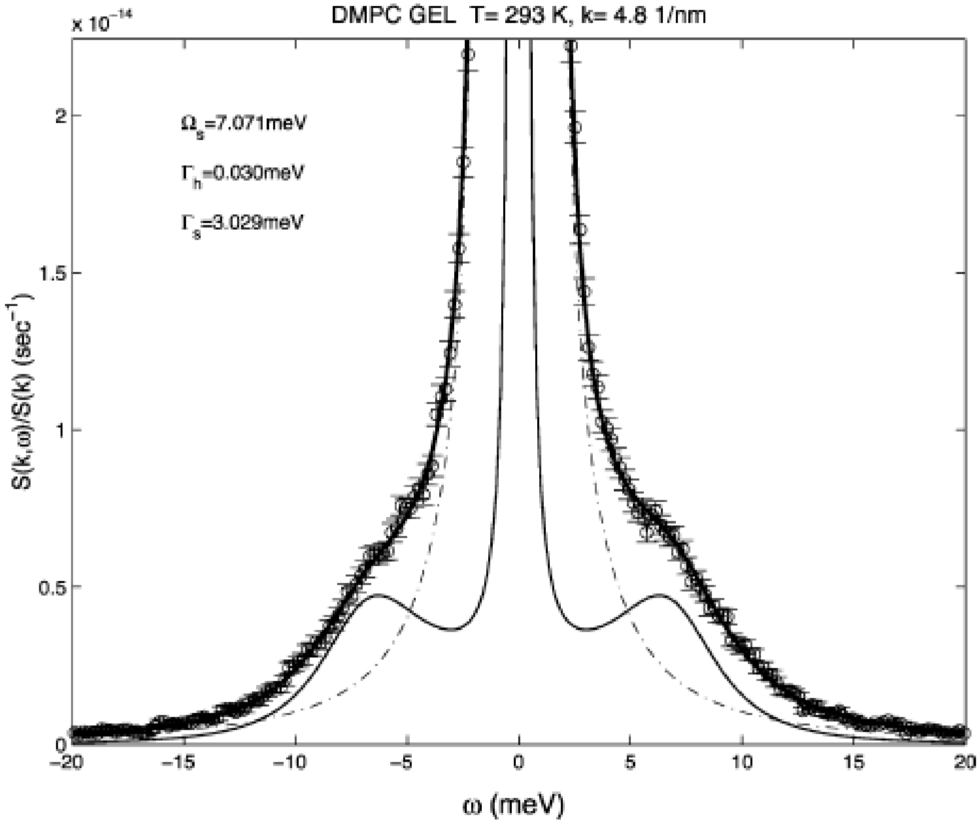

Generalized three effective eigenmode model is a direct extension of the macroscopic hydrodynamic theory including three k-dependent quasi-hydrodynamic modes, namely, the number density, the longitudinal current density, and the energy density.

An overall resolution of 2 meV results in a data set shown wbove. It will be possible to obtain 1 meV overall resolution, soon.

Data analysis

$$S(k,\omega) = \sum_{\alpha,\beta} f_\alpha(k) f_\beta(k) \omega_\alpha \omega_\beta S_{\alpha\beta}(k,\omega)$$

$$S(k,\omega)/S(k) = \frac{1}{\pi}\left\{ A_0 \frac{\Gamma_h}{\omega^2 + \Gamma_h^2} + A_s \frac{\Gamma_s + b(\omega + \Omega_s)}{(\omega + \Omega_s)^2 + \Gamma_s^2} + A_s \frac{\Gamma_s - b(\omega - \Omega_s)}{(\omega - \Omega_s)^2 + \Gamma_s^2} \right\}$$

$\Gamma_h = D_T k^2$: Thermal diffusivity: relaxation rate of non-propagating mode

$\Gamma_s = \alpha k^2$: Damping ~ viscosity

$\Omega_s = c_s k$: adiabatic sound velocity

In-plane phonon dispersion in liquid crystal and gel phases of DMPC

dimyristoylphosphatidylcholine (DMPC)

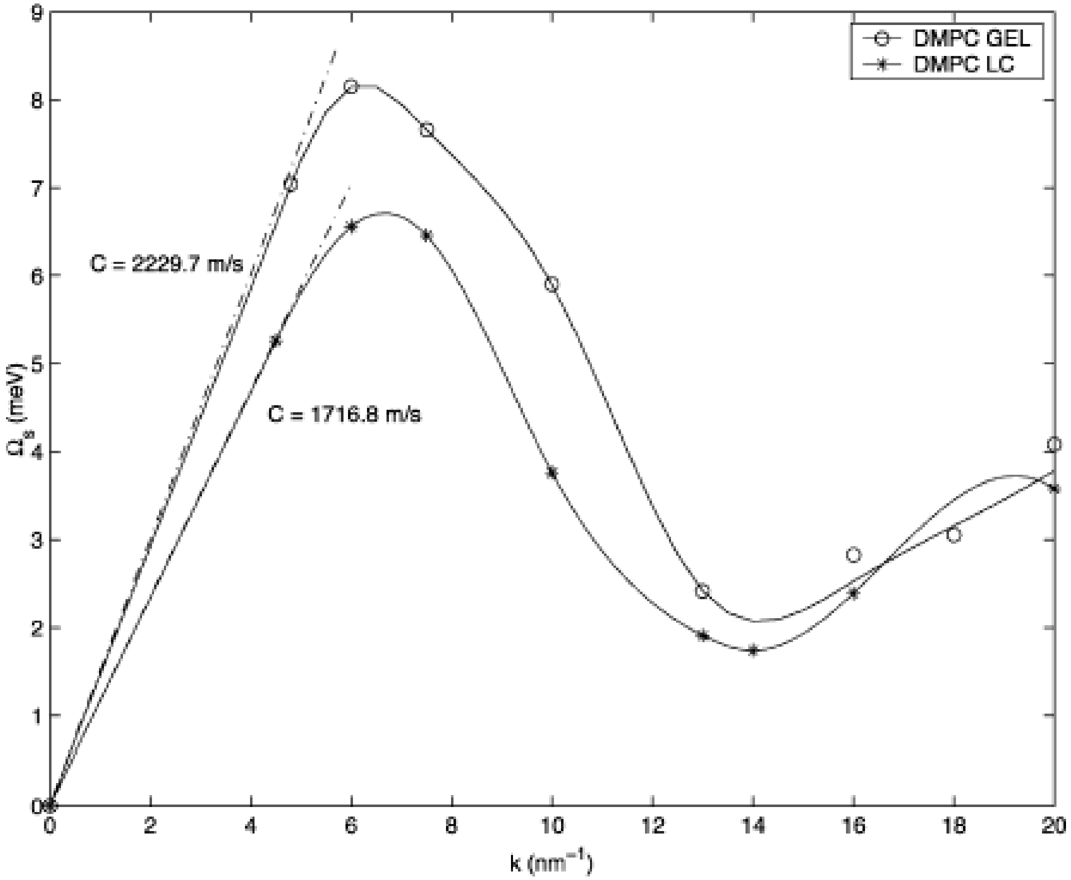

The in-plane phonon dispersion relations of DMPC bilayer for the gel and liquid crystal phases, showing the dependence on the order of the lipid molecules in the bilayer plane.

In the gel phase (T = 293 K), the hydrocarbon chains are ordered, so the sound speed is higher. In the liquid crystal phase (T = 308 K) because the chains are disordered, and the sound speed is lower.

In-plane phonon dispersion in DMPC and DLPC

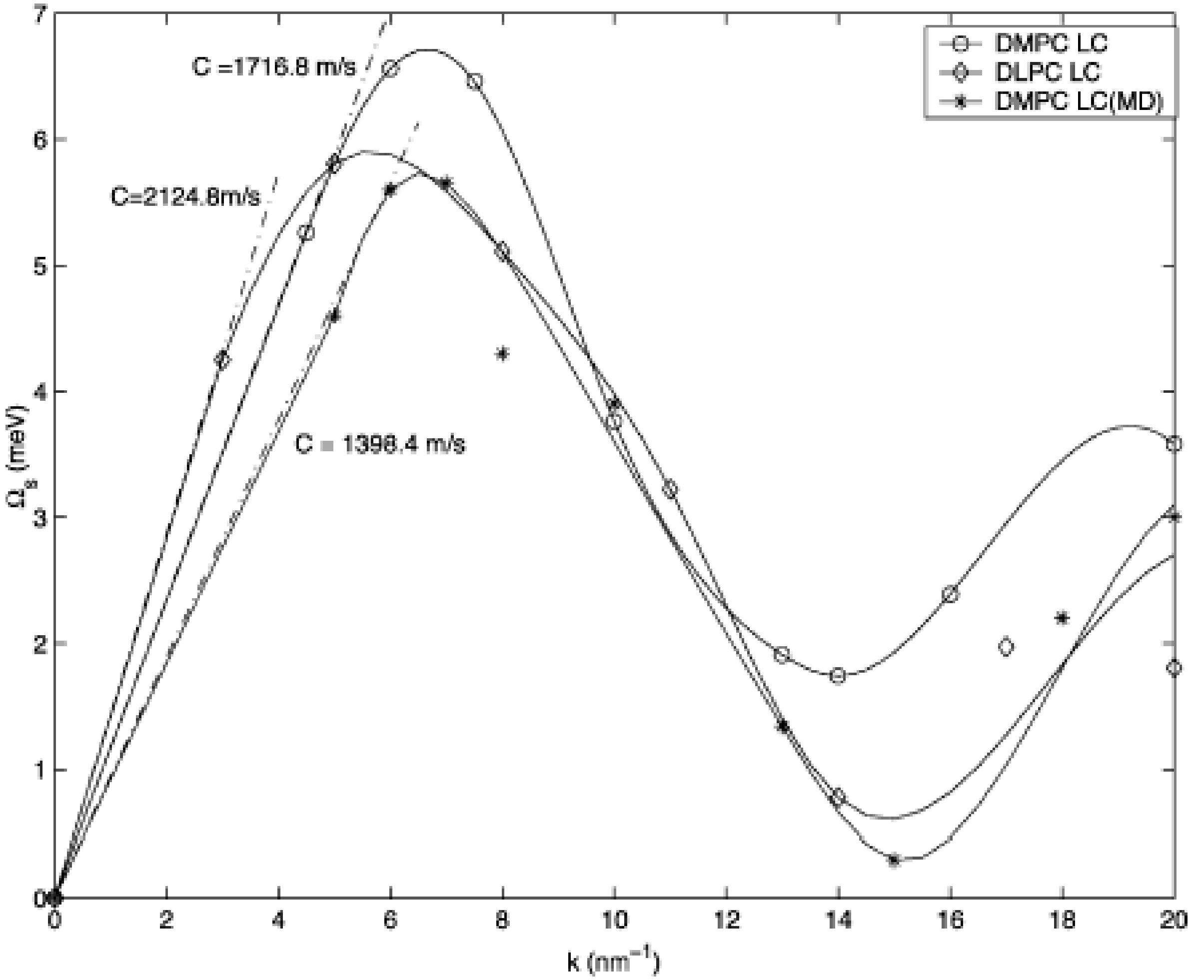

P-J. Chen et al, Biophysical Chemistry 105 (2003) 721–741

Effect of cholesterol addition to DMPC rigidity

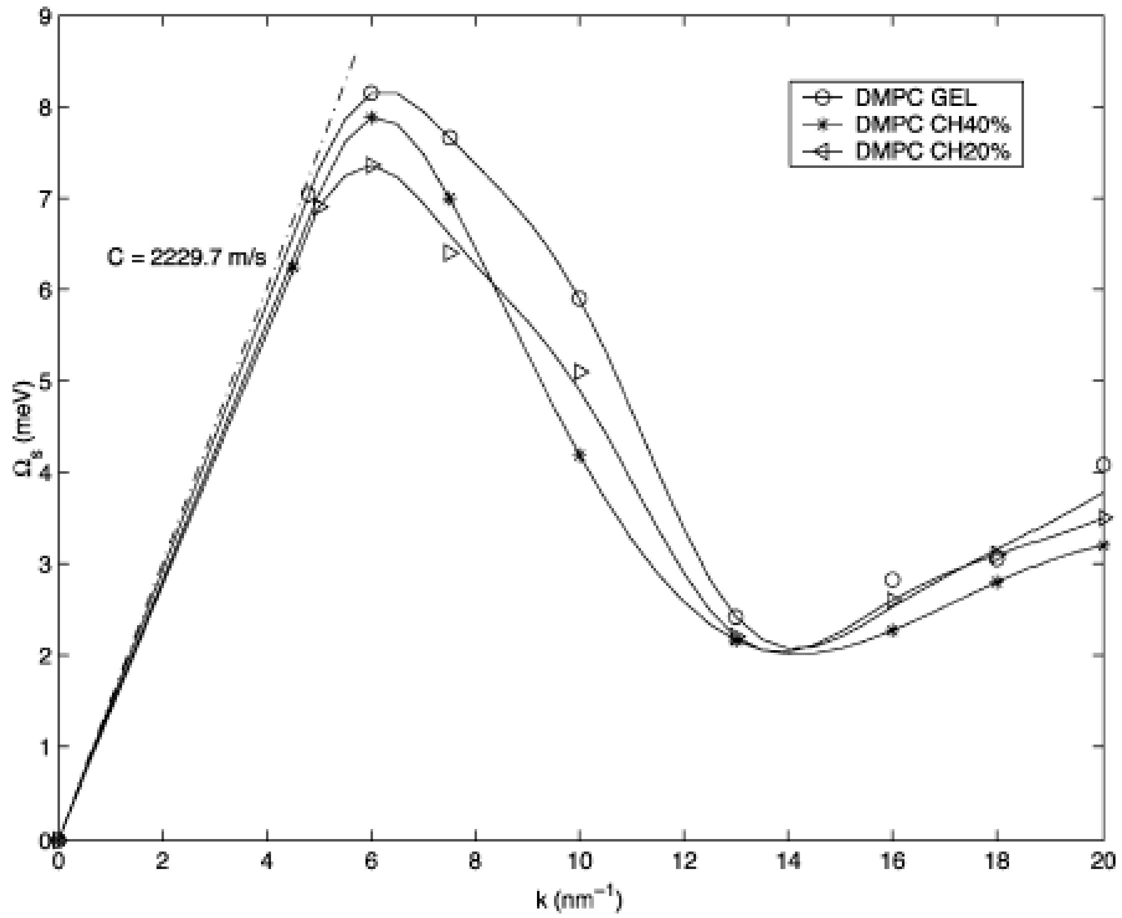

the effect of addition of cholesterol molecules is to make the bilayer more rigid, reducing the distinction between the liquid crystal and gel phases of the bilayer.

P-J. Chen et al, Biophysical Chemistry 105 (2003) 721–741

Thermal diffusivity of cholesterol DMPC

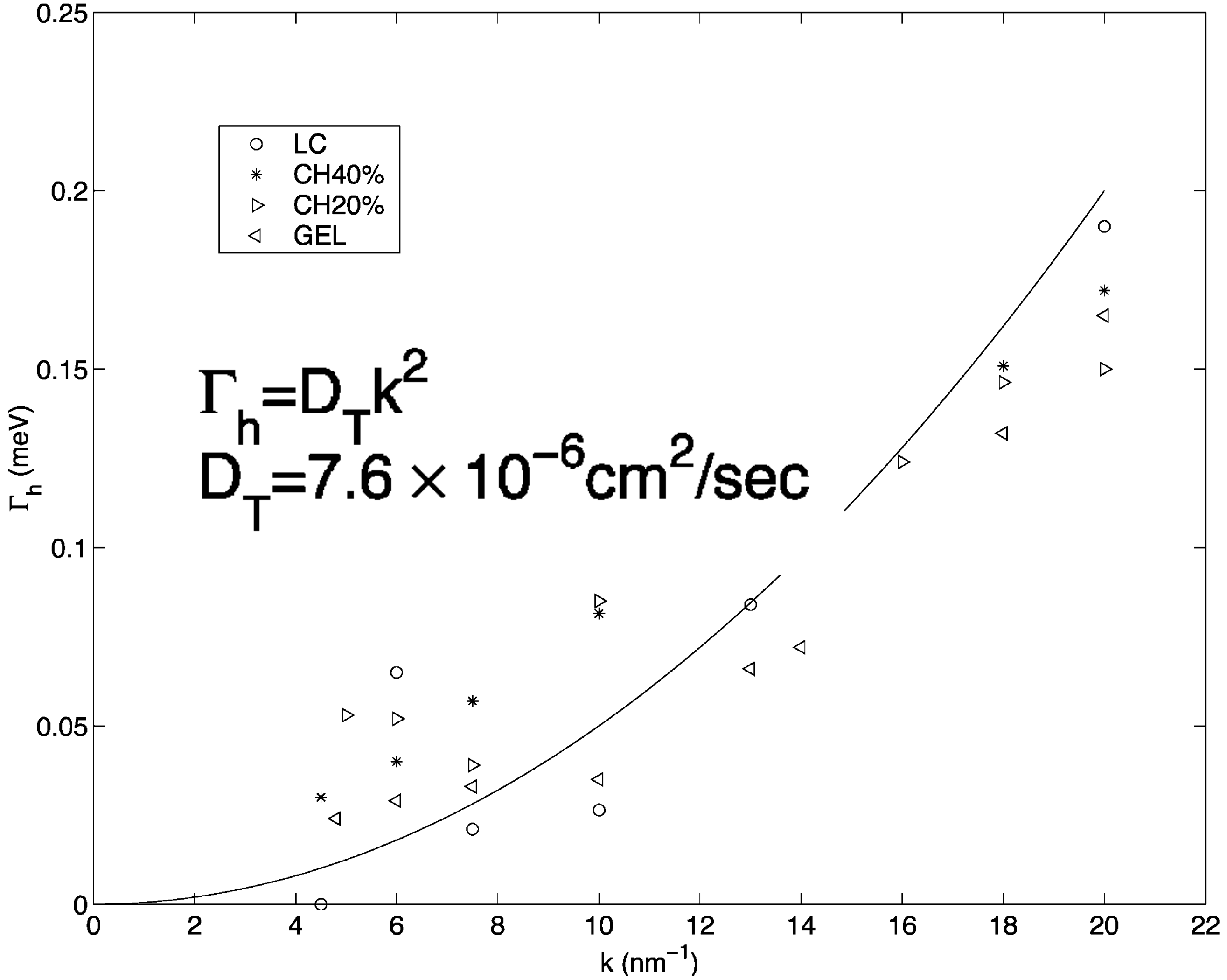

P-J. Chen et al, Biophysical Chemistry 105 (2003) 721–741

Oriented DNA

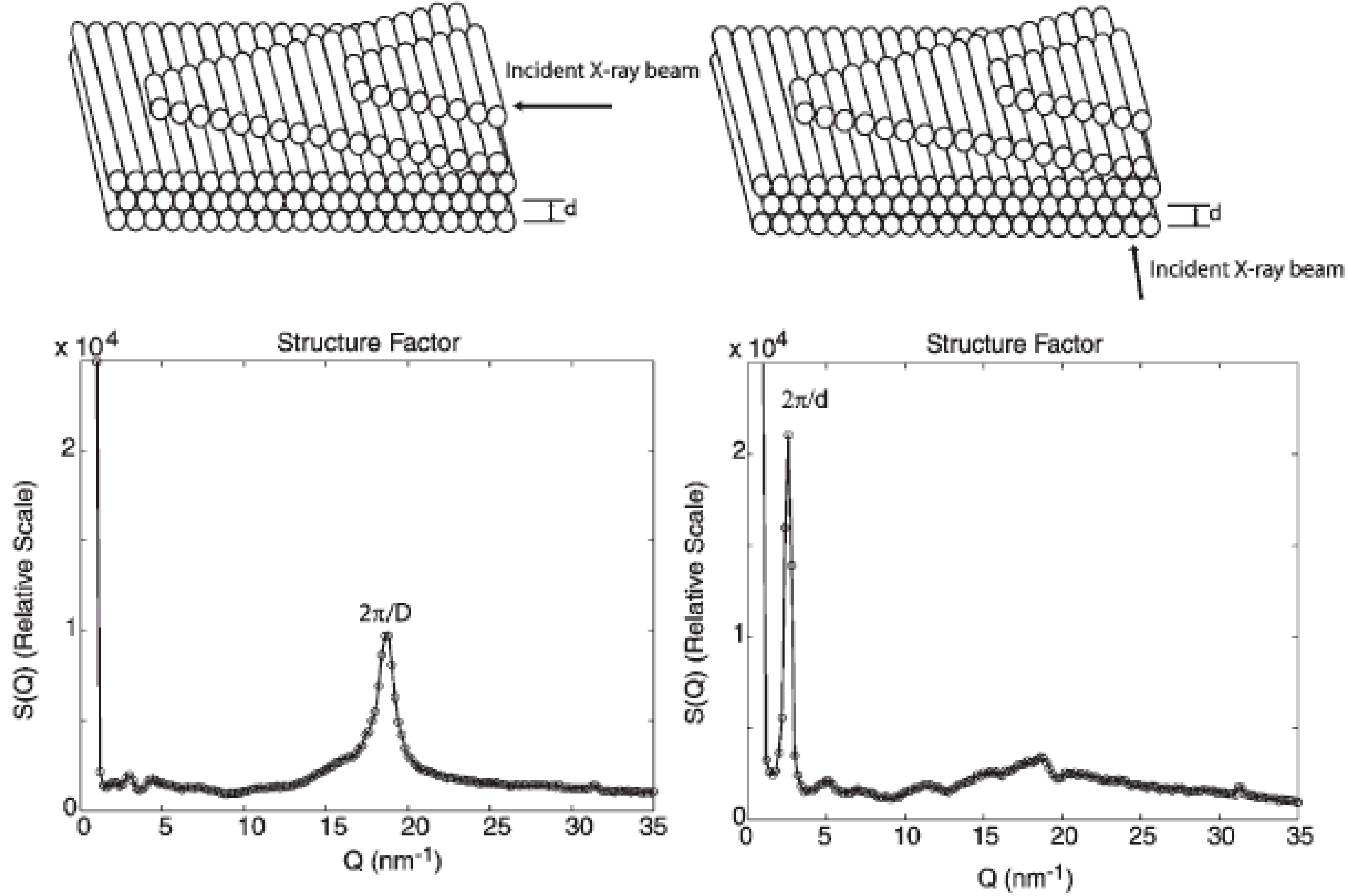

Y. Liu, et al, Phys.Chem.Chem.Phys., 6 (2004) 1499

Oriented DNA

Measurements of phonons propagating along the axis of DNA in a columnar-hexagonal liquid crystalline phase in the presence of different counterions .

The samples are rod-like supra-molecular systems made of shear aligned column hexagonal liquid crystalline phase of DNA dispersed in water.

Two systems are investigated: a 40 wt.% calfthymus Na–DNA in water and a 40 wt.% calf-thymus Na–DNA in 0.085 M MgCl2 . The molecular weight of this calf-thymus DNA is about 8.4 106 Da, which is about 13 000 base pairs.

For a rough estimation by considering all the molecular weight come from nucleotides, there are about 28 water molecules per nucleotide in our samples. This means most water molecules in our samples are tightly bound to DNA molecules.

40 % Calf-thymus Na-DNA in water

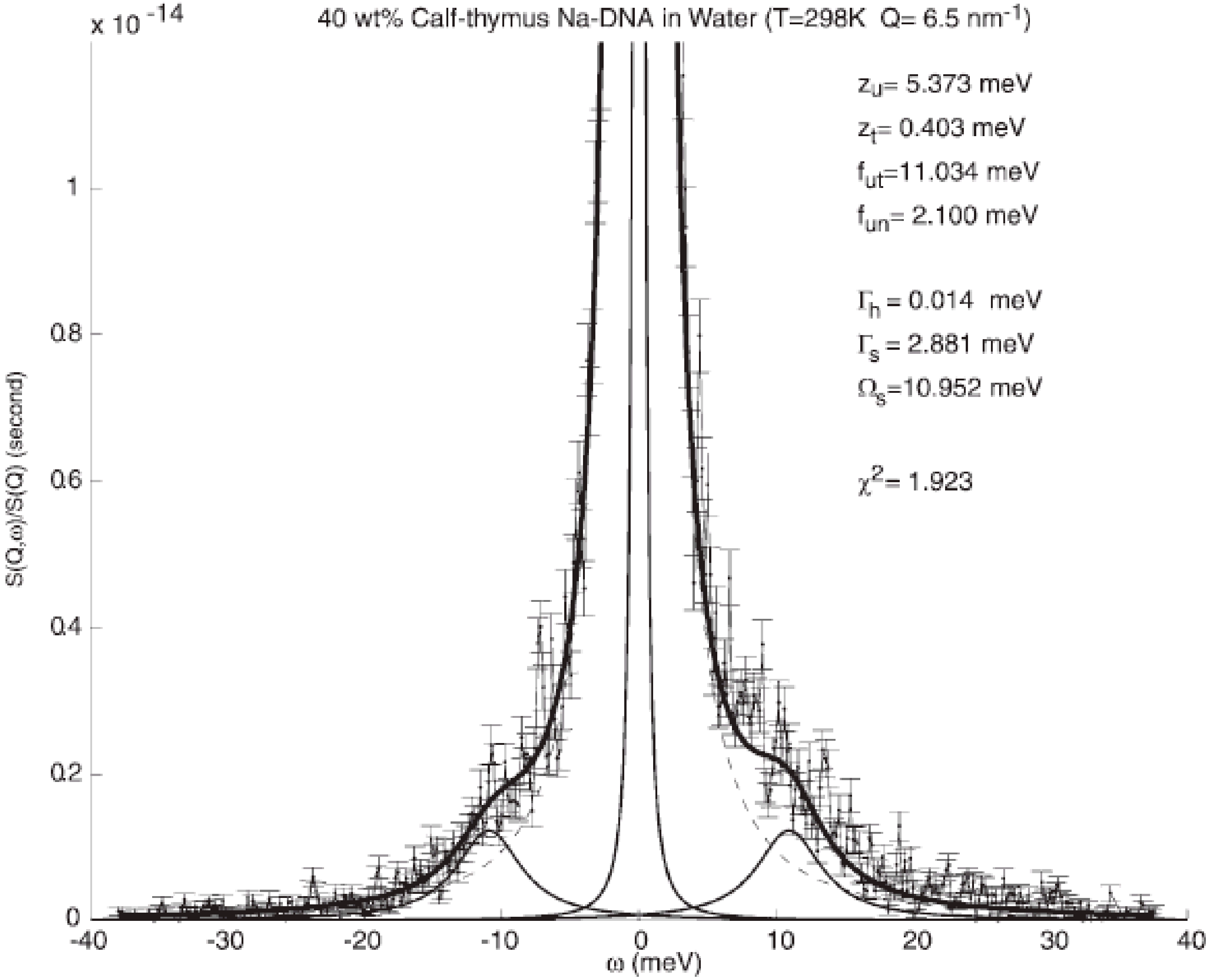

Y. Liu, et al, Phys.Chem.Chem.Phys., 6 (2004) 1499

IXS in DNA in water : what is measured ?

A hydrated DNA molecule consists of H, C, N, O, and P, among which the phosphorus atom has the largest atomic number (Z = 15). Since the X-ray scattering cross-section of an atom is proportional to Z^2, the overall spectral intensity by the phosphorus–phosphorus partial structure factor.

Thus the dynamic structure factor measured with X-ray scattering is largely reflecting vibrational motions of negatively charged phosphate groups attached to the helical back bone of a DNA molecule.

Y. Liu, et al, Phys.Chem.Chem.Phys., 6 (2004) 1499

IXS-CDT Beamline: 30-ID

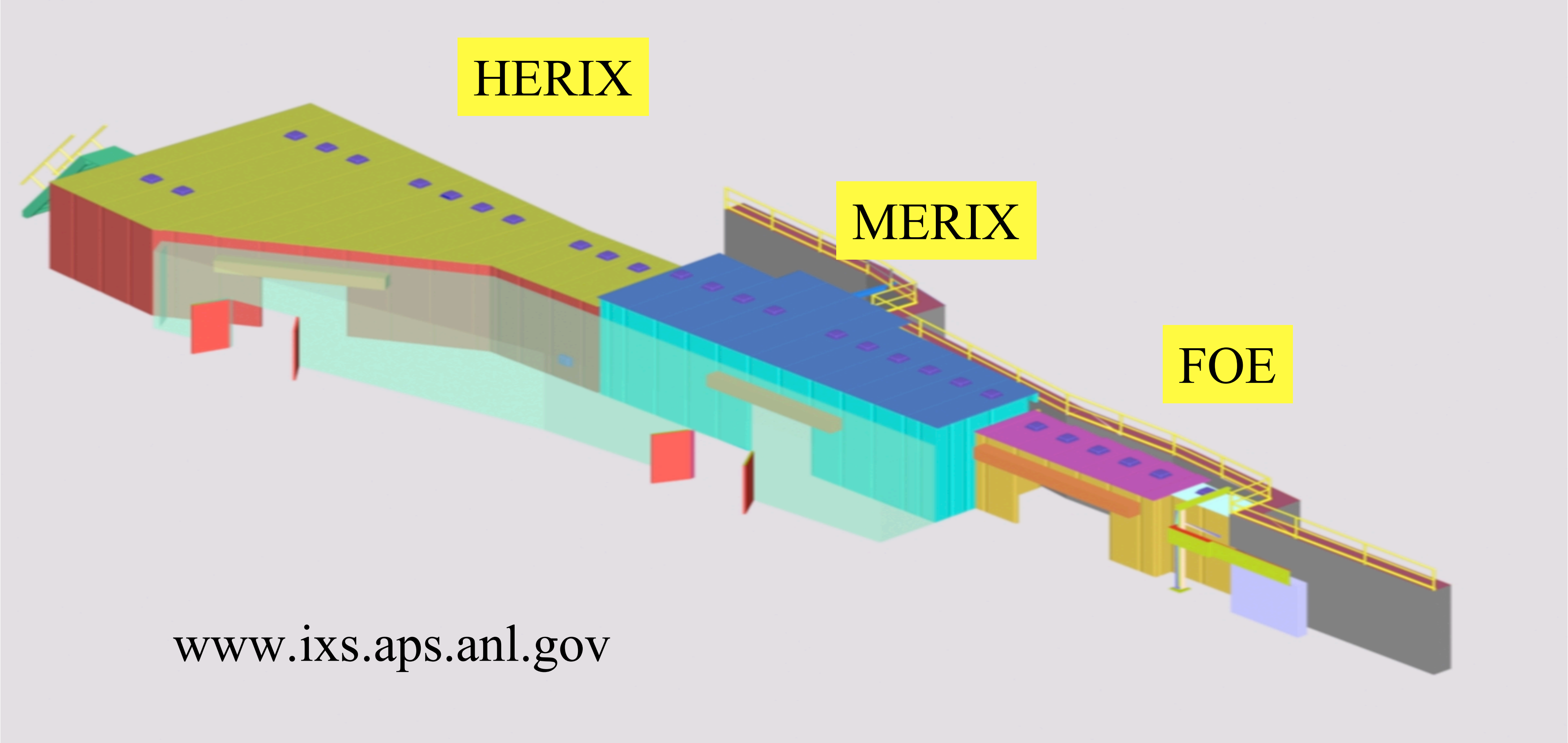

www.ixs.aps.anl.gov

HERIX

ACCEL + SESO
Bi-morph K-B mirror

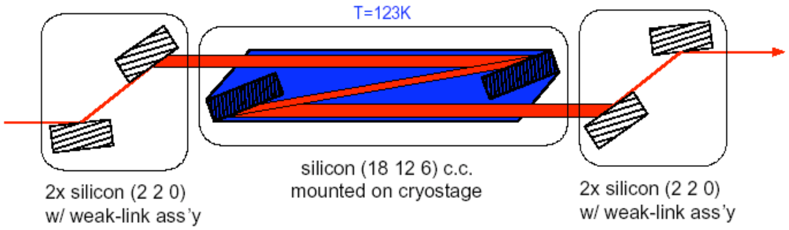

Cryogenically cooled, high-throughput, "in-line"monochromator (Toellner)

MERIX

Ercan's dream machine:
SHERI : Super High Energy Resolution Instrument

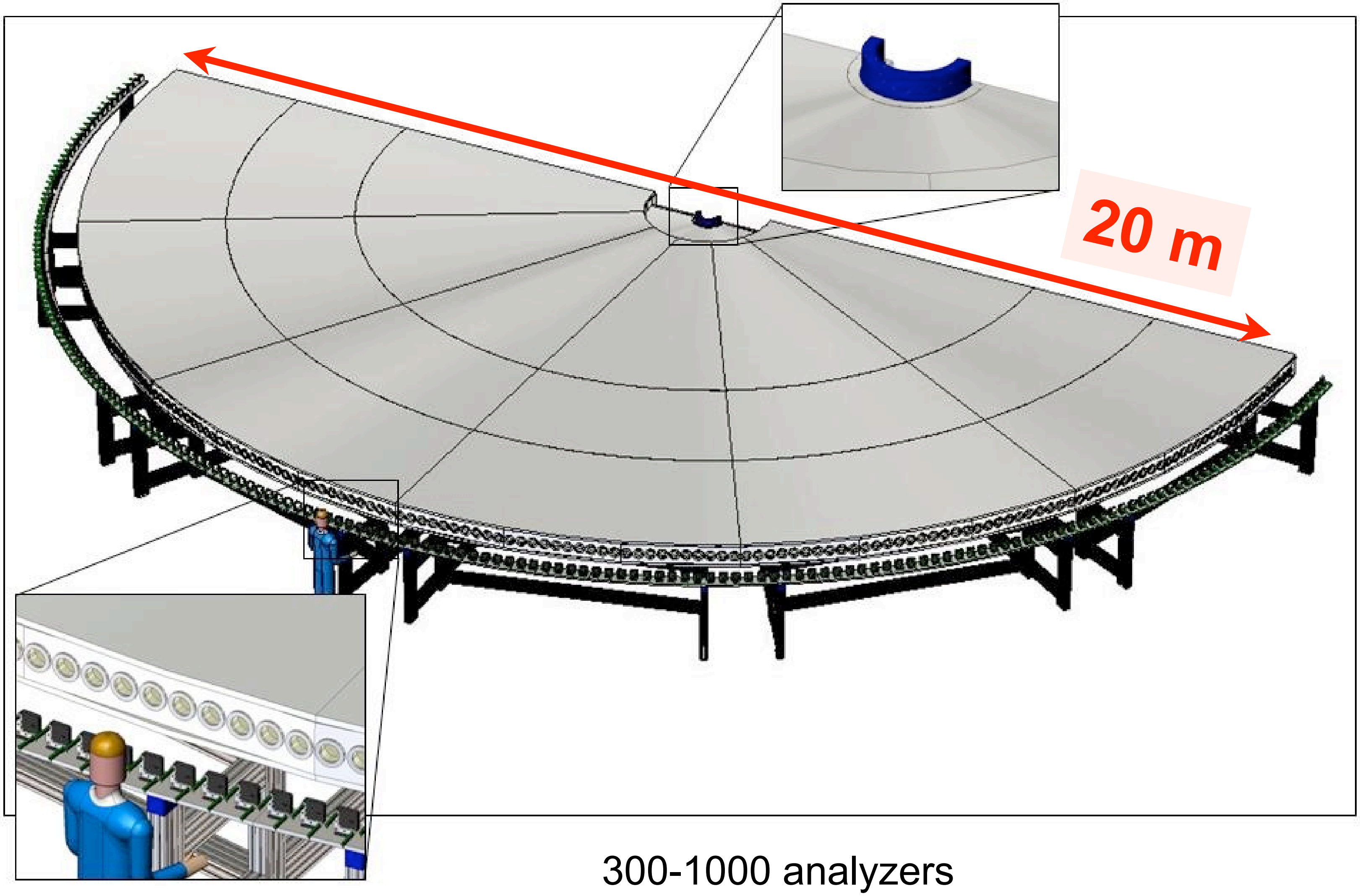

300-1000 analyzers
1% of solid angle, versus 0.01 % today

Ercan's dream machine:
SHERI : Super High Energy Resolution Instrument
0.6 meV @ 25.7 keV

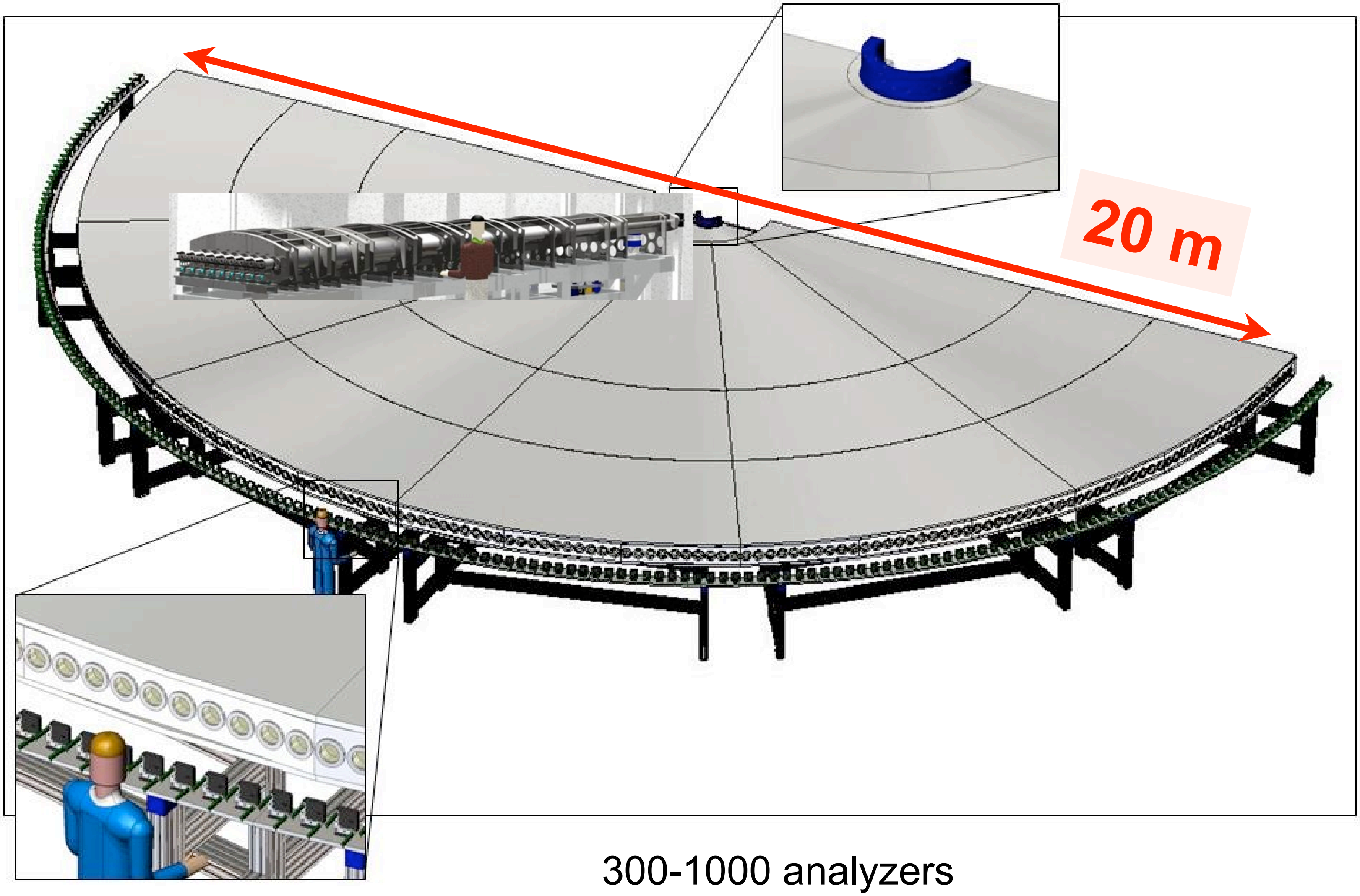

300-1000 analyzers
1% of solid angle, versus 0.01 % today

Choice of energy

Si Reflection at 90 °	Energy (keV)	Resolution (meV)	Reflectivity (%)
18 6 0	21.657	1.23	78
11 11 11	21.747	0.83	70
13 11 9	21.985	0.81	69
15 11 7	22.685	0.70	68
20 4 0	23.280	0.87	76
12 12 12	23.724	0.80	75
14 14 8	24.374	0.69	74
22 2 0	25.215	0.576	71
13 13 13	25.701	0.37	60

Thermodynamics @
High Pressure & high temperatures

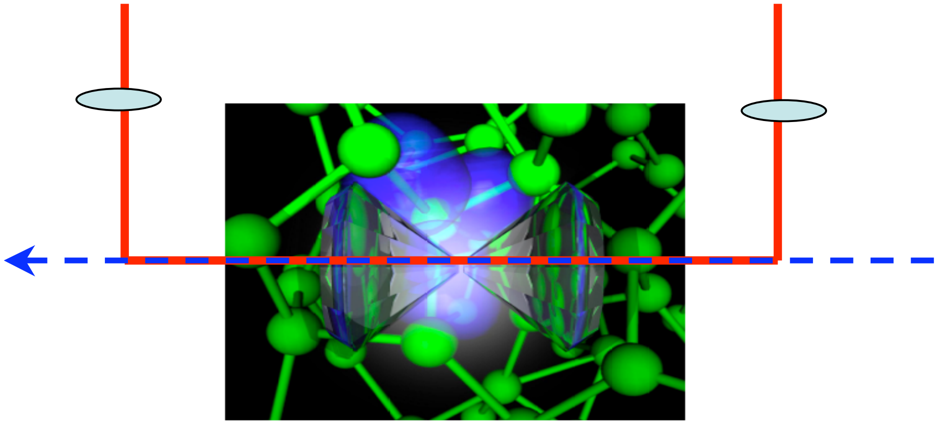

- Sound velocity
- Phonon density of states
- Phonon dispersion
- Vibrational entropy
- Melting point
- Viscosity
- Thermal conductivity

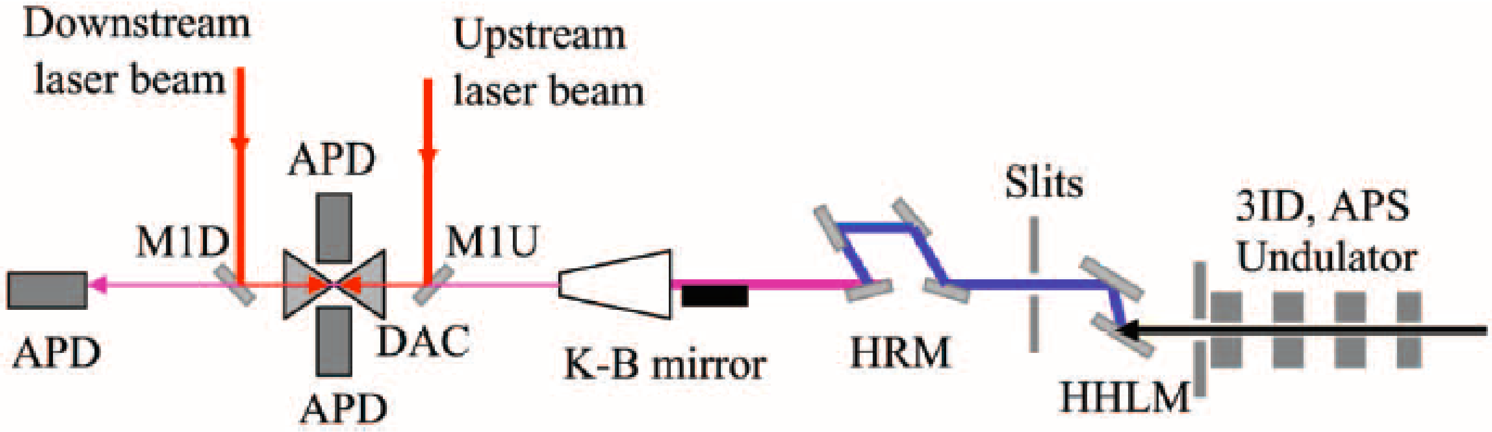

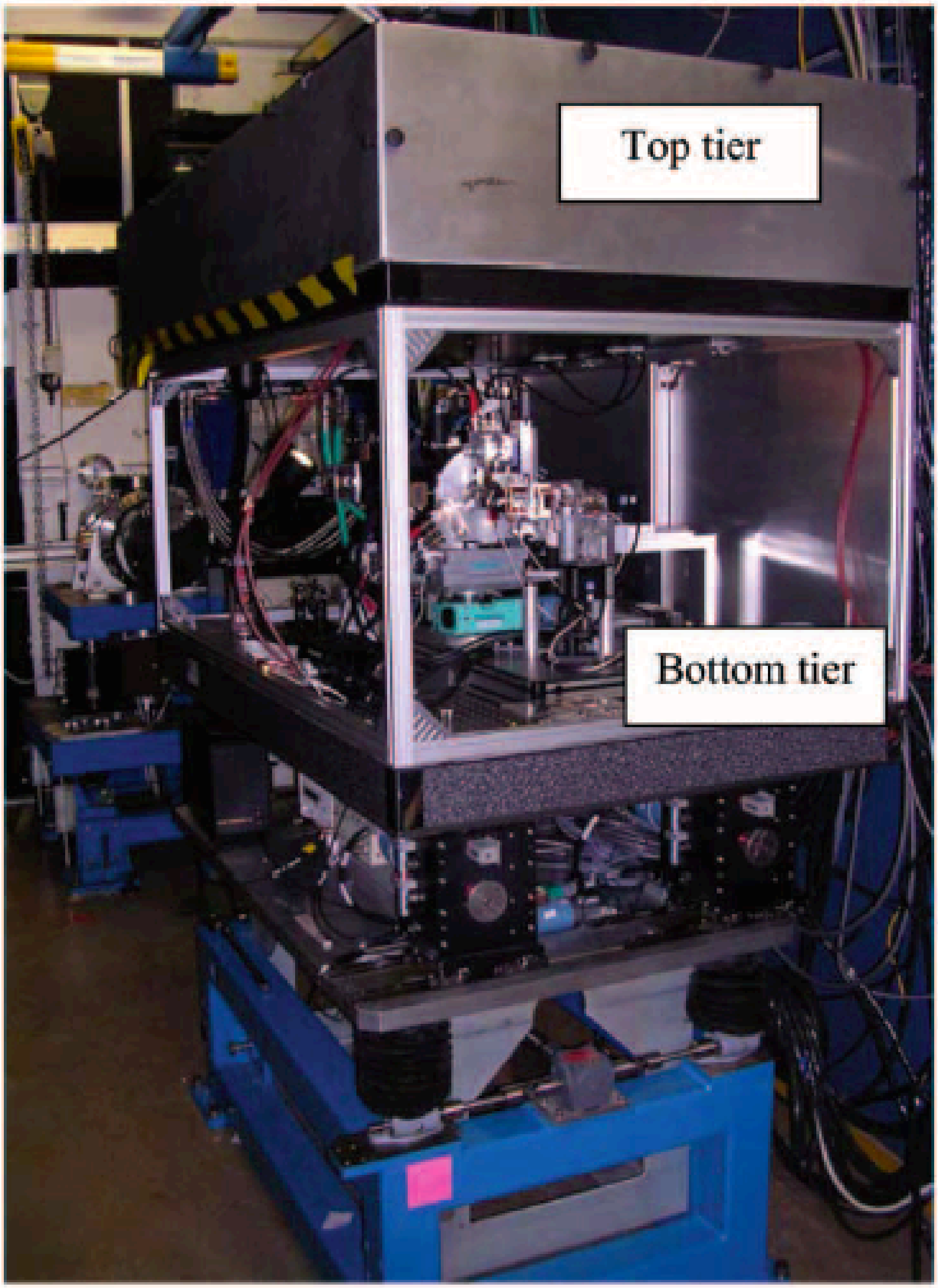
Top tier
Bottom tier

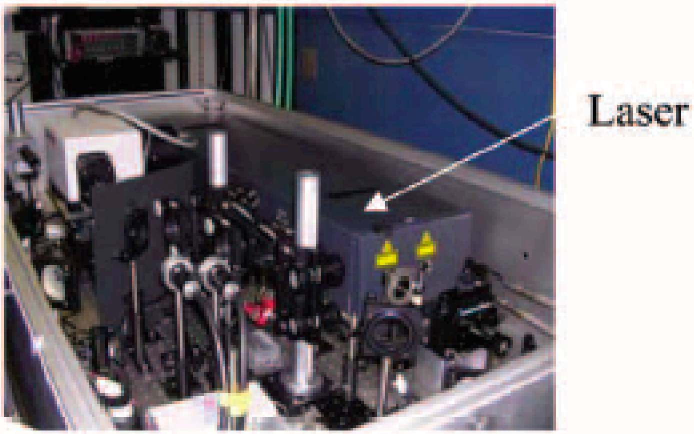
Laser

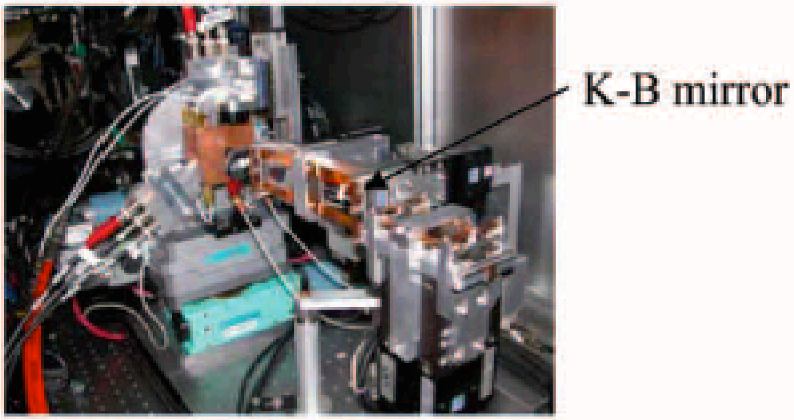
K-B mirror

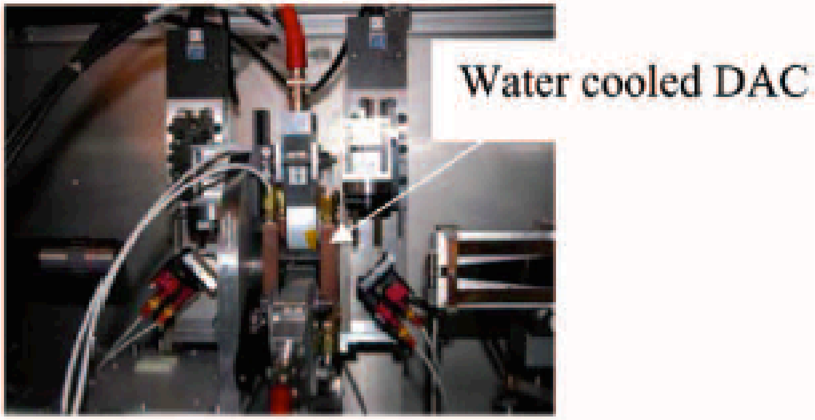
Water cooled DAC

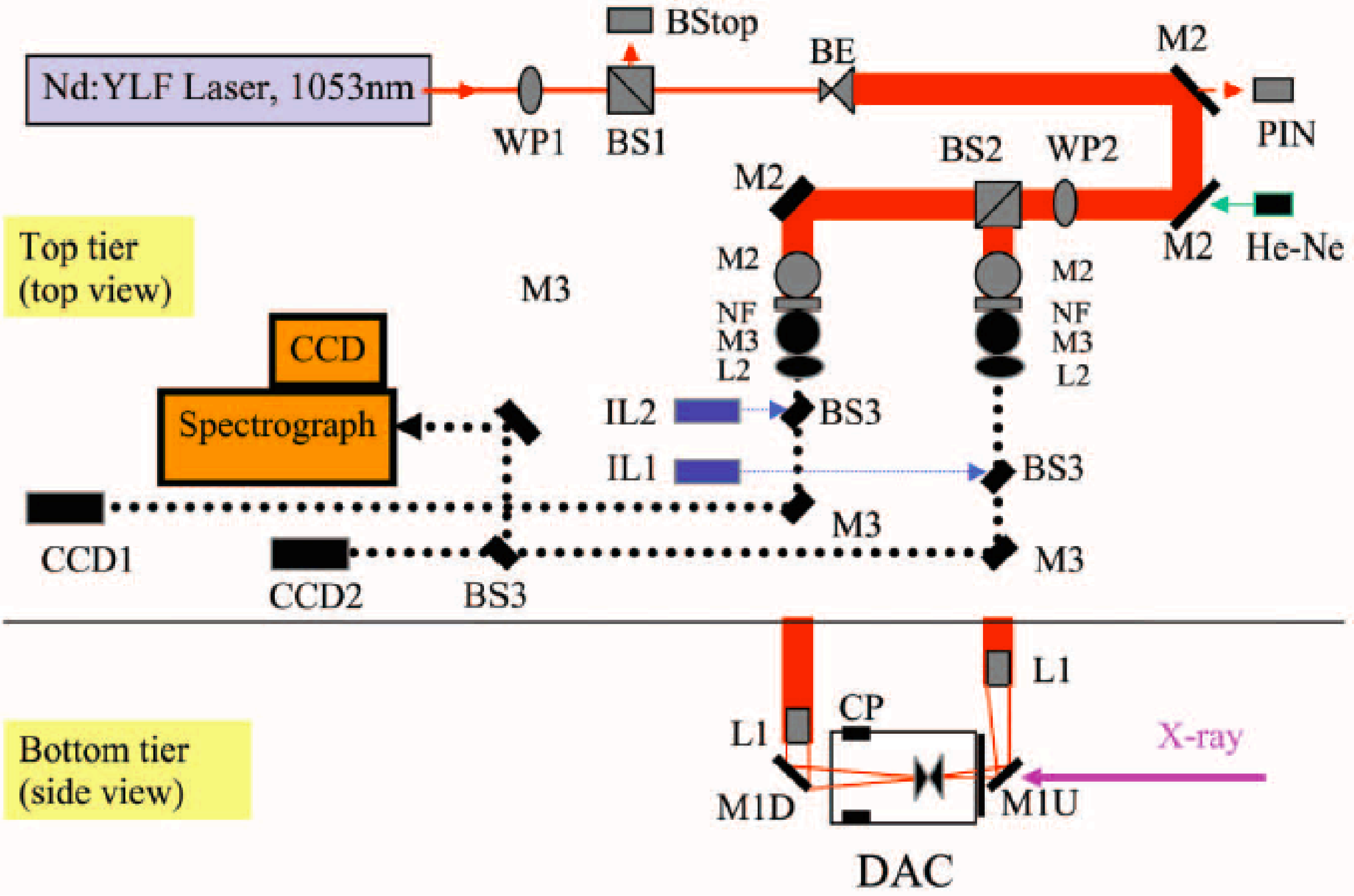

FIGURE 1 Schematic of the double-sided LHDAC system at 3-ID, APS. WP1, WP2: wave plate; BS1, BS2: polarizing cube beam splitter; BS3: 50/50 neutral beam splitter; BStop: water-cooled beam stop; BE: zoom beam expander; PIN: photodiode; M1: beryllium laser mirror coated with gold or carbon mirror coated with silver; M2: dichroic mirror reflecting (>99%) vertical polarized laser beam at 1053 nm; M3: Al-coated mirror; L1: apochromatic objective lens with focal length of 100 mm; L2: achromatic lens with 1000 mm focal length; NF: notch filter; CCD1 and CCD2: CCD cameras; CCD-spectrograph: spectrograph and CCD for temperature measurement; He-Ne: alignment laser; IL1 and IL2: illuminators.

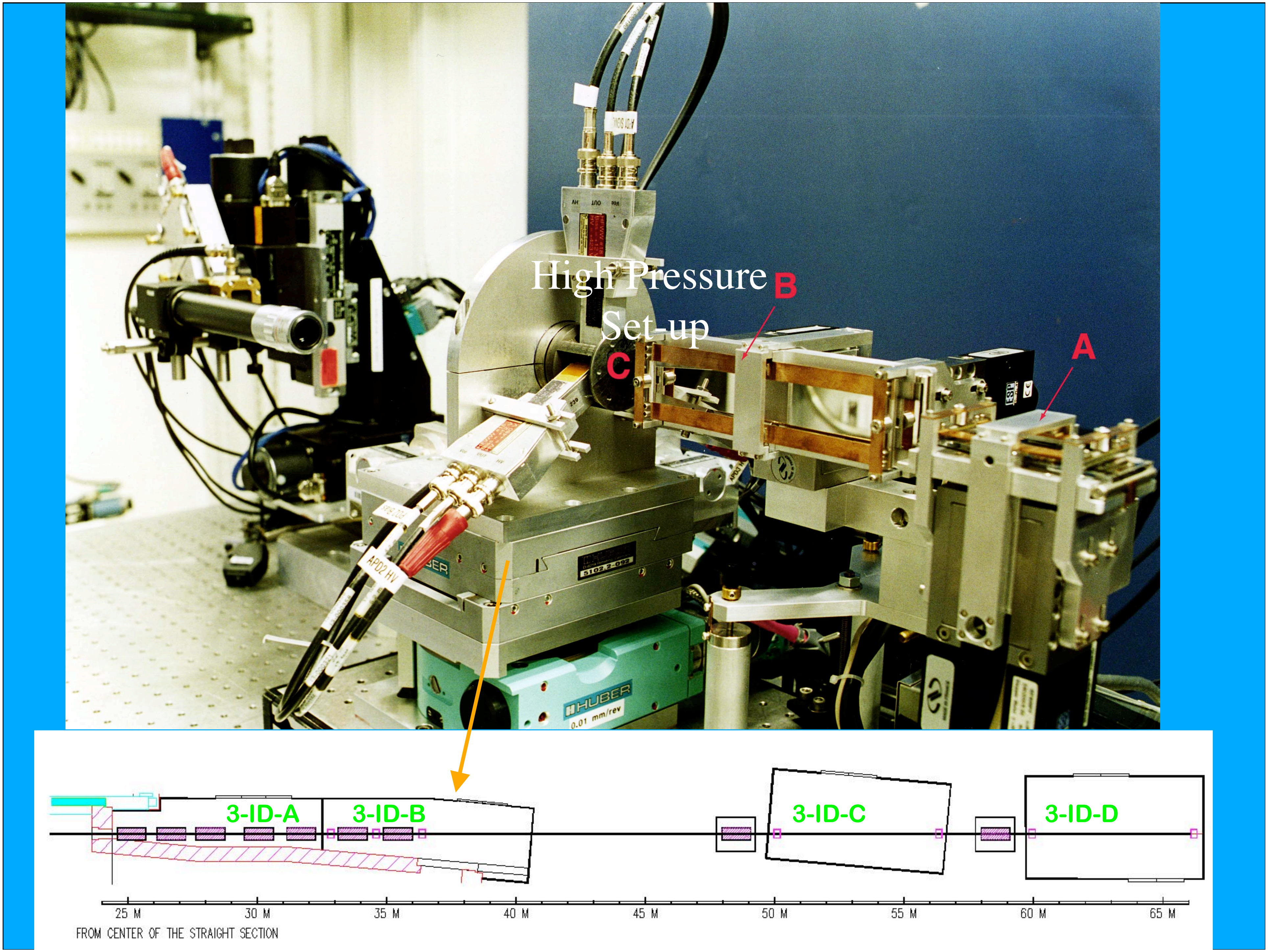

High Pressure Set-up

Earth’s Interior (simplified)

Earth’s seismic structure

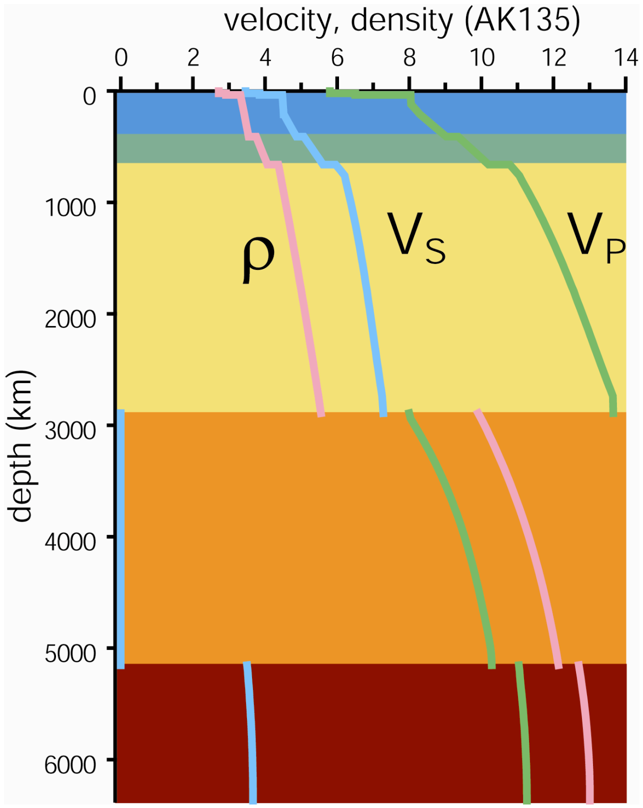

Earth’s stratification

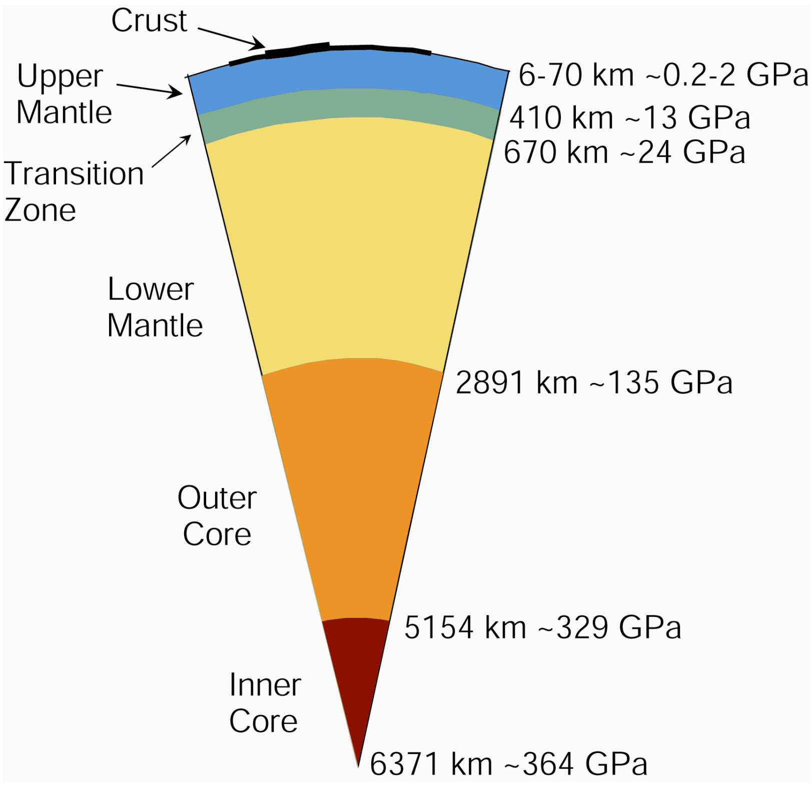

Earth’s composition

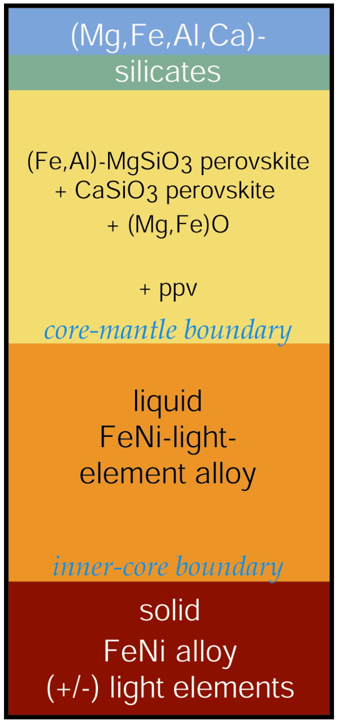

(Mg,Fe,Al,Ca)-
silicates

(Fe,Al)-$MgSiO_3$ perovskite
+ $CaSiO_3$ perovskite
+ (Mg,Fe)O

+ ppv

core-mantle boundary

liquid
FeNi-light-
element alloy

inner-core boundary

solid
FeNi alloy
(+/-) light elements

Seismic wave propagation and the internal structure of the Earth

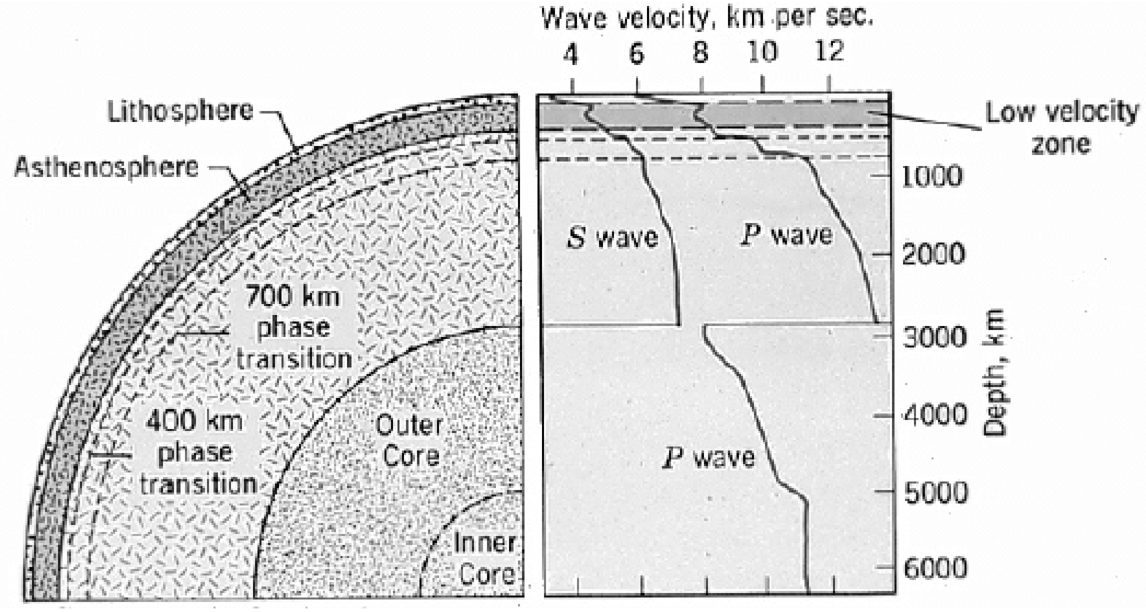

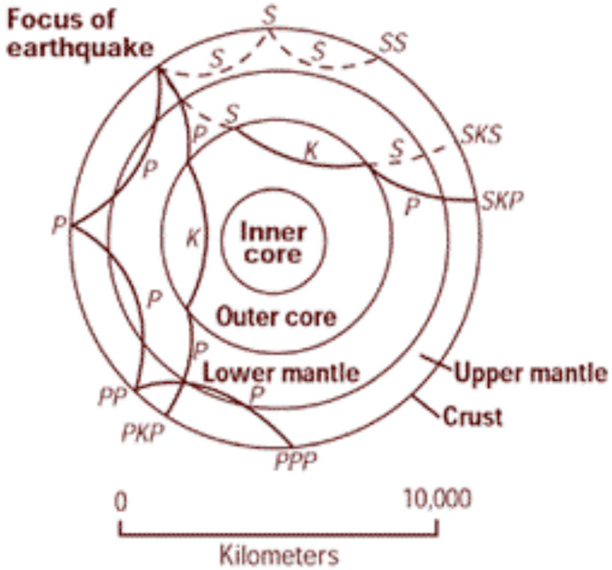

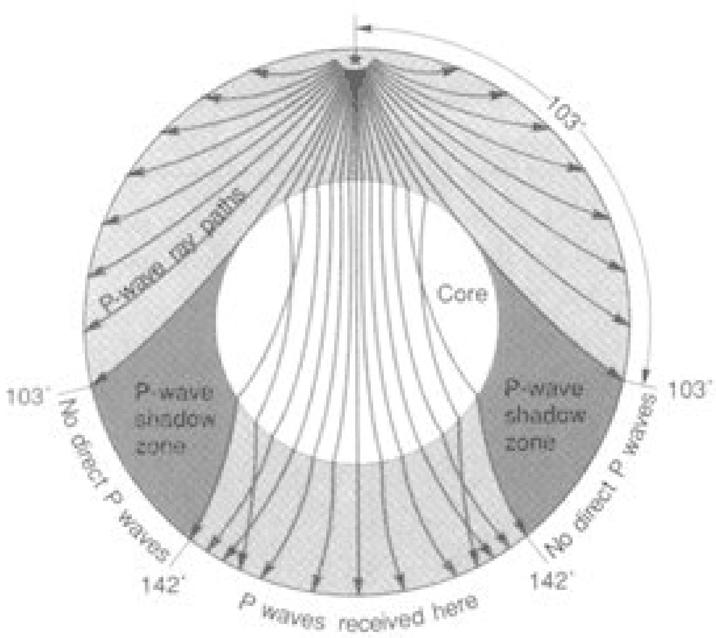

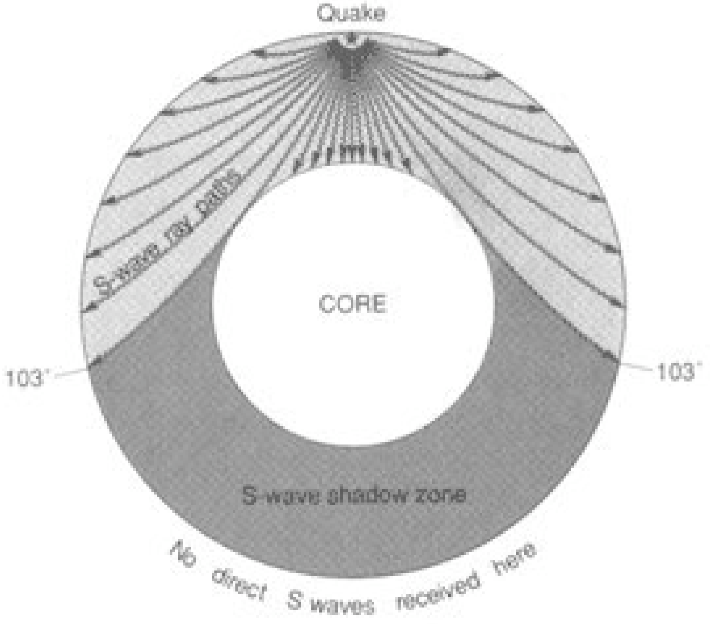

A geotherm together with accessible *P-T* ranges by static techniques

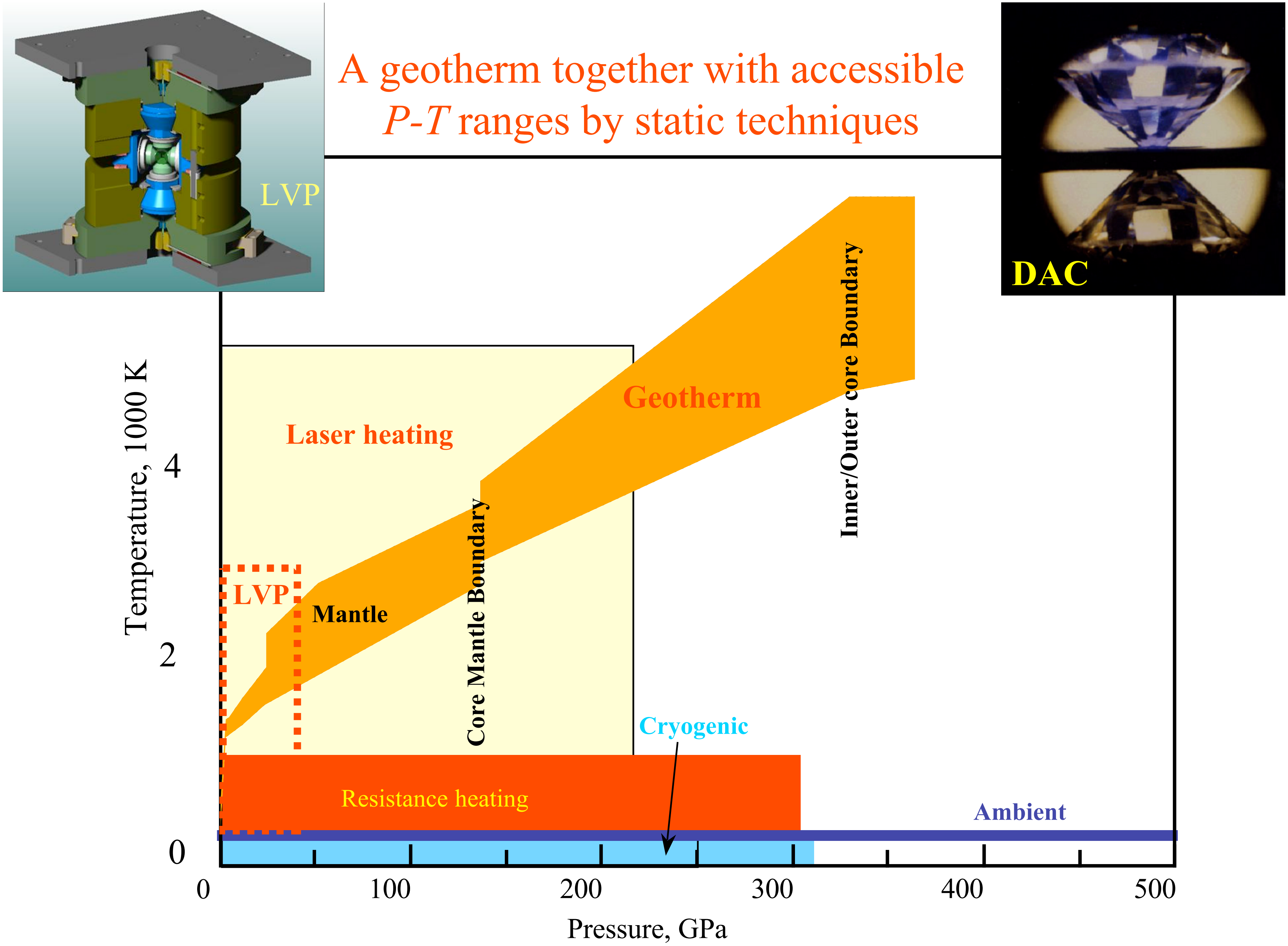

Earth’s Interior (simplified)

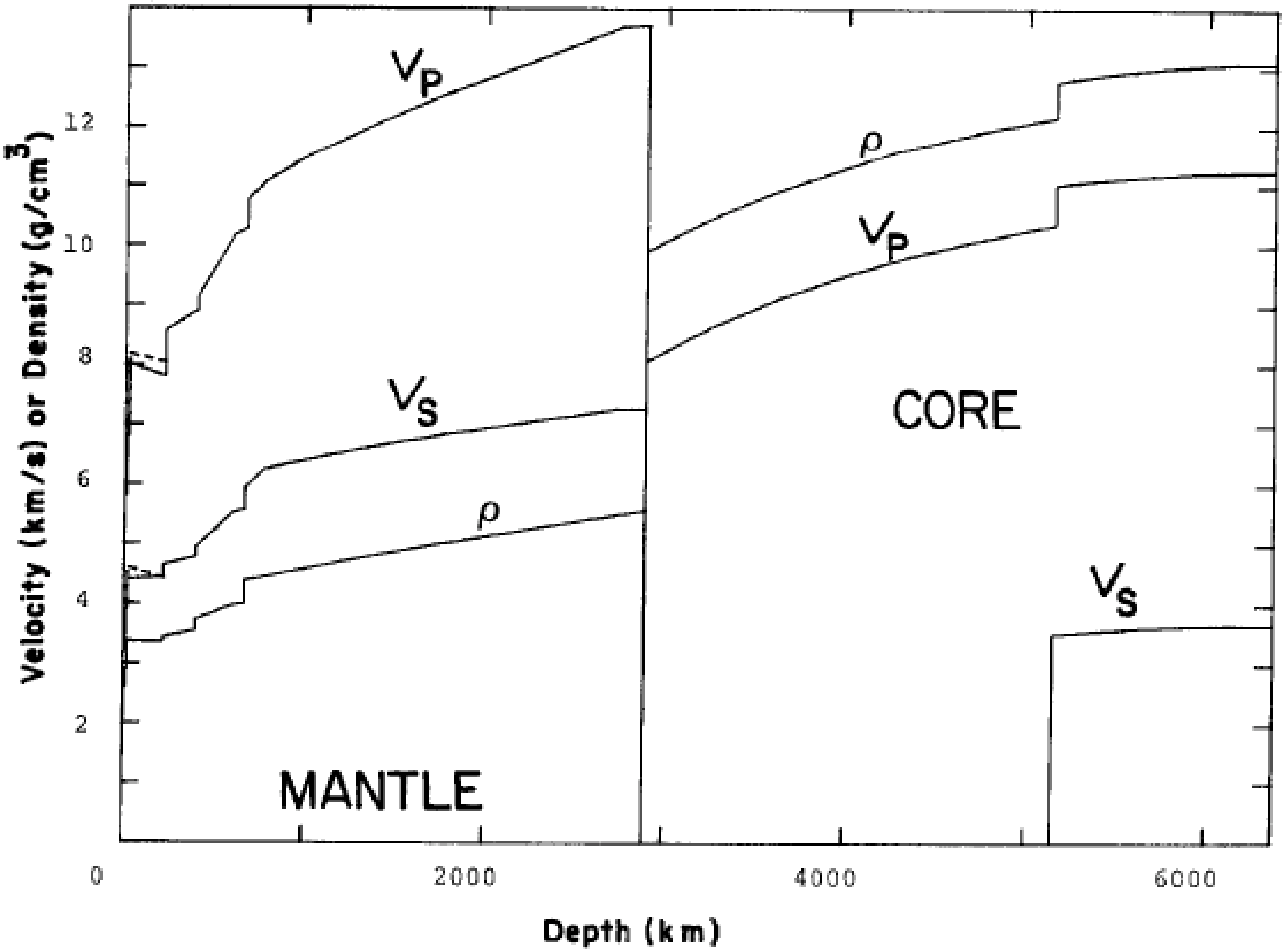

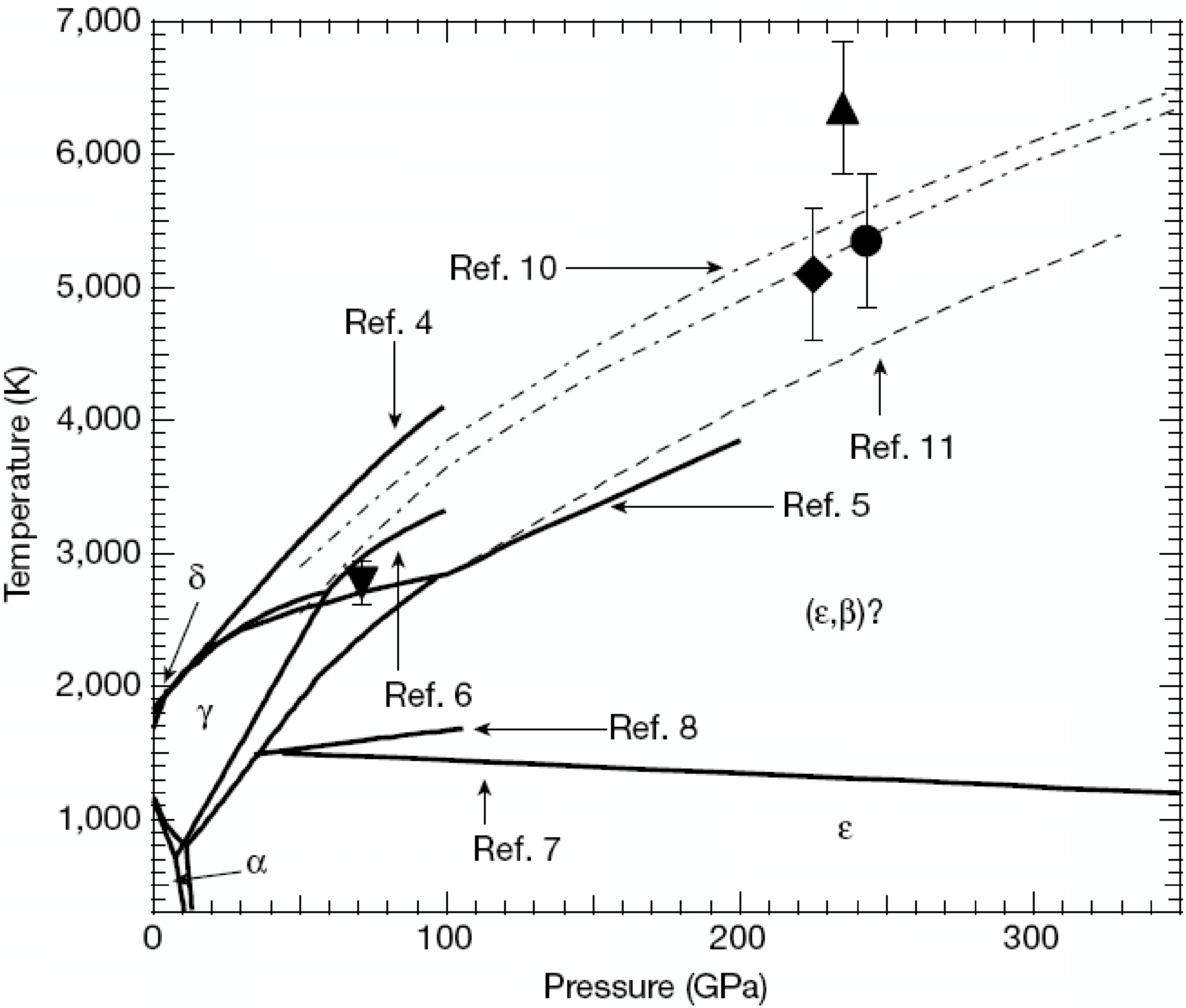

Nguyen and Holmes, Nature, 427, 339, 2004

Detection of nuclear decay

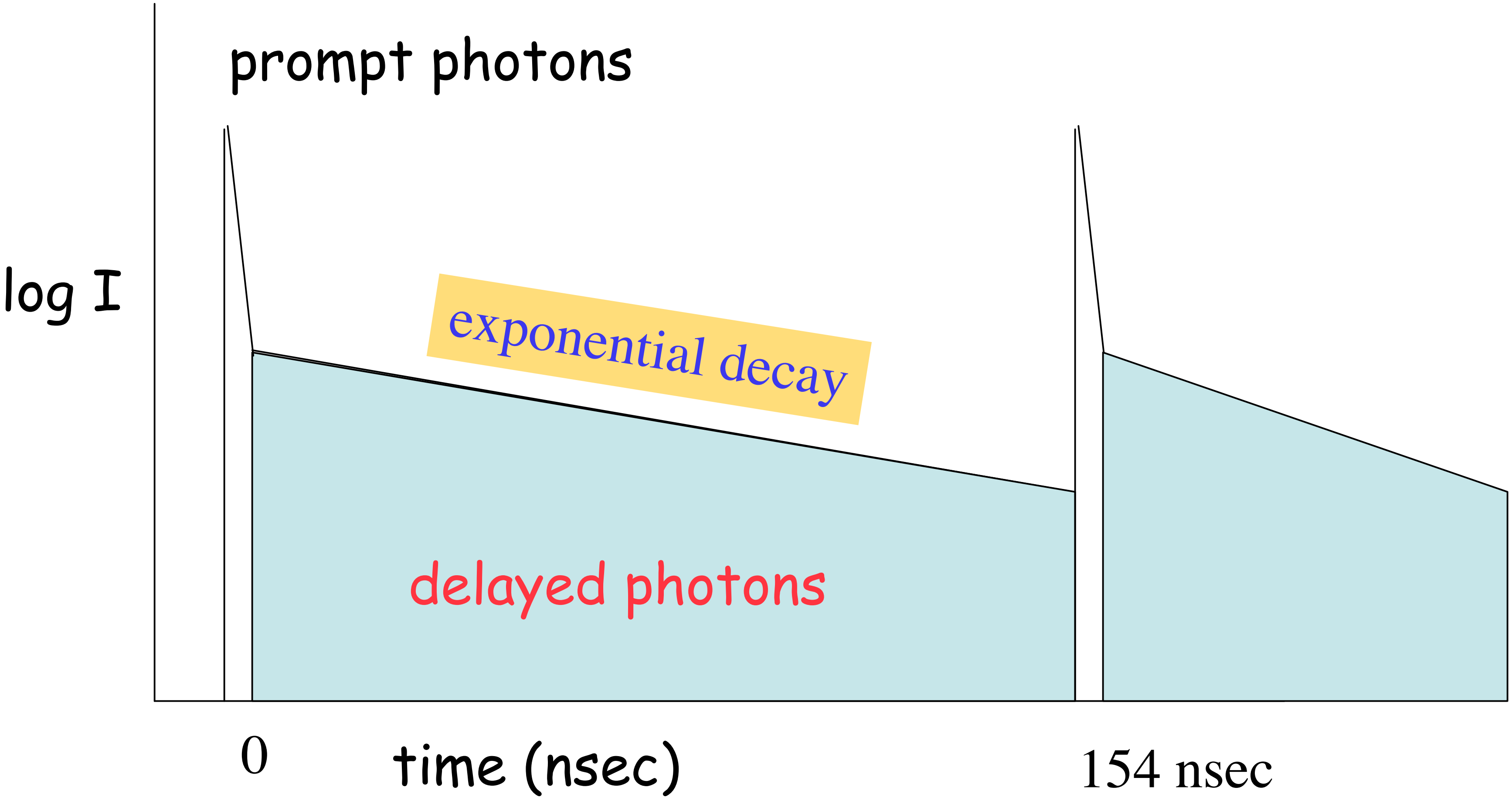

Iron phonon dispersion relations and phonon density of states

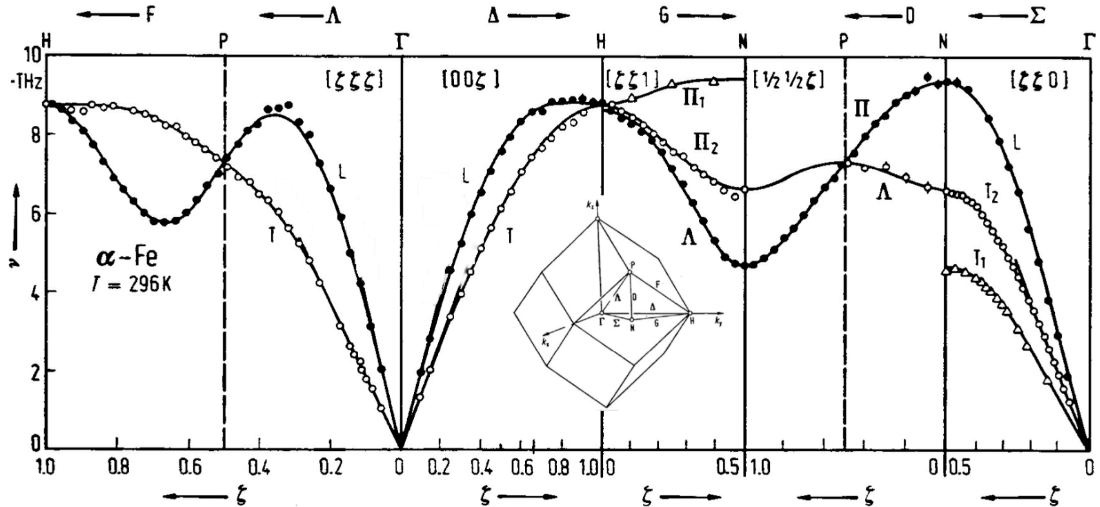

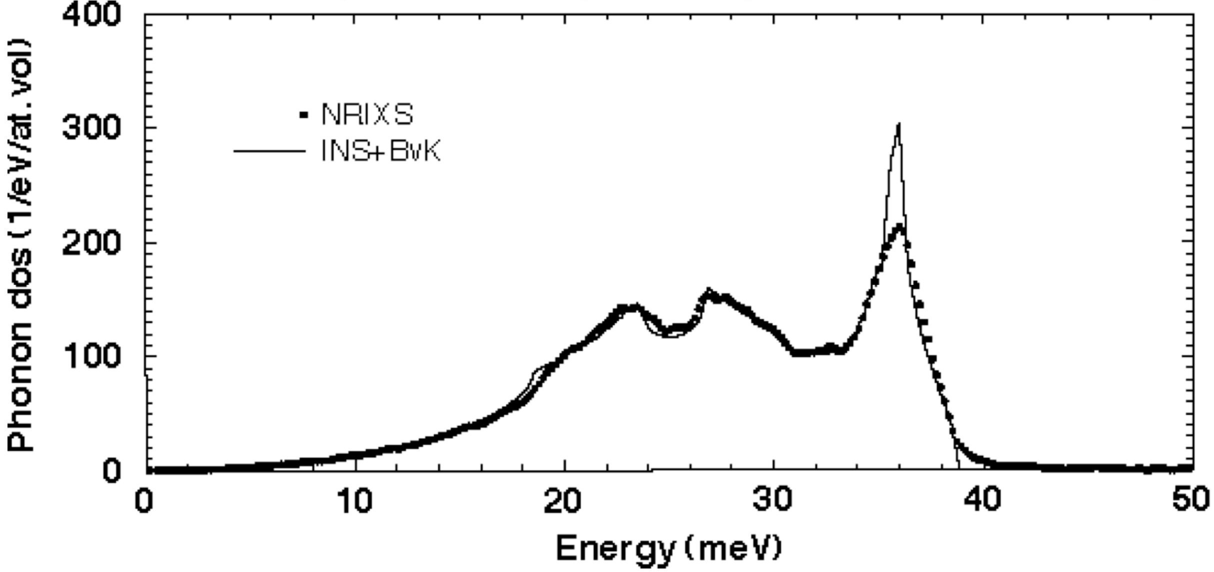

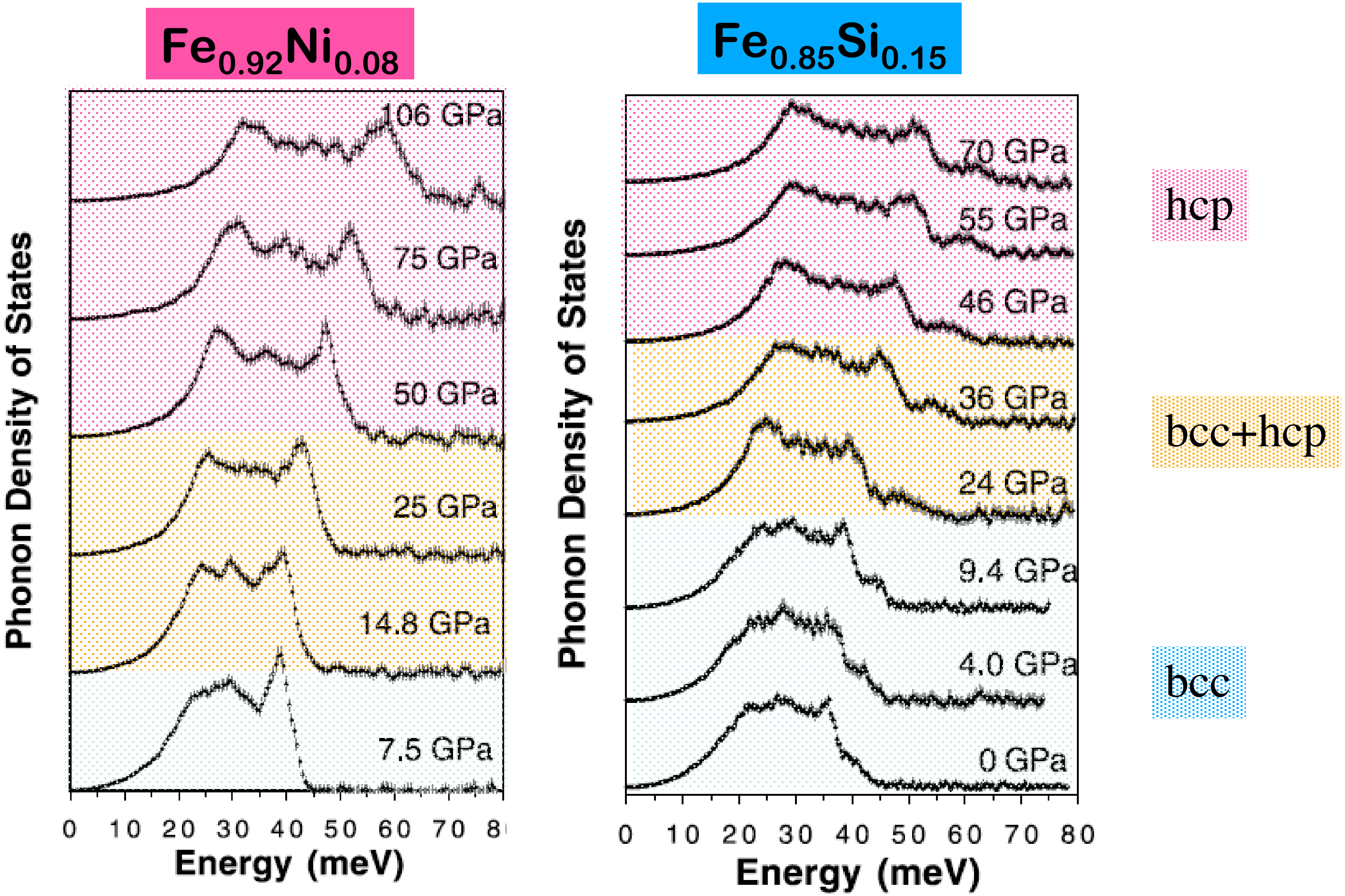

J.F. Lin, et al, Geophys. Res. Lett., 30 (2003) 2112

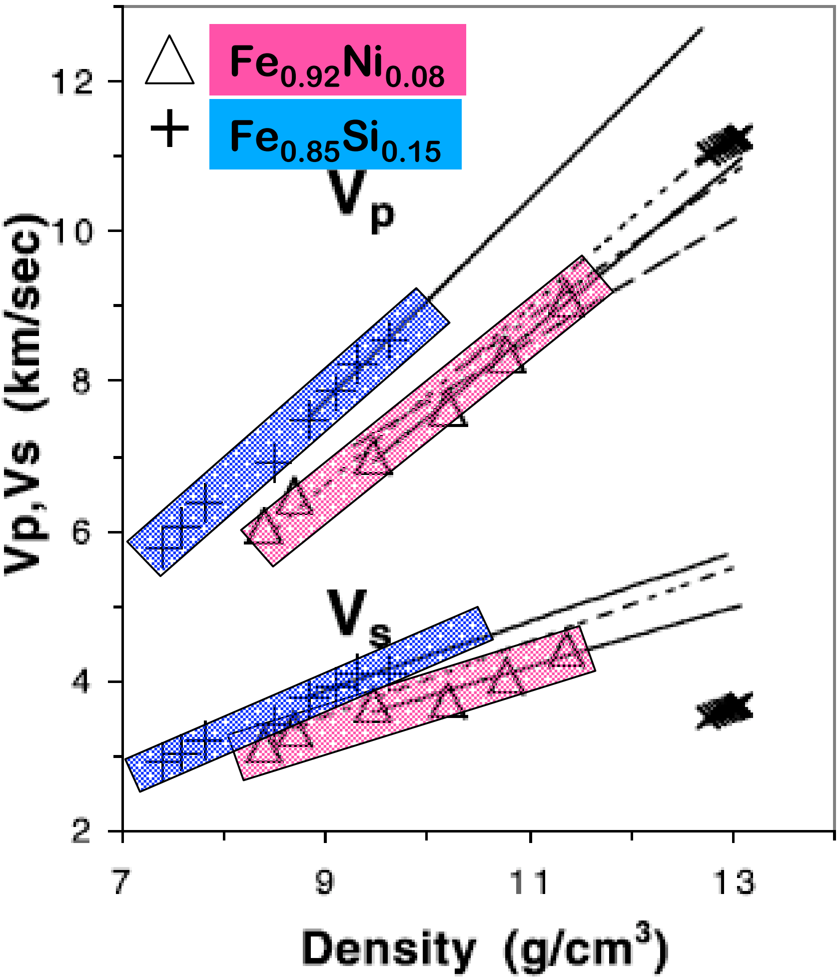

$$\frac{K_S}{\rho} = V_P^2 - \frac{4}{3} V_S^2$$

$$\frac{G}{\rho} = V_S^2$$

$$\frac{3}{V_D^3} = \frac{1}{V_P^3} + \frac{2}{V_S^3}$$

K_S : adiabatic bulk modulus
G : shear modulus
V_P : compression wave velocity
V_S : shear wave velocity
V_D : Debye sound velocity
P : density

Extreme conditions: High pressure & temperature

☆ **The μeV spectrometer would significantly increase accuracy and permit a new approach to investigations of partial melting.**

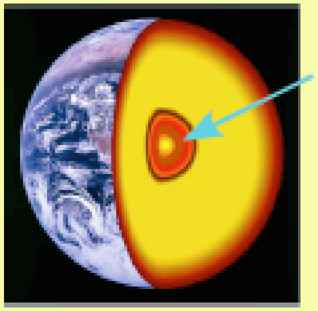

P > 1Mbar
T > 2000K

J.-F. Lin, W. Sturhahn, J. Zhao, G. Shen, H.-k. Mao, R.J. Hemley,
Science 308 (2005) 1892
"Sound Velocities of Hot Dense Iron: Birch's Law Revisited"

- ➢ explicit temperature dependence
- ➢ v $\propto \rho$ rule (Birch's Law) cannot be used for extrapolations

➢ *relevant publications*

H.-k. Mao et al., Science 292 (2001) 914
V.V. Struzhkin et al., Phys. Rev. Lett. 87 (2001) 255501
J.-F. Lin et al., Geophys. Res. Lett. 30 (2003) 2112
W. Mao et al., Geophys. Res. Lett. 31 (2004) L15618
A. Barla et al., Phys. Rev. Lett. 92 (2004) 066401
J.-F. Lin et al., Earth and Planet. Sci. Lett. 226 (2004) 33
H. Kobayashi et al., Phys. Rev. Lett. 93 (2004) 195503
J.S. Tse et al., Nature Materials 4 (2005) 917

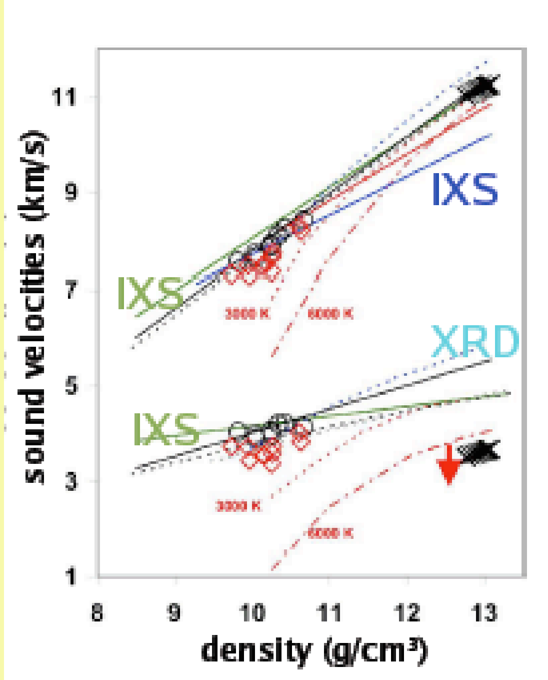

Albert Franics Birch (1903-1992) (1952)

Unwary readers should take warning that ordinary language undergoes modification to a high-pressure form when applied to the interior of the Earth. A few examples of equivalents follow

High Pressure Form	*Ordinary Meaning*
Certain	Dubious
Undoubtedly	Perhaps
Positive proof	Vague suggestion
Unanswerable argument	Trivial objection
Pure iron	**Uncertain mixture of all the elements**

From biography by T. J. Ahrens, National Academy of Science

IXS

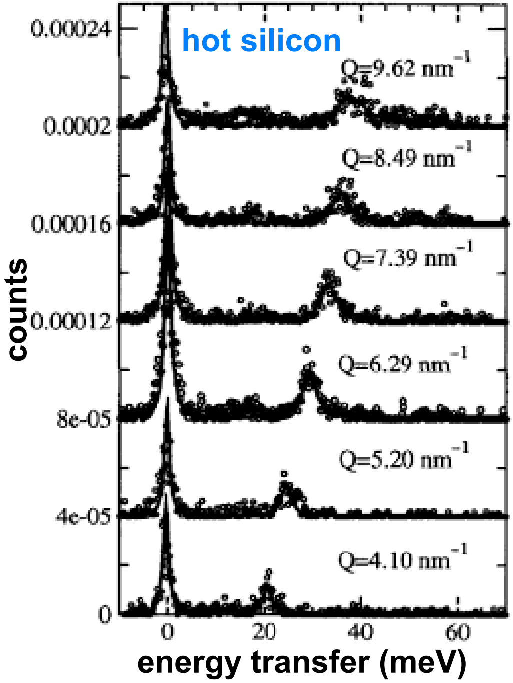

(Atlas *et al.* 2005)

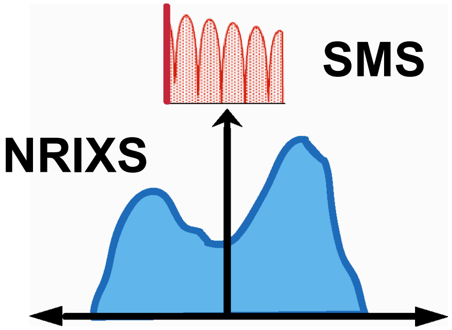

XRD

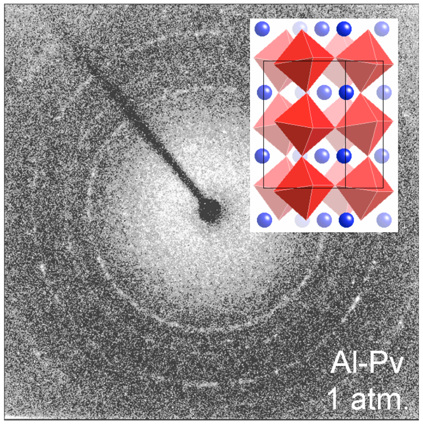

(Jackson *et al.* GRL, 2004)

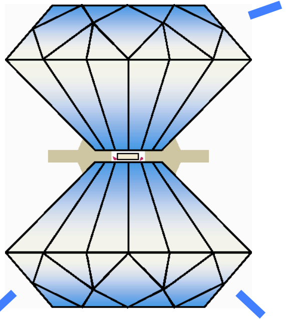

Brillouin Spectroscopy

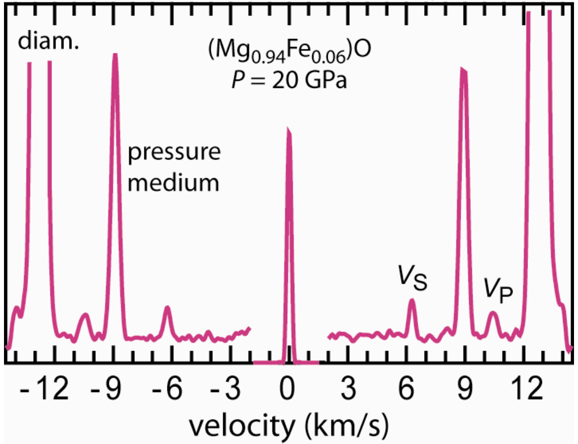

(Jackson *et al.* JGR, in press)

$$\frac{K_S}{\rho} = V_\phi^2 = V_P^2 - \frac{4}{3}V_S^2$$

$$\frac{\mu_S}{\rho} = V_S^2$$

$$\frac{3}{V_D^3} = \frac{1}{V_P^3} + \frac{2}{V_S^3}$$

IXS

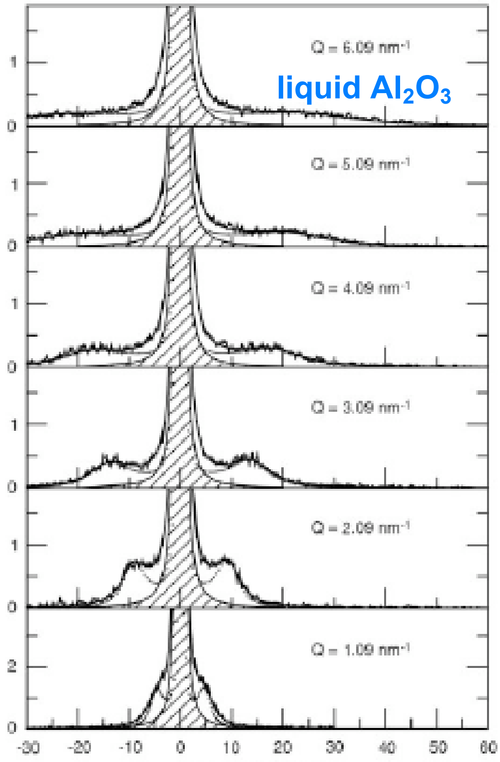

(Sinn *et al.* Science, 2003)

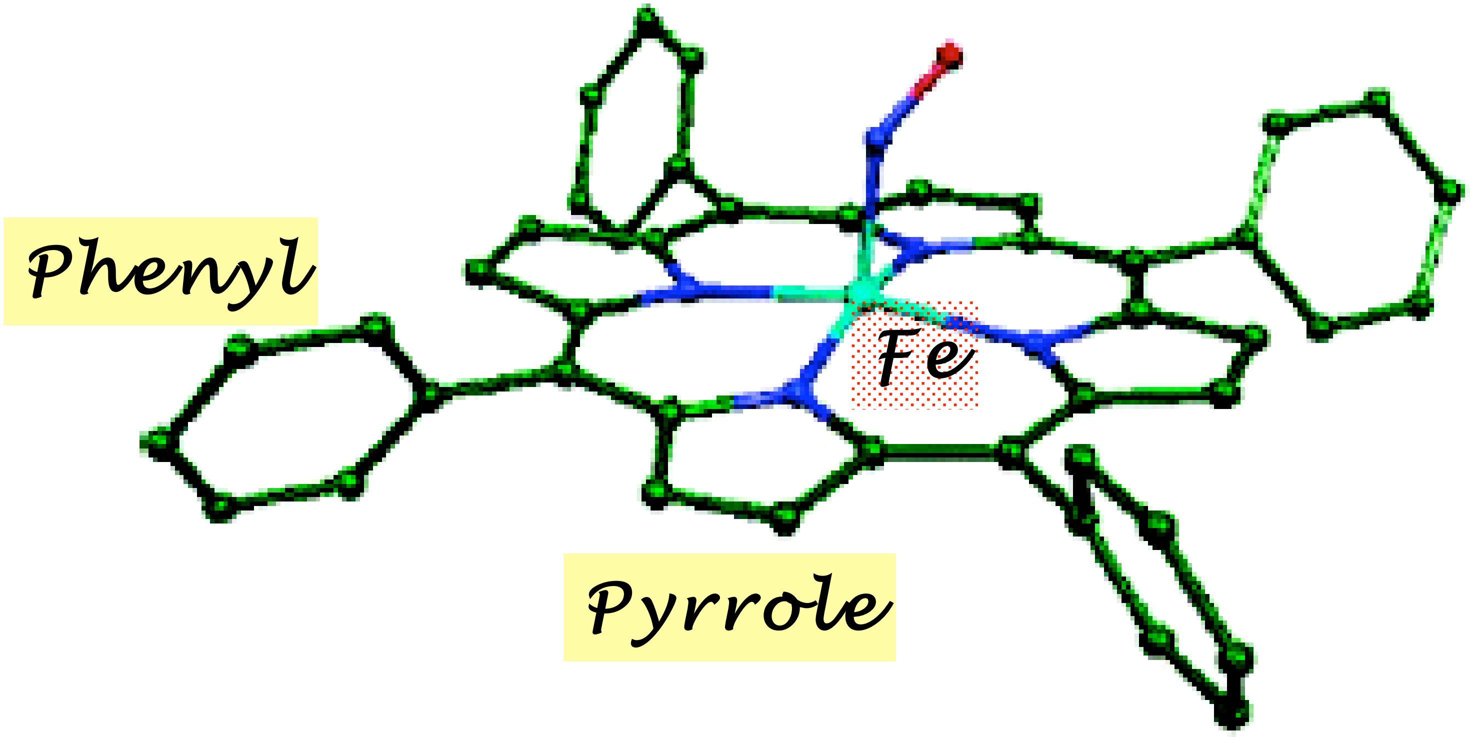

Figure 1. Calculated structure of ferrous nitrosyl tetraphenylporphyrin,

In-plane vibrations of heme Fe have not been identified in Raman spectra due to lack of electric dipole moment in D_{4h} symmetry.

Solvent absorption limit IR studies below 125 meV (1000 cm^{-1}).

Low frequency reactive modes are rarely identified with Raman or IR.

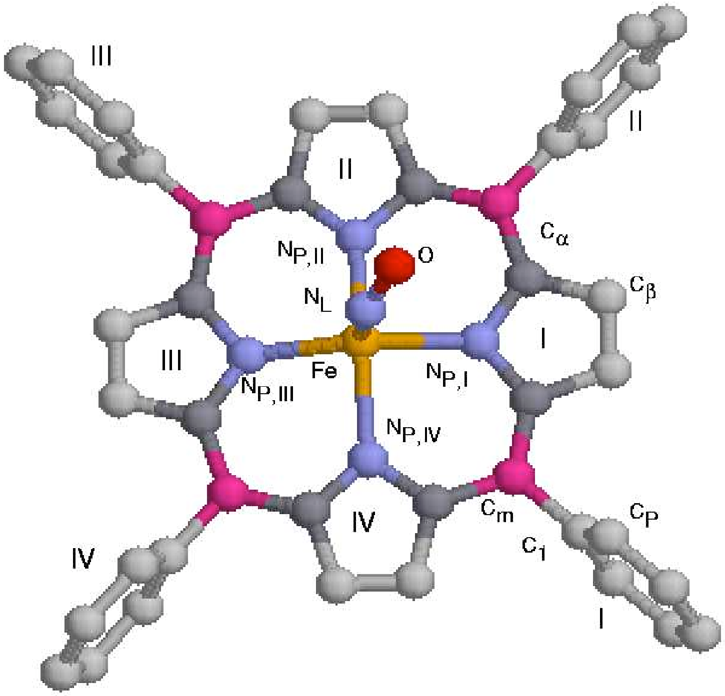

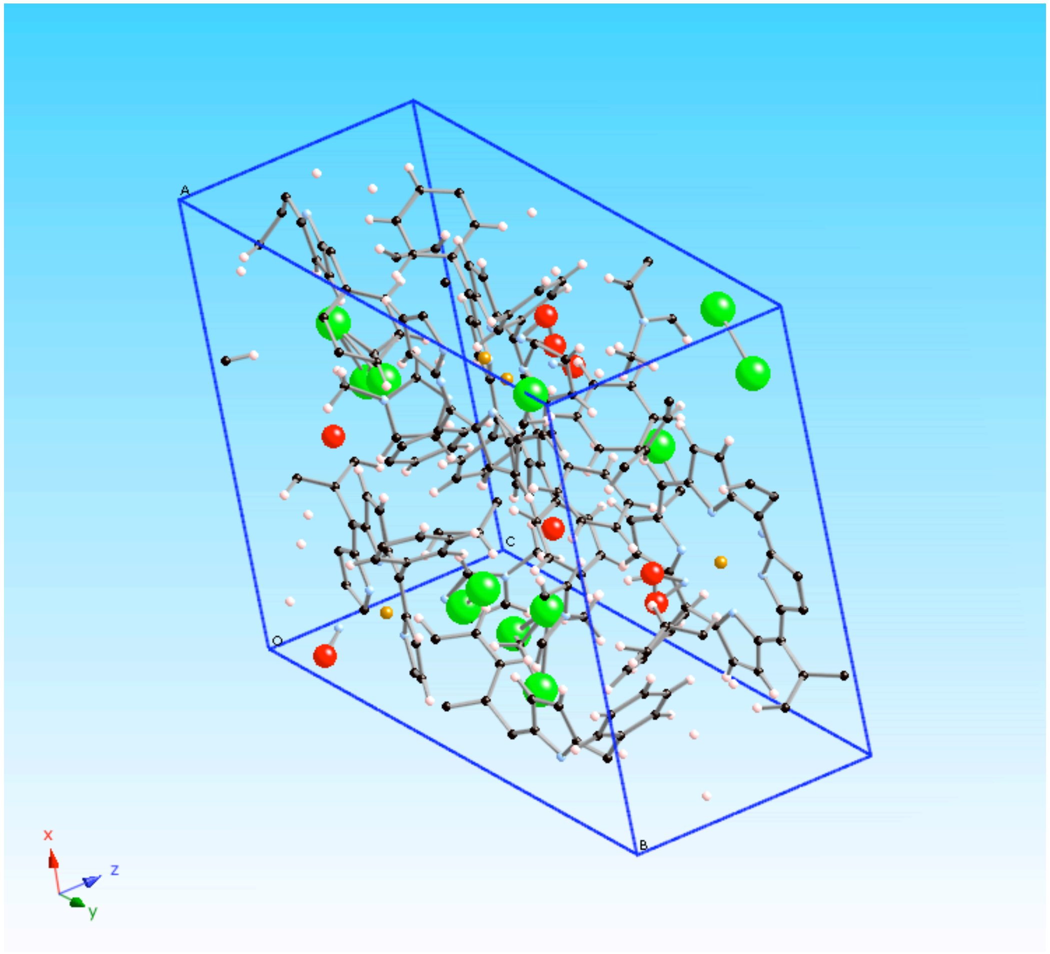

Porphyrins:	**A**	**B**
Tetraphenylporphyrin (TPP)	Phenyl	H
Octaethylporphyrin (OEP)	H	Ethyl

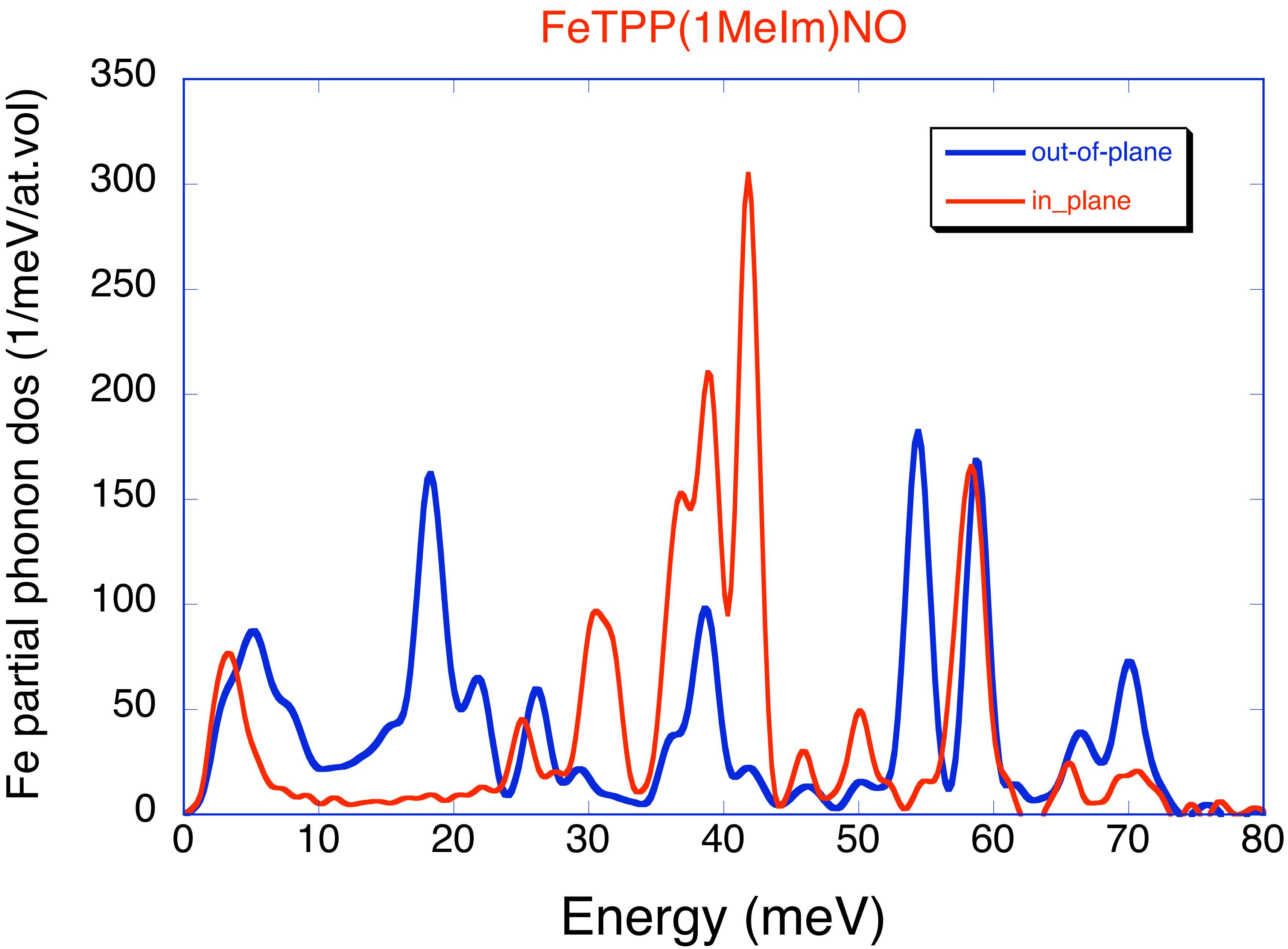
FeTPP(1MeIm)NO
Fe partial phonon dos (1/meV/at.vol)
350
300
250
200
150
100
50
0
0
10
20
30
40
50
60
70
80
Energy (meV)
out-of-plane
in_plane

doming

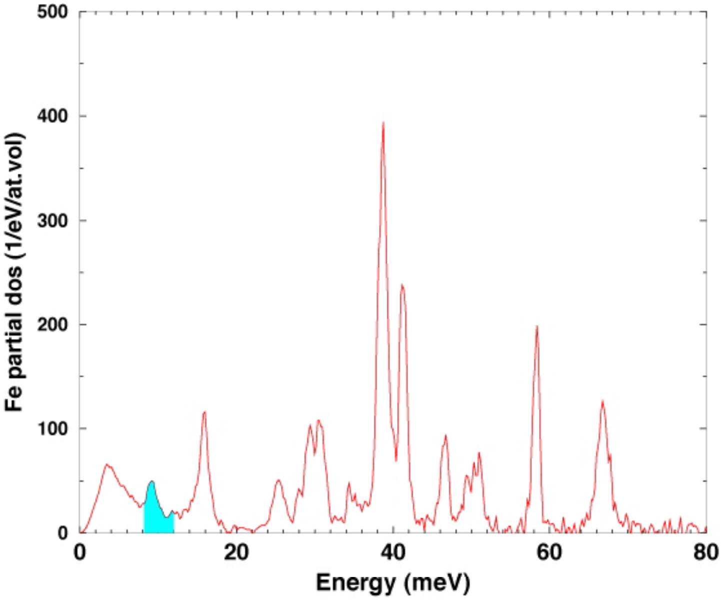

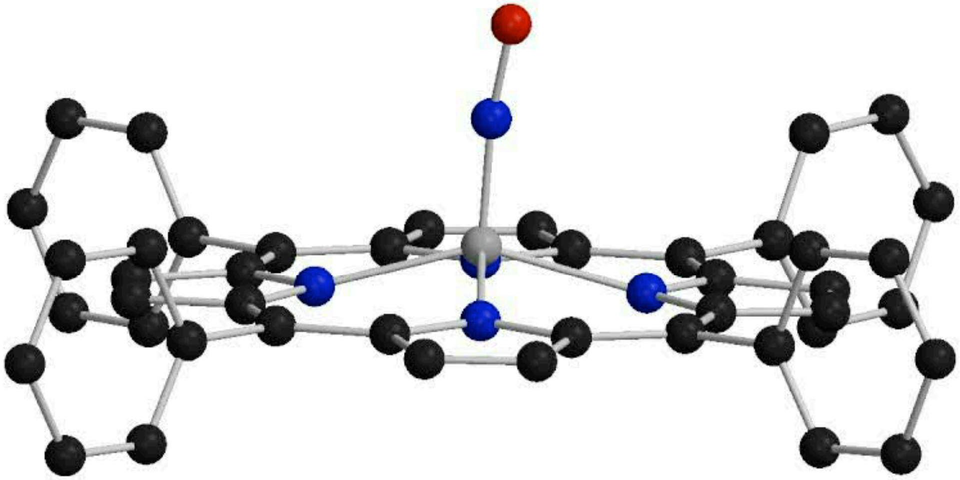

B. Rai, S. Durbin, W. Sturhahn, et al, Biophysics Journal, 2002

tilting

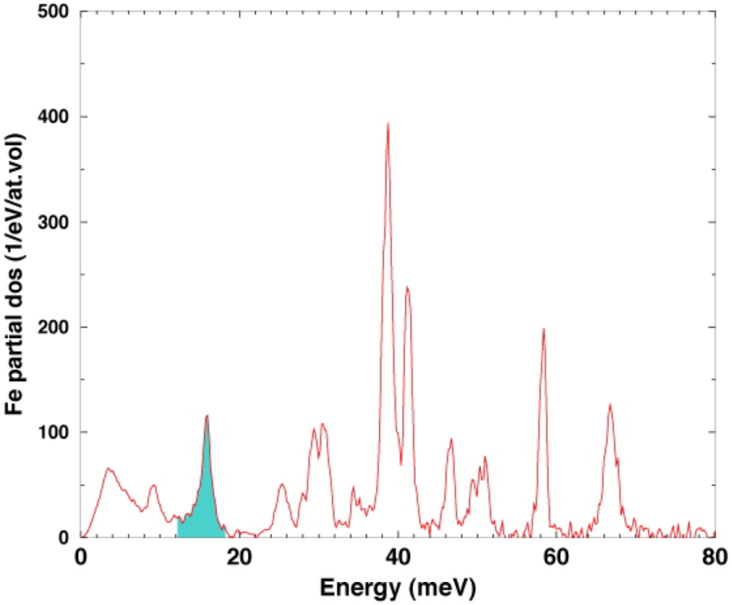

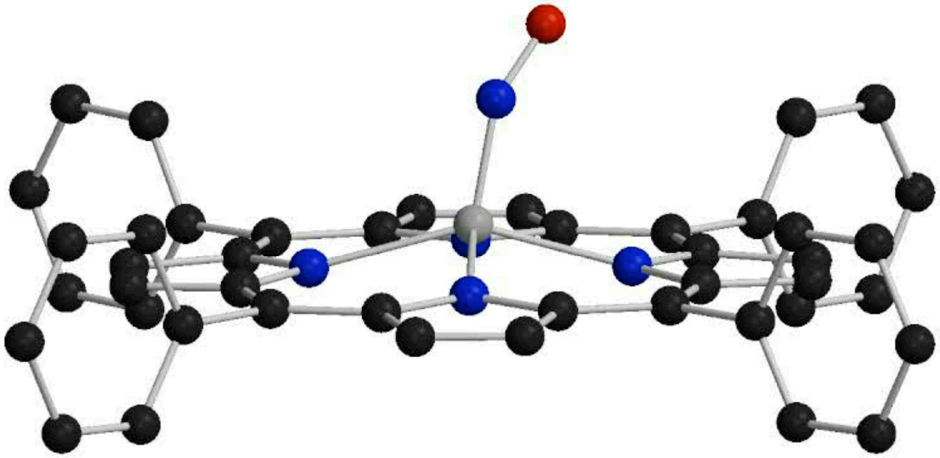

B. Rai, S. Durbin, W. Sturhahn, et al, Biophysics Journal, 2002

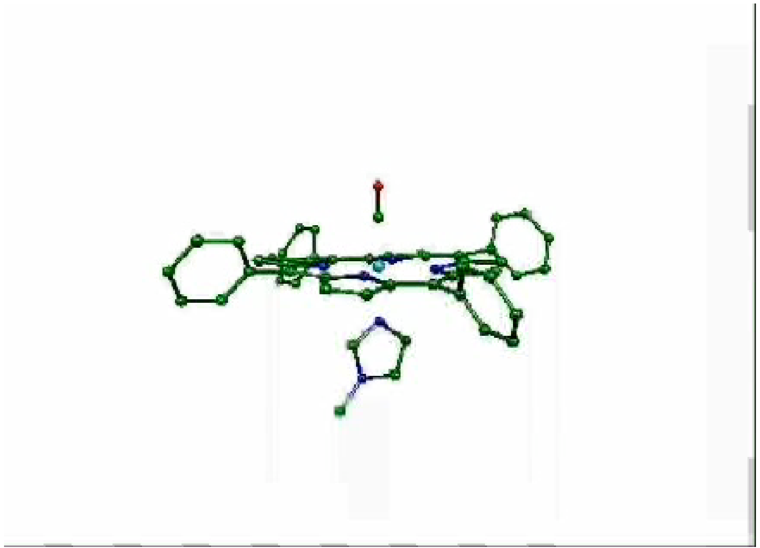

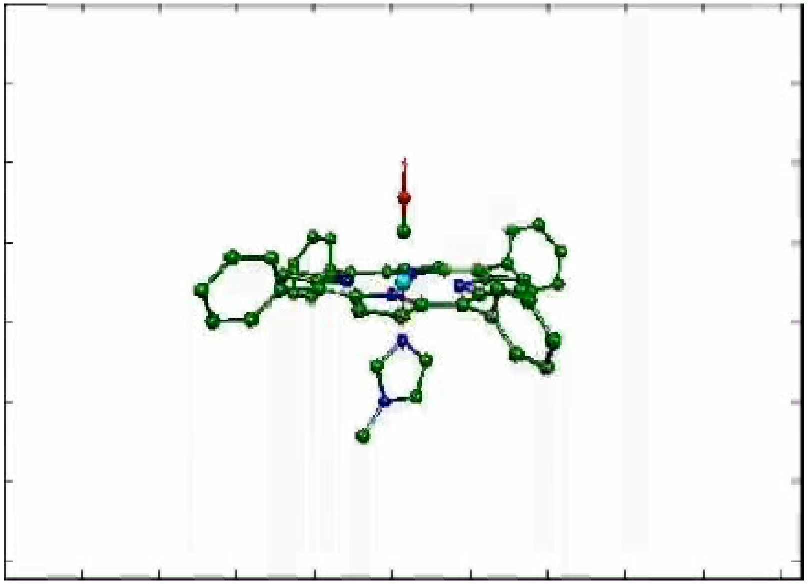

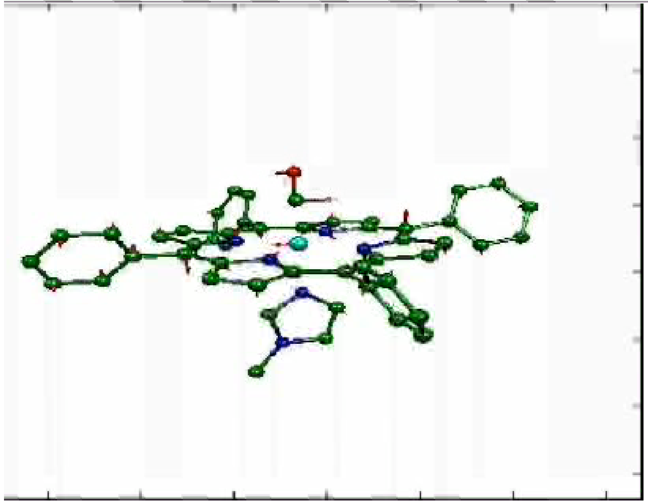

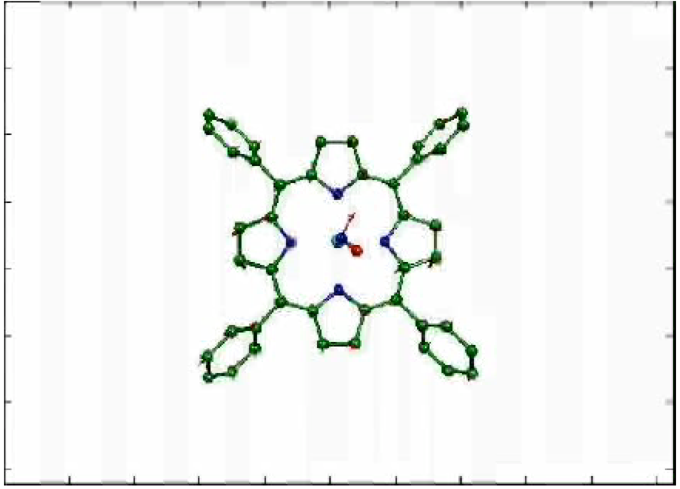

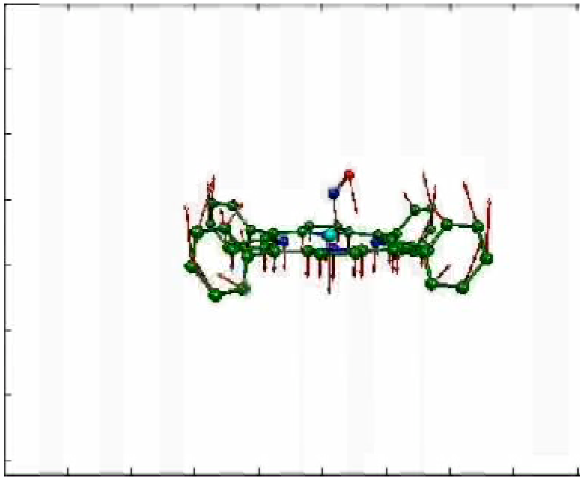

FeTPP(1MeIm)NO

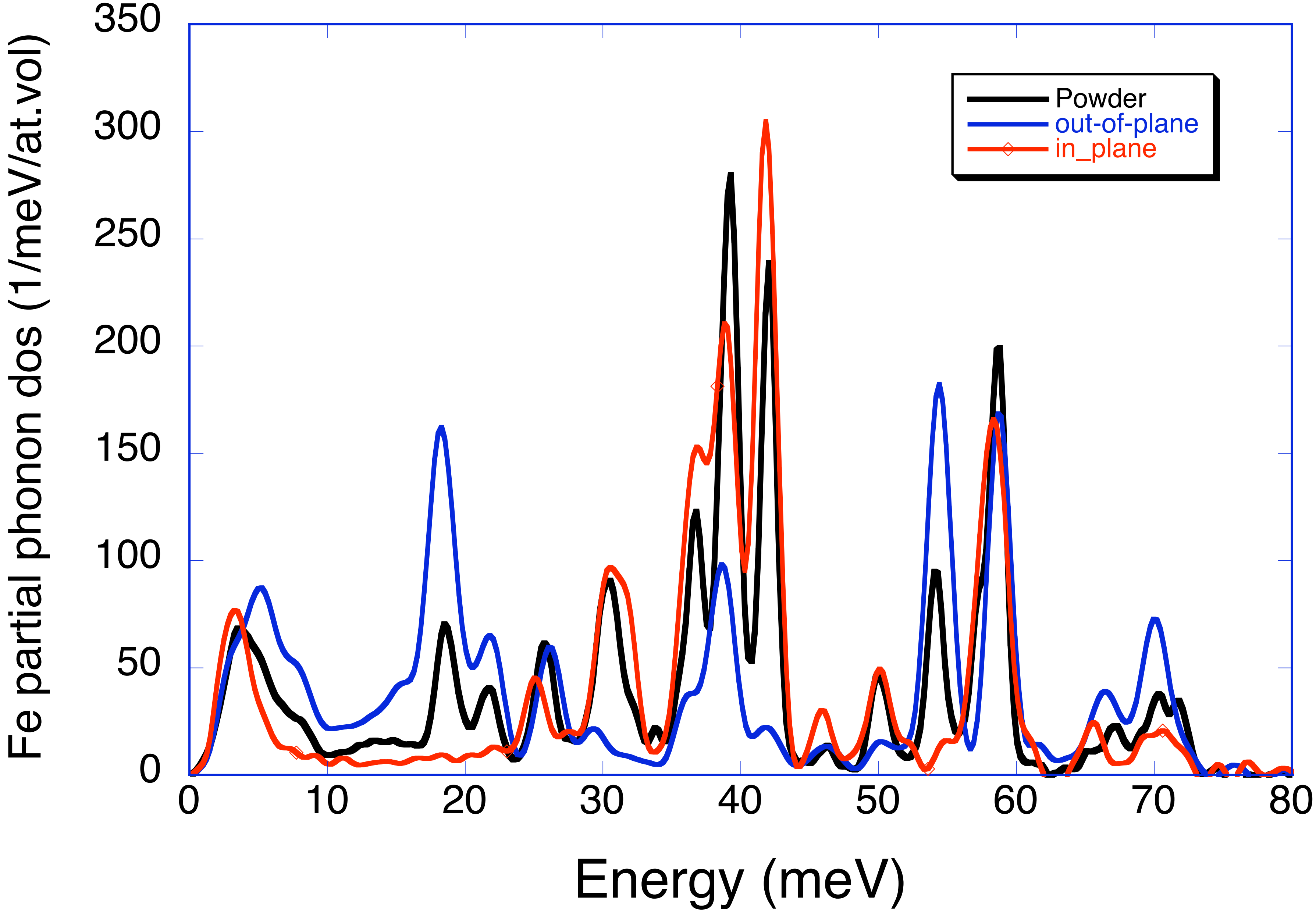

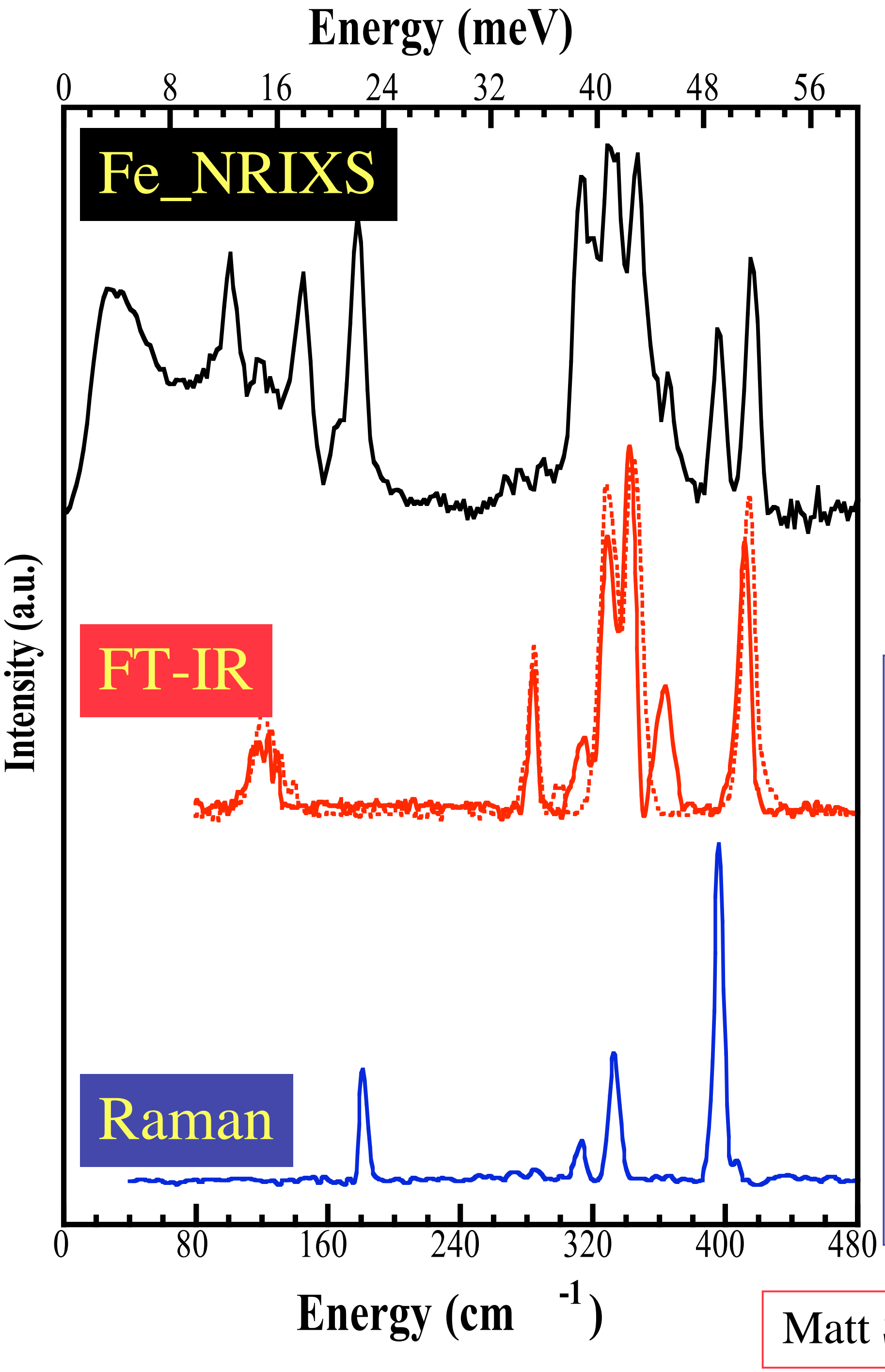

$[NEt_4]_2[Fe_2S_2Cl_4]$.

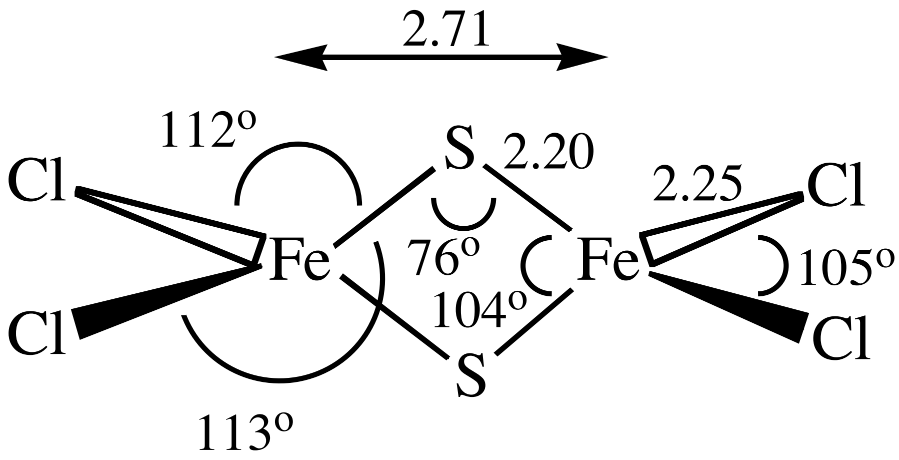

Some unique advantages of NRIXS

- Low frequency motions
2. No selection rule except motion of atoms along x-ray propogation
3. Peak intensity ~ mode participation ~ actual displacement
4. No matrix effects or limitations
5. Element and isotope selective
6. No unpredictable cancellations in scattering terms

Matt Smith, et al, Inorganic Chemistry, 2005, 44,5562

Iron-sulfur cubane compounds

- **Reduced {4Fe4S}$^{+}$ has not been possible to observe with resonant Raman technique, in contrast to oxidized {4Fe4S}$^{2+}$**

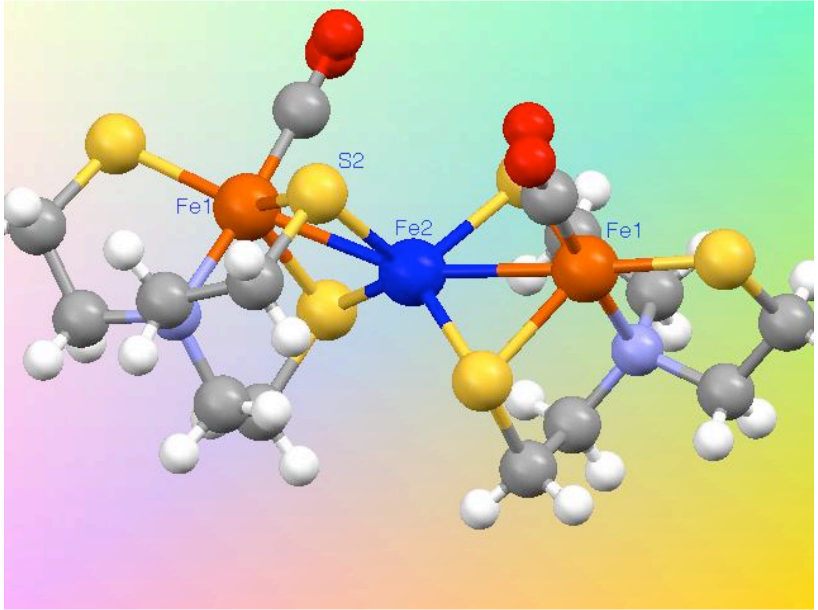

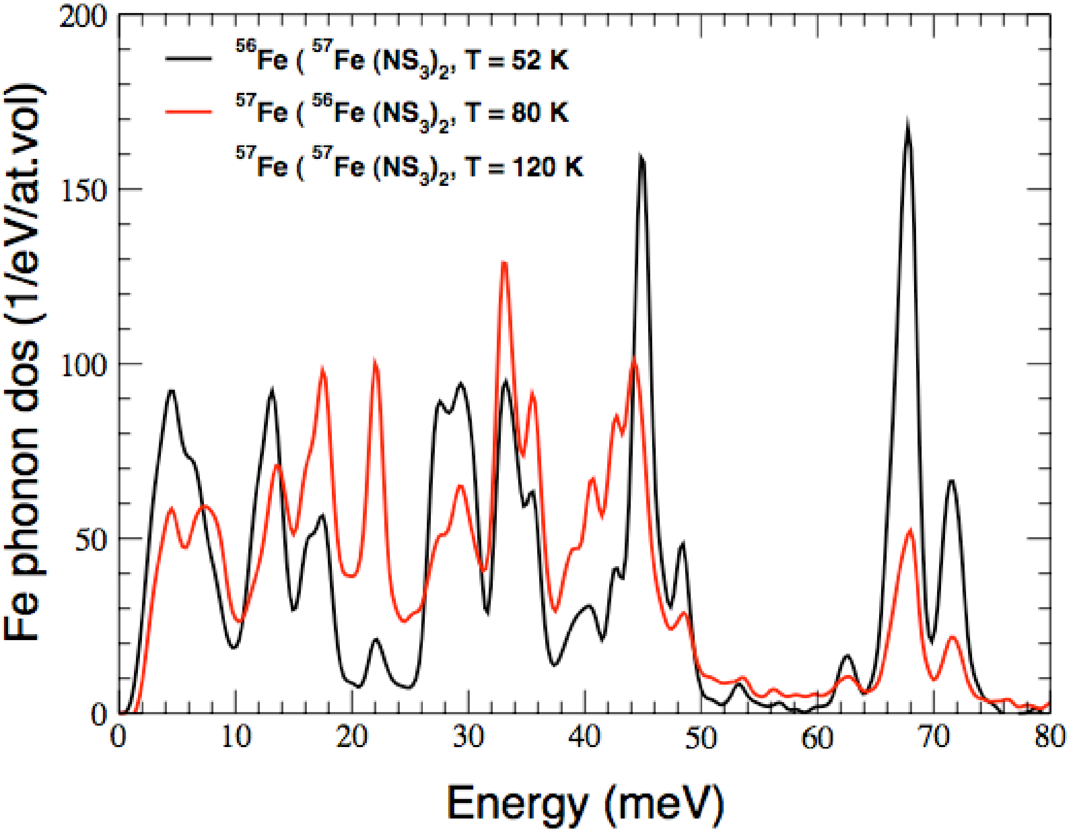

U. Jayasooriya et al, unpublished

Porphyrin model compounds

J. T. Sage, et al, J. Phys. Cond. Matt, 13 (2001) 7707

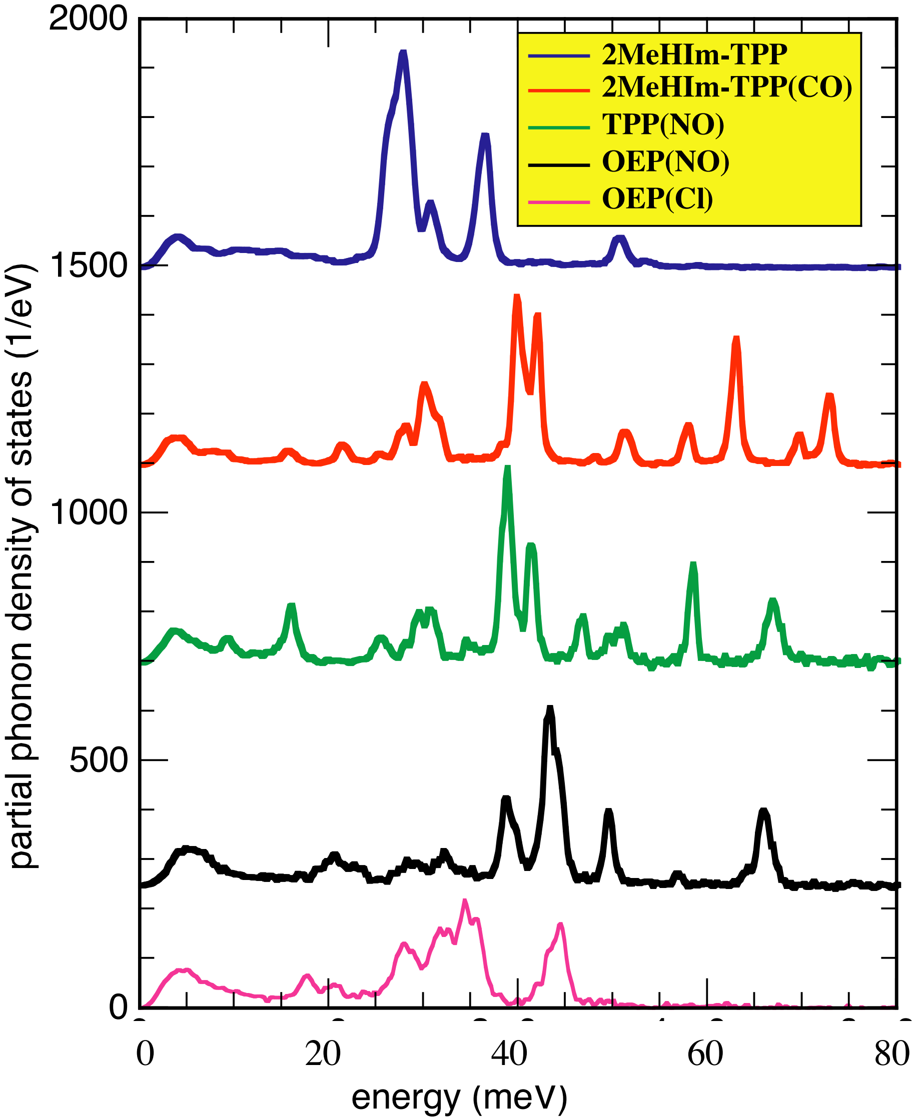

The heme doming coordinate is directly Involved in oxygen-binding reaction.

In proteins, it is important to know whether It acquires a global character.

Doming modes are expected in the range of 6-8 meV.

Porphyrin model compounds mimic the heme group found at the active site of many proteins involved in biological usage of oxygen and nitric oxide.

2MeHIm-TPP: Methyl-Hydrogen-Imidazole tetra phenyl porphyrin

OEP : Octo ethyl porphyrin

TPP : Tetra phenyl porphyrin

Properties extracted from NRIXS data

Property	Information content
Lamb-Mössbauer Factor, or recoil-free fraction	f_{LM}, recoil free fraction obtained from density of states, $g(E)$: $f_{LM} = \exp\left(-E_R \int \frac{g(E)}{E} \cdot \coth\frac{\beta E}{2} dE\right)$
Second order Doppler shift	$\delta_{SOD} = -E_0 \frac{< v^2 >}{2c^2}$
Average kinetic energy	Extracted from second moment of energy spectrum: $T = \frac{1}{4E_R}\left\langle (E - E_R)^2 \right\rangle$
Average force constant	Extracted from third moment of energy spectrum: $\frac{\partial^2 U}{\partial z^2} = \frac{m}{2h^2}\left\langle E^3 \right\rangle$
Phonon density of states	Extracted one-phonon absorption probability, $S_1(E)$: $g(E) = \frac{E}{E_R}\tanh(\beta E/2)(S_1(E) + S_1(-E))$
Specific heat (vibrational part only)	$C_V = 3k_B \int_0^\infty (\beta E/2)^2 \csc h(\beta E)\, g(E) dE$
Vibrational entropy	$S_V = 3k_B \int_0^\infty \left\{\frac{\beta E}{2}\coth(\beta E) - \ln\left[2\sinh(\beta E)\right]\right\} g(E) dE$
Debye sound velocity (aggregate sound velocity)	From low-energy portion of the density of states: $g(E) = \frac{3V}{2\pi h^3 v_D^3} E^2$
Mode specific vibrational amplitude	Contribution of mode α of atom j to zero-point fluctuation [11,12]: $\left\langle r_{j\alpha}^2 \right\rangle_0 = \frac{h^2}{2m_j\omega_\alpha^2} e_{j\alpha}^2$
Mode specific Gruneisen constant	From pressure dependence of phonon frequencies ω_α of acoustic or optical modes: $\gamma_\alpha = -\frac{\partial \ln \omega_\alpha}{\partial \ln V}$
Temperature of the sample	From detailed balance between phonon occupation probability

Classical thermodynamical quantities and phonon density of states

In the Harmonic Approximation (i.e. interatomic forces are linear in atomic displacement) the thermodynamic functions are additive functions of the normal mode frequencies. Thus, they are expressible as averages over frequency distribution function, **g**(ω), or phonon density of states.

1.Helmholtz Free Energy

$$F_V = 3RNk_BT\int \ln\left\{2\sinh\left(\frac{h\omega}{k_BT}\right)\right\}\mathbf{g}(\omega)\mathbf{d}\omega$$

2.Vibrational Energy

$$F_V = 3RN\frac{h}{2}\int \ln\left\{\coth\left(\frac{h\omega}{k_BT}\right)\right\}\omega\cdot\mathbf{g}(\omega)\mathbf{d}\omega$$

3. Specific heat

$$C_P = 3RNk_B\int\left(\frac{h\omega}{2k_BT}\right)^2 \operatorname{csch}\left(\frac{h\omega}{k_BT}\right)\ \mathbf{g}(\omega)\mathbf{d}\omega$$

4.Entropy

$$S = 3RNk_B\int\left\{\left(\frac{h\omega}{2k_BT}\right)\coth\left(\frac{h\omega}{k_BT}\right) - \ln\left[2\sinh\left(\frac{h\omega}{k_BT}\right)\right]\right\}\mathbf{g}(\omega)\mathbf{d}\omega$$

Werner Keune, Duisburg
Phonon confinement in multilayers

Fe / Cr(001) samples (MBE)